

EXPERIMENTAL ANALYSIS AND MODELLING OF GASOIL HYDROTREATMENT PROCESS



UNIVERSITÀ DEGLI STUDI DI CAGLIARI

Michela Medde



DOTTORATO DI RICERCA IN INGEGNERIA INDUSTRIALE
UNIVERSITÀ DEGLI STUDI DI CAGLIARI
XX CICLO

EXPERIMENTAL ANALYSIS AND MODELLING OF GASOIL HYDROTREATMENT PROCESS

MICHELA MEDDE

Supervisors:
Prof. Ing. Roberto BARATTI
Ing. Stefano MELIS



Dottorato di Ricerca in Ingegneria Industriale
Università degli Studi di Cagliari
XX Ciclo

Acknowledgements

The SARTEC Company is kindly acknowledged for the support through its fellowship.

A special thank should go to Prof. Baratti, first of all as my tutor for his continuous support and help but especially at human level for the great opportunity he gave me to grow up as both an engineer and a person. I found in him both professionalism and humanity that helped me facing this work during all the difficult moments.

Thanks to Stefano for all the invaluable suggestions and for the scientific support. I would like to thank him because he has shared many fruitful discussions with me.

Thanks also to all the persons working in the SARTEC Company who helped me along these years offering their collaboration and availability.

Special thanks to my colleagues, to Stefania and Massimiliano, to my friends and my roommates for bearing me during my up and down moments.

Finally, thanks to my family and Claudio for the continuous support to my choice during these years and sharing all my sacrifices and my joys. Everyone of them helped me passing through all the difficult moments pushing me to continue along this way up to now. I am sure it will be like that also in the future and I can say I am lucky for this.

Contents

Introduction	1
Chapter 1. Generality	3
1.1 Gasoil	5
1.2 Diesel demand in the world.....	9
1.3 Environmental specifications	12
1.4 Meeting demand and specifications	16
1.5 Alternative fuels	19
1.6 Motivations	20
Chapter 2. Hydrotreating	23
2.1 Unit description	25
2.2 Hydrotreating reactions	27
2.2.1 Hydrogenation reactions	27
2.2.2 Hydrodesulfurization reactions	30
2.2.3 Hydrodenitrogenation reactions	34
2.2.4 Hydrodeoxygenation reactions	36
2.3 Hydrotreating feeds	37
2.4 Commercial catalysts	37
2.5 Characteristic operating conditions	42
2.6 Reactor fluidynamic	44
Chapter 3. Pilot Unit	49
3.1 Pilot unit description	51
3.1.1 Gaseous feed section.....	53
3.1.2 Liquid feed section.....	53
3.1.3 Reaction section	54
3.1.4 High-pressure separation section	56
3.1.5 Stripping section	56
3.1.6 Treatment, recycle and discharge section	57
3.1.7 Product storage section	57
3.2 Pilot unit fluid dynamic.....	57
3.3 Experimental test on the pilot unit	58
Development of the phenomenological model.....	63
Chapter 4. Feedstock and product characterization	65
4.1. State of art	67
4.2. Definition of the aromatic, sulfur and nitrogen compounds.....	71
4.2.1 Aromatics speciation.....	71
4.2.2 Sulfur compounds speciation.....	76
4.2.3 Nitrogen compounds speciation.....	78

4.3. Definition of the compounds for cracking reactions	79
Chapter 5. Model formulation.....	83
5.1 Hypotheses of the model	85
5.1.1 Axial dispersion influence	85
5.1.2 Mass Transfer Resistances	88
5.1.3 Other hypotheses	92
5.2 Mathematical model development	92
Chapter 6. Hydrogenation and hydrodesulfurization kinetics.....	95
6.1. Hydrogenation reactions	97
6.1.1 Mechanism of hydrogenation of the aromatic compounds	97
6.1.2 Hydrogenation kinetics	100
6.2 Mechanism and kinetics of hydrodesulfurization of sulfur compounds	104
Chapter 7. Hydrodenitrogenation kinetics.....	111
7.1 Introduction and state of art	113
7.2 Mechanisms of hydrodenitrogenation	114
7.3 Kinetics of hydrodenitrogenation	117
7.4 Inhibition effect of the nitrogen compounds	121
Chapter 8. Model results.....	125
8.1. Introduction	127
8.2 Preliminary remarks	129
8.3 Hydrogenation results for a low level of temperature: catalyst 1 (cat 1)	130
8.3.1 Calibration test (Set #1)	130
8.3.2 1 st Validation test (Set #2)	133
8.3.3 2 nd Validation test (Set #3)	135
8.4 Hydrogenation results for a low level of temperature: catalyst 2 (cat 2)	137
8.4.1 Calibration test (Set #4)	137
8.4.2 1 st Validation test (Set #5)	138
8.4.3 2 nd Validation test (Set #6)	139
8.5 Hydrogenation results for a high level of temperature: catalyst 1 (cat 1)	141
8.5.1 Calibration test (Set #3)	141
8.6 Hydrogenation results for a high level of temperature: catalyst 2 (cat 2)	142
8.6.1 Calibration and validation tests (Set #5 and Set #7)	142
8.7 Hydrogenation results for different feeds: catalyst 2 (cat 2)	144
8.8 Hydrodesulfurization results for a low level of temperature	146
8.8.1 Calibration tests for both cat 1 and cat 2 (Set #1 and Set #4)	146
8.8.2 Validation test: cat 2 (Set #5 and Set #6)	149
8.9 Hydrodesulfurization results for a high level of temperature	151
8.9.1 Calibration and validation tests for cat 2	151
8.10 Hydrodenitrogenation results	152
8.10.1 Calibration test (Set #4)	152
8.10.2 Validation tests (Set #5 and Set #6)	153
8.10 Industrial model results	155
Chapter 9. Cracking reactions	157

9.1 Kinetics	159
9.2 Cracking Model.....	161
9.3 Results.....	162
Conclusions	163
Appendix	167
Introduction.....	167
Content and distribution of the aromatic compounds	167
Content and distribution of the sulfur compounds	172
Acronyms.....	177
Bibliography.....	179

Figures Index

Fig.1. 1 Refinery scheme.....	7
Fig.2. 1 Typical scheme of hydrotreating unit.....	26
Fig.2. 2 Aromatic saturation as a function of reactor temperature and pressure on a Middle East heavy gas oil: (□) 4.5 MPa, (+) 6.5 MPa, (*) 12.5 MPa.....	30
Fig.2. 3 Classification of sulfur compounds.....	31
Fig.2. 4 Reaction network of thiophene	32
Fig.2. 5 Reaction network of benzothiophenes	33
Fig.2. 6 Reaction network for dibenzothiophenes hydrodesulfurization and hydrogenation catalyzed by CoMo/ γ -Al ₂ O ₃ or NiMo/ γ -Al ₂ O ₃	33
Fig.2. 7 Nitrogen distribution in a SRGO, LCO and VGO	34
Fig.2. 8 Reaction network of benzofuran (Angelici, 1997).....	36
Fig.2. 9 MoS ₂ nanostructure.....	38
Fig.2. 10 Co-Mo-S nanostructures	39
Fig.2. 11 Particle shapes of industrial hydroprocessing catalysts. (Ancheyta et al., 2005).....	40
Fig.3. 1 Simplified scheme of hydrotreating pilot unit.....	51
Fig.3. 2 Completed scheme of hydrotreating pilot unit.....	52
Fig.3. 3 Example of loading scheme for a hydroprocessing reactor.....	55
Fig.3. 4 Thermowell and thermocouples location inside the pilot unit reactor	55
Fig.4. 1 Classification of the aromatic compounds lumps.....	75
Fig.4. 2 Chromatogram of sulfur compounds obtained from the analytical method PFPD	77
Fig.4. 3 Approximation of experimental SimDis curve by the cumulative gamma distribution.....	80
Fig.4. 4 Identification of intervals along the temperature range in the SimDis curve	81
Fig.4. 5 Cumulative distributions of the different molecular lumps.....	82
Fig.5. 1 . Influence of IPMT for low LHSV (1,75 h ⁻¹); Feed: SRGO+LCO; Pressure: 90 bar	91
Fig.5. 2 Influence of the IPMT for high LHSV (5 h ⁻¹); Feed: SRGO+LCO; Pressure: 90 bar	91
Fig.6. 1 Lumping scheme of the aromatic compounds.....	99
Fig.6. 2 Reaction network for dibenzothiophenes hydrodesulfurization.....	105
Fig.7. 1 Quinoline HDN complete reaction network.....	115
Fig.7. 2 Indole HDN complete reaction network	116
Fig.7. 3 Quinoline HDN simplified reaction network	117

Fig.7. 4 Indole HDN simplified reaction network.....	117
Fig.8. 1 Typical values of heats of reaction for hydrogenation, hydrodesulfurization and hydrodenitrogenation.....	129
Fig.8. 2 Hydrogenation: Comparison between experimental data and model results (Set#1).....	132
Fig.8. 3 Hydrogenation: Comparison between experimental data and model results (Set#2).....	134
Fig.8. 4 Hydrogenation: Comparison between experimental data and model results (Set#3).....	136
Fig.8. 5 Hydrogenation: Comparison between experimental data and model results (Set#4).....	138
Fig.8. 6 Hydrogenation: Comparison between experimental data and model results at 365°C (Set#3).....	142
Fig.8. 7 Hydrodesulfurization: Comparison between experimental and model R ₃ and R ₄ concentrations, (Set#1).....	147
Fig.8. 8 Hydrodesulfurization: Comparison between experimental and model R ₃ and R ₄ concentrations, (Set#4).....	148
Fig.8. 9 Hydrodesulfurization: Comparison between experimental and model total sulfur content, (Set#1-Set#4).....	148
Fig.8. 10 Hydrodesulfurization: Comparison between experimental and model R ₁ , R ₂ , R ₃ , R ₄ concentrations (Set#6).....	150
Fig.8. 11 Hydrodesulfurization: Comparison between experimental and model total sulfur concentrations (Set#6).....	150
Fig.8. 12 Hydrodesulfurization: Comparison between experimental and model total sulfur concentrations (Set#5).....	151
Fig.8. 13 Hydrodenitrogenation: Comparison between experimental and model total nitrogen concentrations (Set#4).....	153
Fig.8. 14 Hydrodenitrogenation: Comparison between experimental and model total nitrogen concentrations (Set#6).....	154
Fig.8. 15 Hydrodenitrogenation: Comparison between experimental and model total nitrogen concentrations (Set#5).....	155
Fig.9. 1 Variation of the kinetic constant vs. cracking position (x).....	160
Fig.9. 2 Dealkylation matrix.....	160
Fig.9. 3 Cracking: Comparison between experimental and model results.....	162
Fig.A 1 High Performance Liquid Chromatography schematization.....	168
Fig.A 2 Typical chromatogram from HPLC.....	170
Fig.A 3 Typical gasoil deconvolution by Peakfit algorithm.....	171
Fig.A 4 Chromatogram of feedstock obtained from the analytical method PFPD..	173

Fig.A 5 Chromatogram of product obtained from the analytical method PFPD	173
Fig.A 6 Baseline position, 1 st approach	174
Fig.A 7 Baseline position, 2 nd approach	175

Introduction

Oil industry is continuously evolving chasing the fast development of the contrasting requirements of modern life. From one side, it tries to satisfy the growing energy demand adopting its production to provide the energy resources required by the market while considering at the same time the increasing pressure to the environmental protection.

For this reason, the increasing demand for diesel fuels coupled with the progressive tightening of environmental specifications has brought new emphasis on the research on gasoil production. Worldwide refineries, also in consideration of the varying quality of the feedstock, are trying to optimize the current process operations to maximize the utilization of the available sources. Depending of the specific constraints, this is realizable through the construction of new plants or the revamp of pre-existing units coupled to the utilization of state of the art catalysts. In any case, optimization of operating conditions is crucial.

In this context, this thesis proposes a phenomenological model that could be used to optimize the operating conditions of hydroprocessing plants that, due to their hydrogenation, hydrodesulfurization and hydrodenitrogenation reactions, are the refinery plants devoted to the improvement of gasoil quality. In this way the optimization of the process can always guarantee the satisfaction of more critical specifications.

This work is a part of a wider project on the hydroprocessing plant founded by Ministry of University and Research to whom a previous PhD thesis focused on the hydrogenation reaction, developed by Lara Erby, belongs too.

The first step will be presenting the more critical specifics, especially in terms of total sulfur, and polyaromatic content, density, cetane number and distillation temperature (Chapter 1). After that, this work will complete the previous hydrogenation study and provide a new contribute in terms of hydrodesulfurization and hydrodenitrogenation reactions by formulation of a phenomenological model.

Such formulation starts from the experimental tests carried out using the pilot unit located in SARTEC Company. The main property required for such model is a high versatility that is the ability to describe the process for all the possible situations in terms of feedstock, catalysts and operating conditions. To achieve such characteristic, a deep knowledge of both the industrial plant (Chapter 2) and the pilot unit (Chapter 3) is needed. In fact, they provide useful information to establish the rigorousness of the model and probable assumptions in the formulation of mass and thermal balances (Chapter 5).

On the other hand, good process knowledge is required about feeds and products characterization in order to make explicit the kinetic terms for reactions occurring in the plant. Therefore, starting from a lumped approach, the characterization of the hydrocarbons present in gasoil has been developed (Chapter 4).

This is essential to reduce the gasoil complexity and to identify a reduced number of kinetic expressions able to describe all the kinetic behaviors for all the compounds in feedstock and product.

The kinetic expressions have been obtained studying the reaction networks of hydrogenation, hydrodesulfurization (Chapter 6) and hydrodenitrogenation considering their novel competition on the catalyst. A special attention has been dedicated to the nitrogen compounds cross effect on the hydrodesulfurization and hydrogenation (Chapter 7).

Along this thesis, some tests showed also the presence of cracking reactions, although usually they do not occur on the typical hydrotreating catalysts. Therefore, also the cracking reactions have been included in the model increasing the level of detail in the gasoils characterization required to describe the side chains breaking off (Chapter 9).

Model results are related to both calibration and prediction tests with the objective to demonstrate its ability to satisfy the goal of model versatility. The developed model reliability is strengthened by its application on a real industrial plant especially showing out the importance of the hydrodenitrogenation reaction usually neglected by the common hydroprocessing studies (Chapter 8).

Chapter 1

Generality



Middle distillate fuels meet the personal and commercial energy needs of a large portion of the world's population. These fuels include diesel fuel, kerosene, jet fuel and home heating oil. This thesis focuses on diesel fuel and especially this Chapter concerns with the important changing diesel perspective. Worldwide refineries are living one of the most challenging periods of their histories in fact, the world demand for gasoil is growing at a faster rate than the demand for energy in general and it is expected to increase by 2.2% per year from 2006 to 2011. Currently the global refining industry is driven by demand for transportation fuels with their required specification. Consequently, the challenge is finding ways to meet the growing demand for diesel fuel to produce higher-quality diesel and sell it into an economy that may not be prepared to pay the price for environmentally improved fuel.

1.1 Gasoil

Before studying what is the current situation in the world in term of demand, quality and attitude of diesel fuels, it is necessary to explain in some detail what diesel fuels are. Diesel fuel is sometimes called gasoil but this is an inappropriate definition because they correspond only when gasoil is the combustibile for diesel engines. Anyway, from here these terms will be used without distinction because after a brief classification of the different gasoils they will be meant as diesel fuels.

Gasoil is a complex mixture of several classes of hydrocarbon compounds like paraffines, naphthenes and aromatics. Organic sulfur and nitrogen compounds are also naturally present while oxygen compounds are present in such small quantities that they may be considered negligible.

The market offers several kinds of gasoils whose properties depend on the destination uses.

Currently gasoil is employed as:

1. Heating oil for thermal plants and home heating;

This gasoil is burned in the thermal power plants. Because of the application, typical targets for the properties are different from those for auto-traction gasoil. For example, the main characteristic is a very high calorific value while for oil used in the diesel engines the high quality of the combustibile is determined by parameters like lubricity, polyaromatics, cetane number and sulfur contents.

2. Combustible for diesel engines;

Major uses are:

- On road transportation
- Off-road uses
- Rail transportation
- Military transportation
- Sea transportation

Combustible for auto-traction is employed to feed diesel engines, both those for big and slow motor vehicles destined to transport of goods or sea transportation and those for small and fast automobiles.

3. Special gasoils:

- ✓ Farming gasoil
- ✓ Alpine gasoil

Farming and alpine gasoils can be defined as combustible for diesel engines as well, but they are classified as special gasoils because they must have specific properties due to their employment. The farming (or agricultural) diesel oil is used as fuel for agricultural vehicles and as combustible for the activities related to agriculture. These products are subjected to different taxation than other oil products and for this reason, at least in Italy, they are green colored before the commercialization. Instead, the alpine diesel is employed as fuel for diesel engines that should work at low temperatures. In fact, using a particular refining process, this product can be employed until temperatures lower than minus 21° C.

4. Used as raw material for the chemical industry;

Tab. 1.1 resumes some important properties of gasoils described above:

	Density at 15°C [kg/m ³]	Sulfur content [%w]	Viscosity at 40°C [cSt]	Distillated at 250°C [%v]	Distillated at 370°C [%v]	Cetane Number
Heating gasoil	815÷865	0.2	2÷7.4	65	-----	-----
Auto-traction gasoil	820÷845	0.005	2÷4.5	64.5	95	51
Agricultural gasoil	820.6 at 40°C	0.05	4.29	64	95	49
Alpine gasoil	820÷860	0.005	2÷4.5	64.5	95	51

Tab 1.1 Principal properties of different kinds of gasoil

As shown in the Table 1.1, the properties that distinguish a gasoil change as a function of the use destination. In the specific instance, for the gasoil meant as diesel fuel, the main properties are cetane number, distillation curve, density, polyaromatic hydrocarbons and total sulfur content.

The **cetane number** is a measure of auto-ignition quality. It is defined as the percentage of normal cetane in a mixture of normal cetane and alpha-methyl naphthalene. Higher cetane numbers indicate better quality because generally result in a decrease in carbon monoxide, hydrocarbons and nitrogen oxides emissions.

Distillation curve of diesel fuel indicates the fuel amount that will boil off at a given temperature. The curve can be divided into three parts: the light end, the region around the 50% evaporated point (linked to other fuel parameters such as

viscosity and density) and the heavy end, characterized by the T90, T95 and final boiling points.

The **density** relates to the fuel energy content; the higher the fuel density is, the higher its energy content per unit volume. Too high fuel density for the engine calibration has the effect of over-fuelling, increasing black smoke and other gaseous emissions.

Polyaromatic hydrocarbons (PAHs) are increasingly attracting special attention because many are known harmful to the human health. They are suspected to be carcinogen and cardiovascular, gastrointestinal, reproductive and respiratory toxicant. They are also classified as persistent organic pollutants because tend to breakdown slowly in the environment.

Sulfur content, which tends to increase sulfur dioxide (SO₂) and particulate matter (PM) emissions from all vehicle categories, from the least controlled to the most controlled. Sulfur dioxide is an acidic irritant that also leads to acid rain and to the sulfate particulate matter formation.

Such properties represent the quality specifications that the refiners have to satisfy to introduce this combustible into the markets:

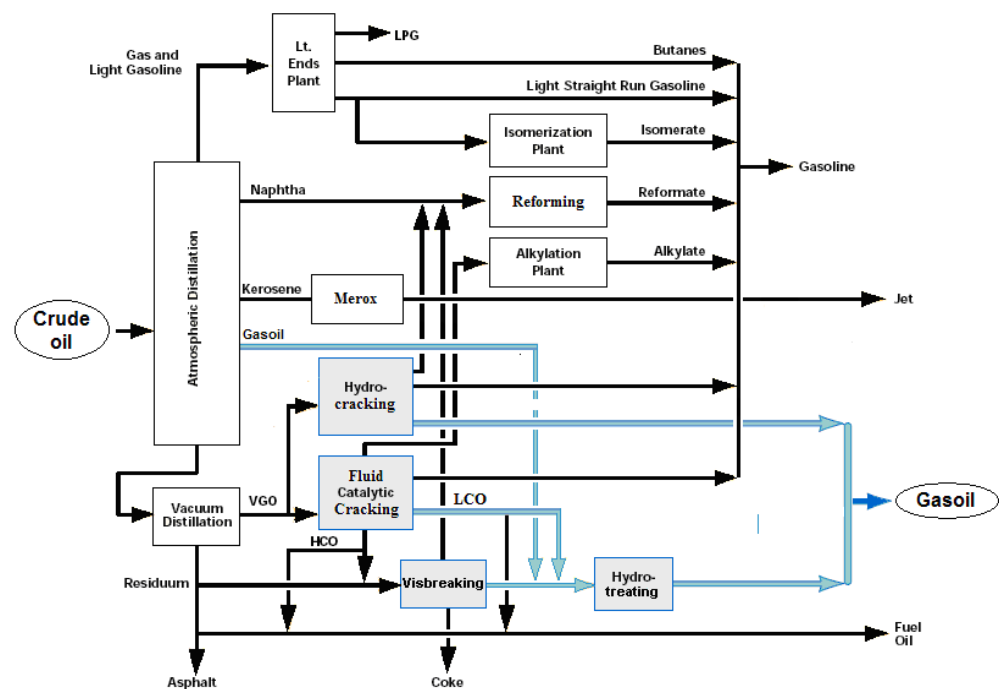


Fig.1. 1 Refinery scheme

Gasoil is one of the most important high value products obtained from crude and several processes can produce it. These processes could be divided into three different categories:

- Separation processes: the feed to these processes is separated into more components as a function of physical properties like boiling point (distillation).
- Upgrading processes: these processes improve gasoils quality using chemical reactions just to remove some undesired compounds (hydrotreating).
- Conversion processes: these processes change the molecular structure of the compounds of the feedstock increasing gasoil yield.

As shown in Fig. 1.1, in atmospheric distillation gasoil (277-343 °C) boils nominally between the kerosene and vacuum gasoil boiling points. The yield and the quality of atmospheric gasoil, similarly to the other distillation products, depend on the type of crude oil feedstock. Gasoils directly obtained from crude oil distillation are called straight run gasoils.

This kind of gasoils is also used as an important feedstock for middle distillates production and especially kerosene jet fuels, diesel and heating oil, usually after desulfurization. A fraction is used as olefin feedstock and the rest to enhance fluid catalytic cracking (FCC) feeds, this going on especially in the United States of America in order to increase gasoline yields. Gasoil can be produced also from the residual distillation product of high-boiling hydrocarbons. This feed is processed in a vacuum distillation unit to produce very heavy feedstock like asphalt, coke and vacuum gasoil. Vacuum or heavy gasoil is a distillate of petroleum with a boiling range of about 343-565°C and actually it is growing in importance as a feedstock to fluid catalytic cracking and hydrocracking in naphtha and diesel production.

In the past years, vacuum residue has been used as a low value, high sulfur fuel oil for onshore power generation or marine fuel. However, to remain competitive on the markets, refiners must obtain as much high value as possible leaving the minimum residue or coke possible. As result, vacuum residue may be sent to other plants performing thermal processes like visbreaking and coking to produce additional gasoil to feed the hydrotreating plant. The gasoil weight percentage from visbreaking or coking is 14.5 and 50.8 of the whole of the products, respectively.

Consequently, as shown in the Fig. 1.1, following the blue lines, the final diesel fuel produced by a refinery is a blend between all available gasoils: straight run gasoil, FCC light cycle oil and hydrocracked gasoil. Both straight run gasoil and FCC light cycle oil need to be hydrotreated to upgrade their quality.

Blending the available streams (and appropriate additives) may be made in order to achieve different performances, to satisfy several regulatory, economic and inventory requirements and to obtain gasoils for different applications.

Anyway, most of the plants used to produce gasoil, like hydrotreating and hydrocracking, have the disadvantage to require a high supply of hydrogen. The

main hydrogen source is the reforming plant usually present into refineries to produce high-octane gasoline. Nevertheless, hydrogen from the reforming is not enough to satisfy the hydrotreating and hydrocracking plants hydrogen demand. Some refiners have solved the problem tapping gasification processes of the heavy residue used to produce electric energy from the rejected items. Others use dried gas from FCC, recycle gas from hydrotreating and hydrocracking. Others use plants that realize partial oxidations or resort to external systems or producers.

This is an important aspect because introduces the need to find the best compromise among production and hydrogen consume that the refiners cannot neglect in hydrotreating plants construction.

1.2 Diesel demand in the world

As said before, several gasoil applications exist and the demand for this fuel is currently increasing very fast. Actually, diesel demand around the world is significantly heterogeneous because of different regional markets and environmental specifications concerning all kinds of fuels. There is some sea interregional trade, usually during peaks in demand that occur during seasonal demand for heating oil but usually each country lives a different status.

Considering the market related to gasoil as a petrochemical feedstock, its usage is concentrated mainly in the United States of America and Western Europe. Use in other regions is limited because naphtha is more plentiful from refineries, since less is consumed for gasoline production. In the USA, gasoil is consumed in refining processes to produce gasoline blending components. On the other hand, dealing only with auto-traction combustibles, gasoil is extremely popular in Europe and demand continues to grow very fast, while diesel market in the USA is practically nonexistent and gasoline remains the main fuel.

A diesel engine powers one out of 50% of cars sold in Europe today and it is expected that this percentage is going to further increase in the future. At the contrary in the USA, during the year 2000, diesel cars accounted for 0.26% of all new cars sold. The new advanced-technology diesel can be employed to get better fuel efficiency, more power and more durability. In fact, in term of fuel efficiency, diesels engines use 30-60% less fuel than gasoline engines of similar power. Moreover, diesels give more power producing more drive-force at lower engine speeds than gasoline engines, and more durability because diesel engine is built to last well over 320000 km. Finally, since diesels burn less fuel than gasoline vehicles, they produce significantly lower greenhouse gases emissions like carbon dioxide.

Use of last diesel technology has nearly eliminated the noise and the smoke. With the application of advanced technologies such as direct injection lean-burn

combustion, particulate traps and catalytic converters, diesel vehicles are now a clean and quiet alternative to less efficient gasoline powered cars. European governments encourage diesel technology use to reduce greenhouse gas emissions and to limit reliance on foreign oil. Fuel tax structures make diesel fuel cheaper than gasoline, and vehicle sales taxes encourage diesel technology purchase. European emissions regulations are designed aggressively to reduce diesel emissions such as nitrogen oxides and particulate matter.

Tables 1.2 and 1.3 describe 2003 and 2006 gasoil consumption status in five major regions respectively. They show how gasoil demand and supply increased more and less everywhere in the last years with exception of Japan where they remained almost the same.

2003				
Millions of Metric Tons				
	Production	Consumption		
		Chemicals	Fuels	Total
USA	320.9	4.8	321.8	326.7
Europe	269.0	5.6	266.6	272.2
Middle East	97.2	-----	-----	78.0
Japan	57.5	-----	-----	57.8
China	89.4	2.8	85.1	88.0

Tab. 1.2 Supply/Demand for gasoil in the year 2003

2006				
Millions of Metric Tons				
	Production	Consumption		
		Chemicals	Fuels	Total
USA	348.0	6.3	341.7	348.0
Europe	273.0	7.1	276.2	283.3
Middle East	101.9	-----	-----	93.0
Japan	55.4	-----	-----	60.1
China	119.5	2.7	114.3	117.0

Tab. 1.3 Supply/Demand for gasoil in the year 2006

Table 1.4 presents forecasts about gasoil consumption in the same areas up to 2011.

Consumption of Gasoil by Major Region

	Millions of Metric Tons		
	Gasoil		
	Chemicals	Fuels	Total
USA			
2006	6.1	341.7	347.8
2011	5.9	349.0	354.9
Europe			
2006	7.1	276.2	283.3
2011	7.4	305.0	312.4
Middle East			
2006	-----	-----	93.0
2011	-----	-----	96.4
Japan			
2006	-----	-----	60.1
2011	-----	-----	60.1
China			
2006	2.7	114.3	117.0
2011	2.9	159.2	162.1

Tab. 1.4 Gasoil fuel consumption 2006-2011

During 2006-2011 periods, consumption for gasoil in the fuel market will be minimal in the United States of America, Japan and in the Middle East. On reverse, looking to data reported in Table 1.5 about average annual growth rates, Western Europe's gasoil consumption for fuels would continue increasing. China will see a strong growth in gasoil fuels demand becoming, before 2011, the second largest energy consuming country worldwide.

Average Annual Growth 2006-2011

	Gasoil		
	Chemicals	Fuels	Total
USA	-0.6%	0.4%	0.4%
Europe	0.8%	2.0%	2.0%
Middle East	-----	-----	0.7%
Japan	-----	-----	-0.1%
China	1.4%	6.9%	6.7%

Tab. 1.5 Average Annual Growth Rate for Gasoil consumption 206-2011

1.3 Environmental specifications

Increasing gasoil fuels demand should face more and stricter environmental regulations, so that emissions control is now considered one between the performance aspects in comparing different fuels that can make the difference. Moreover, environmental pollution is a worldwide issue but different minimum air-quality targets have been established for different regions like Europe and America. The emissions targeted for any legislative control are:

- Hydrocarbons: they contribute to ozone formation that is an indicator of photochemical smog and a toxic gas for the humankind. Not all hydrocarbons contribute equally to ozone formation. Their reactivity depends on their chemical structure and atmospheric conditions. Under most of the conditions, olefins and aromatics are more reactive than paraffines. Toxicity depends on their structure. Most hydrocarbons are suspected to be or already known carcinogens but others are nontoxic at low concentrations. All hydrocarbons in the atmosphere are considered Volatile Organic Compounds (VOCs), as well as many other organic compounds types.
- Carbon monoxide (CO): a gas formed by fuels incomplete combustion; it is a health hazard because the presence of CO alters oxygen dissociation from other hemoglobin sites in the blood, and compromises oxygen delivery to tissues.
- Carbon dioxide (CO₂): it is a greenhouse gas. Its accumulation in the atmosphere effectively increases radiating energy input to the Earth causing the global warming.
- Nitrogen oxides (NO_x): they contribute to ozone formation and, reacting with water, form nitric acid that is one of the acid rain responsible agents. While NO is non-toxic by itself, NO₂ includes effects on breathing and to the respiratory system, damaging lung tissues. Road haulage accounts for about 50% of total emissions, more than the electricity supply industry and the industrial and commercial sectors considered together.
- Sulfur oxides (SO_x): they are produced primarily by combustion of fuels containing sulfur. Combined with water, they form sulfuric acid, which is the main acid rain component. Furthermore, SO_x irritate the respiratory tract causing coughing, mucus secretion and aggravated conditions such as asthma and chronic bronchitis.
- Particulates: they are possible carcinogens. They are classified into two different categories. PM_{2.5} (d < 2.5μm), composed by ammonium sulfate and nitrated, organic species and trace metals, settle in the deep part of respiratory tracts and, being very difficult to remove, they reduce pulmonary

functionality and cause chronic bronchitis. PM_{10} ($d < 10\mu m$), settling in the upper part of respiratory, is simpler to remove and cause only respiratory diseases like asthma.

- Air Toxics: they are pollutants like benzene, Polycyclic Organic Matter (POM), acetaldehyde and formaldehyde. Among this group, only POM is found in diesel fuel.

For each of them a specific standard to comply with exists but like for the heterogeneous global gasoil demand, at the same way also about environmental standards different specifications in different countries exist. Target values for some important air pollutions are reported in the following table:

Pollutant	EU Target-Band Values $\mu g/m^3$		Corresponding USA Federal Standard
	Upper	Lower	
NO _x (as NO ₂):			
<i>1 hr avg.</i>	200	93	-----
<i>Annual mean</i>	50	-----	100
CO (8hr avg.)	10	5	10
Benzene:			
<i>Annual mean</i>	10	10	-----
<i>Longer-term target</i>	2.5	2.5	-----
Ozone:			
<i>8 hr avg.</i>	120	120	156
<i>1 hr avg</i>	180	180	235

Tab. 1.6 Comparison between air quality targets for Europe and America

Tab. 1.6 shows that European standards are more stringent than USA targets, in fact Europe represents the most advanced region in terms of environmental regulations and, on a comparative worldwide basis, these standards represent the most conservative targets. Studies about environmental regulations are focused only on Europe and United States because in other parts of the world like Asia and Middle East similar emissions standards do not exist yet and the gasoil quality required is lower.

The attempt to reduce the main emission species focuses on their sources and it is a well-known fact that one of them is the vehicles fuel. Therefore, within the next few years, European and United States governmental specifications will require refiners

to produce gasoils with more restrictive characteristics. Legislation is focusing on following diesel properties that affect emissions:

- Sulfur content: which affects SO_x and particulate formation
- Density: which affects driving range
- Cetane number: which affects burning characteristics
- Distillation: which affects particulate formation
- Aromatics: which affect unburned hydrocarbons, NO_x and particulate formation

Aromatic compounds saturation in distillate fractions and in particular in diesel fuel has received considerable attention in recent years. A high aromatic content is associated with poor fuel quality, giving a low cetane number in diesel fuel and a high smoke point in jet fuel. There is also evidence that particulate emissions in diesel exhaust gases correlate with the fuel aromatic content.

Actually, the most important parameter remains the sulfur content. In fact, a drastic reduction of total sulfur content in a gasoil will be necessary to reduce air pollution from diesel engines. The United States reduced sulfur level to 500 wppm in 1993 and Europe followed in 1996. Since then, this sulfur limit in diesel fuel has been adopted by many other regions of the world.

Nowadays, world countries have different environmental regulations for gasoil depending on the different importance this fuel plays in each of them. Although the USA is not yet so dependent on diesel for personal transportation, this fuel is becoming the major one for goods transportation.

Parameter	Limits		Test Method
	Min.	Max.	
Cetane number	51.0	-----	ISO 5615
Density at 15°C [kg/m^3]	-----	845	ISO 3675
Distillation, 95% point, [°C]	-----	360	ISO 3405
PHA, [%w]	-----	11	IP 391
Sulfur content, [wppm]	-----	350 (in 2000)	ISO/DIS 14596
		50 (in 2005)	
		10 (in 2009)	

Tab. 1.7 Diesel fuel specifications proposed by EU Commission

In Europe, gasoil, and in particular gasoil for transportation, must be in keeping with the 2003/17/CE directive application related to the gasoline and gasoil quantity. In particular, it must satisfy the characteristics reported in the Tab. 1.7.

Several European countries have introduced reduced taxes on environmental friendly fuels, for example, diesel fuel in the Nordic countries has more restrictive specifications than EU proposal.

In the United States, the “Clean Air Act” had been approved in the year 1970 giving to the US Environmental Protection Agency's (EPA) the task to define the diesel specifications but other groups can have a marked effect on future specifications:

- CARB: California Air Resources Board
- EMA: Engine Manufactures Association

Diesel Specification	United States of America		
	U.S. EPA	CARB Reference	EMA Premium Diesel
Cetane number	40	48	50
Distillation [°C] max.:			
90%	338	288-321	332
95%	-----	304-350	355
Density at 15°C [kg/m ³]	-----	820-870	
Aromatics, %w			
<i>Total</i>	-----	10%v	-----
<i>PAHs, di/tri, %w</i>	-----	1.4	-----
Sulfur, wppm, max.	500/15	15/500	500

Tab. 1.8 Diesel fuel specifications in the United States

In Tab. 1.8, the different specifications proposed by the above mentioned groups are reported. All of the European, CARB and EMA specifications are considerably more difficult to satisfy than the current EPA standard diesel fuel specifications.

The U.S. Environmental Protection Agency's (EPA) is working to reduce emissions from diesel vehicles. Its program pairs engine technology and fuel changes to reduce significantly diesel vehicle pollution. Under this program, new diesel engines will be equipped with sulfur-sensitive emissions control technologies that will require diesel fuels with significantly reduced sulfur levels to function properly.

Instead, EMA proposal focuses on higher cetane number and CARB has concentrated on total aromatic compounds.

As mentioned previously, one of the most important specifications is represented by total sulfur content. Consequently, future trend will be to produce Ultra Low Sulfur Diesel (ULSD) that is a fuel with very low sulfur content.

In the USA, EPA proposed to change all diesels to ULSD within 2007 with exception of some states like California and Alaska, which ask time up until 2010. The allowable sulfur content for ULSD (15 wppm) is much lower than the previous standard (500 wppm) and it is comparable to European standard (50 wppm at this time and 10 wppm within 2009). Implementing the new fuel standards for diesel,

nitrogen oxide emissions will be reduced by 2.6 million tons each year and particulate matter will be reduced by 100000 tons a year. On the other hand, the process used to remove the sulfur also reduces the aromatic content and fuel density resulting in a minor decrease in energy content (by about 1%), in a reduced peak power and fuel economy. However, the reduction is slight and therefore negligible.

1.4 Meeting demand and specifications

Existing refineries are currently sufficient to satisfy the gasoil demand and quality required by the current environmental regulations in most of the areas, but this could not be possible in the future if gasoil demand will continue increasing faster than refining capacity and if the specifications target will become more restrictive. That means, it will become more and more difficult meeting demand and trying, at the same time, to satisfy fuels specifications.

It is worth to stress that gasoil properties obtained from separation processes depend on the initial crude oil properties and they differ substantially in the worldwide distributed extracting oil-fields. These varying characteristics often affect the refining and processing operations because the required severity for the upgrading and conversion processes increases with the decrease of gasoil quality.

Among all the specifications, the sulfur amount in crudes is the most important both for crude refiners and for consumers using oils produced by it.

Crude oils sulfur content has a direct relationship with the sulfur percentage found in fuel oils; 70-80% of the sulfur in crude oils ends up in the distillate and residual fractions.

There are light, high gravity crudes (30-42 API), which are generally low sulfur, while heavy, viscous and low-gravity crudes (10-24 API) have high sulfur. This shows that as the crude gravity raises, the sulfur content decreases.

Crude oils are found in all areas of the world, from the hot, arid Middle East lands to the frozen Arctic Circle tundra. In addition, many offshore drilling rigs, notably in the North Sea that is a comparatively new crude field, produce large crude volumes.

In the United States of America, both low- and high sulfur crudes are extracted. The following sulfur percentages are typical in crude oils found in the following states: Oklahoma, 0.73%; Texas, 0.35% and 1.50%; Michigan, 0.51%; Illinois, 0.37%; Louisiana, 0.40%; and Wyoming, 3.20%. Crude from Alaska's Prudhoe Bay has about 1% sulfur content.

Most of the actual crudes not coming from USA oil-fields have high sulfur. Large part of these crudes originates in the oil-rich Middle East, with sulfur contents ranging from 1.3% in Arabian and Iranian crudes to 2.5% in Kuwait crude. About the Mediterranean area, Libya, Algeria, Tunisia, and Nigeria have much lower sulfur

contents oils, but their import volume is much lower. Mexican and Venezuelan crudes are high sulfur, ranging from 2.5 to 4%.

Global refining configuration will have to face in the years to come the fuels quantity and quality evolution. In the past, gasoline represented the main refining product but now it is coming substituted from gasoil. Therefore, typical refineries configuration will not focus on plants such Fluid Catalytic Cracking (FCC) or thermal cracking, developed in the past to produce mainly gasoline. Further, the kind of gasoil produced for the market will not be the same because the Light Cycle Oil (LCO) from FCC will contain a too high aromatic content and it will be even not suitable to blend gasoil, unless treated in hydrotreatment.

It will be not sufficient to purchase from other refiners diesel blend stocks with low sulfur and aromatic contents or with a high cetane number because the streams supply and their price will be prohibitive in a short time.

For this reason refiners have to do something different; they could improve the actual infrastructures utilization or, for example, optimize the fractionation to maximize diesel production. Nevertheless especially, they must focus on other types of processes, like hydrotreating and hydrocracking, working with plants more suitable to produce a very high quality gasoil.

Possible solutions are the existing plants optimization or the grass root plants construction if not present in the refinery yet.

Most of the refineries already possess the hydrotreating plant. In this case, they could use severe operating conditions for hydrogenation, hydrodesulfurization and hydrodenitrogenation and new generation catalysts, very reactive and selective, to optimize their yields and their products quality.

Following the way of optimization, they do not have to replace old plants with new ones, as they just could improve the global refining arrangement using hydroprocessing plants to increase the quality of gasoil produced by thermal or catalytic cracking. Namely, in the optimal configuration, refiners could use old traditional plants to still produce large gasoil quantities and satisfy the gasoil demand introducing new hydrotreating processes to satisfy the new environmental specifications.

They could also introduce hydrocracking units or more severe forms of hydrogen replacement to process even heavier feeds (like vacuum gasoil) to produce high-value naphtha or distillate products.

The choice between different options in order to improve diesel properties and meet the new specifications depends mainly on which properties we want to get better. For example, as said earlier, the most important goal is total sulfur content reduction to satisfy the very stringent target of 10 wppm. The problem gushes out from the considerable differences between gasoils in term of sulfur content. In fact,

hydrotreating capacity can satisfy this target only when a low sulfur gasoil is processed, while it could not be sufficient to produce an ULSD when feed contains a high sulfur level. Consequently, to meet the increasing demand for diesel and at the same time, a lower sulfur level, most refiners have probably to increase the capacity of existing hydrotreaters or to install additional ones. Another strategy could be changing catalyst or changing operating conditions to obtain a higher severity operation, for example increasing the pressure inside the unit or the catalyst volume or, moreover, decreasing space velocity improving sulfur removal.

Several options are available also for reducing the aromatics content. The purchase of more-paraffinic crudes resulting in gasoils poor in aromatics is often not sufficient to satisfy the strict specifications. Therefore, sometimes it is necessary to convert high aromatic gasoil, such as Light Cycle Oil from Fluid Catalytic cracking (FCC LCO) into diesel with a higher paraffinic amount. Even in this case the aromatic compounds conversion can be improved modifying operative conditions, for example increasing hydrogen partial pressure, decreasing space velocity, or changing catalyst. Instead, the temperature effect is more complex because initially aromatic conversion increases when temperature increases while later, when equilibrium limitations are met, it reaches a maximum and starts to decrease. Moreover, this effect is more complex because the maximum depends on pressure and space velocity.

Aromatic saturation is a very important alternative because it allows improving other gasoil properties that have specific targets like distillation temperature, density or endpoint.

Aromatic saturation is a way to improve cetane number too; in fact, a reduction in polyaromatic compounds turns into a lower content of multiple ring aromatics molecules that have the lowest cetane number. That means cetane number can be improved even maintaining the same total aromatics content but changing the hydrocarbon type. In fact, the n-paraffin molecules have the highest cetane numbers followed by olefins, isoparaffins, and finally polyaromatic compounds. Cetane number increases also by removal of organic sulfur and nitrogen species because most of them contain aromatic rings that are opened or saturated by hydrodesulfurization and hydrodenitration. Furthermore, hydrocracking can be used to improve cetane number opening ring structure.

1.5 Alternative fuels

Growing demand for fuel compared with the environmental specifications leads to look for different kinds of combustibles other than gasoil or other fossil fuels from petroleum.

These fuels are called “alternative fuels” and in the common language, they are defined as petroleum substitutes. The term ‘alternative fuel’ can imply any available fuel or energy source, and does not refer to a renewable energy source.

Alternative fuels, also known as non-conventional fuels, are any materials or substances that can be used as a fuel, other than conventional fuels. Conventional fuels include fossil fuels and in some instances nuclear materials such as uranium. The most important alternative fuel is biodiesel.

Biodiesel is a domestically produced, renewable fuel that can be manufactured from vegetable oils, animal fats, or recycled restaurant greases. In the United States, soybean oil is the largest source of biodiesel, although oil from other plants can be used as well. Biodiesel is a mixture of fatty acid methyl esters. Vegetable oils, which chemically are triglycerides of fatty acids, are not good biodiesels. However, the oils can be combined with methanol in a process known as transesterification to produce a material with better properties. The resulting mixture of fatty acid methyl esters has chemical and physical properties similar to those of conventional diesel fuel.

Fuel Property	Biodiesel	Low sulfur diesel	ASTM D 975 Specification
Flash point [°C]	100	60	52 min
Viscosity, 40°C, [cSt]	4.7	32	1.9-4.1
Sulfur %w	<0.01	0.03	0.05 max
Cetane number	48-52	45	40 min.
Heating value, [kJ/m ³]	~35.7x10 ⁶	~36.2x10 ⁶	
Relative density	0.88	0.83-0.86	

Tab. 1.9 Comparison of typical properties of biodiesel and low sulfur diesel
(Source: National Soy Diesel Development Board)

Table 1.9 compares properties of a typical biodiesel with a typical low sulfur diesel. The energy content of biodiesel is slightly lower than that of conventional diesel but it contains essentially no sulfur or aromatic. It has a relatively high pour point, which could limit its use in cold weather.

Biodiesel is safe, biodegradable, and reduces air pollutants such as particulates, carbon monoxide, hydrocarbons, and sulfur dioxide emissions. Biodiesel offers

safety benefits over petroleum diesel because it is much less combustible, with a flash point greater than the low sulfur diesel. It is safe to handle, store, and transport. The main disadvantage of biodiesel is fuel cost that is two-thirds higher than conventional diesel fuel. Until the price comes down, its use will be limited respect to diesel fuel use. Moreover, biodiesel systems generally have lower emissions, but using biodiesel actually increases the amount of nitrogen oxide (NO_x).

Blends of 20% biodiesel with 80% petroleum diesel can generally be used in unmodified diesel engines; however, biodiesel can also be used in its pure form but it may require certain engine modifications to avoid maintenance and performance problems and may not be suitable for wintertime use.

1.6 Motivations

This Chapter showed the two different problems that substantially are the motivations of this work. The former is the increasing demands of diesel fuels and, the latter the progressive restrictive environmental regulations, in particular in terms of total sulfur content (currently bound is equal to 50 wppm but is going to become 10 wppm in 2009). These introduce a new emphasis on the optimization of refining process with the aim to face two problems with nearly divergent tendencies. In fact, the problem results in a simultaneous increase of quality and quantity of gasoil considering the scarceness of oil-fields and the insufficient quality of crude oils already available. All plants in the refinery must be strengthened and optimized to guarantee the maximum yield and the maximum production of product with a high value. Especially for conversion and upgrading processes (hydrotreatment plants), the aim is to develop a model that could be used to optimize the plant operating conditions in order to guarantee the maximum production of gasoil with properties respecting the target of the environmental regulations. Such model development needs a deep knowledge of the real processes, a detailed characterization of the complex feedstock and products that exceeds the level of detail allowed from the typical experimental techniques and a rigorous kinetic study of the hydrotreatment reactions. Therefore, its realization definitely is not only the formulation of the constitutive equations and this work consists of the making of the detailed speciation of the several compounds of gasoil according the development of new experimental methods and a rigorous study of their kinetic behaviors. However, certainly the mass and energy balances formulation is also realized. The model has been developed using a pilot unit similar to the industrial plant where tests “ad hoc” have been realized choosing the appropriate operating conditions. The main goal of the work is to propose a phenomenological model to optimize the process conditions like flow rate, temperature and pressure as a function of feed properties and to develop a

model able to describe the real properties of gasoil in each situation, for all feeds, catalysts, values of temperature, pressure and Liquid Hourly Space Velocity (LHSV).

Chapter 2

Hydrotreating



Until the 1940s, there was little incentive for the petroleum industry to improve product quality by means of hydrogen treatment. Since the early 1950s, however, several influences have determined the development of various hydroprocessing (or hydrotreating) processes. The increased production of high-sulfur crude oils and consequently the need to remove sulfur compounds from oil fractions, more stringent product specifications because of environmental requirements, and the production of increased quantities of cracked material from conversion processes boosted the installation of adequate hydrotreating capacities in refineries. Hydrotreating plants represent the highest capacities of all-secondary refining.

2.1 Unit description

The terms hydrotreating and hydroprocessing are used rather loosely for designating processes where operations like hydrodesulfurization, hydrocracking and hydrogenation occur (Trambouze, 1993). However, rigorously hydroprocessing includes hydrocracking and hydrotreating and the distinction among them is made.

Hydrotreating is one of the most commonly used refinery processes, designed to improve the quality of the feed removing contaminants such as sulfur, nitrogen, polyaromatics, or metals. The feedstock used in the process range from naphtha to vacuum residues, and the products in most applications are used as environmentally acceptable clean fuels.

Hydrocracking is an important conversion technology for producing high-value naphtha or distillate products from a wide range of refinery feedstock. The feedstock includes heavy vacuum gas oil, heavy synthetic crude gasoil, thermally or catalytically cracked stocks, or solvent extracted vacuum bottoms. It purposes decrease of molecular weight and boiling point, saturates from aromatics, molecular size reduction and residue upgrading.

This thesis focuses on the hydrotreating plant, therefore this will be the only technology showed in this Chapter to propose the industrial real plant description.

Into the hydrotreating plant, feeds react under high hydrogen pressure in presence of a catalyst under specified operating conditions in terms of temperature, pressure, and space velocity. Hydrogenation (HDA) is the main reaction but hydrodesulfurization (HDS), hydrodenitrogenation (HDN) and hydrodeoxygenation (HDO) take place simultaneously during the hydrotreatment. Some hydrodemetallation (HDM) and hydrocracking may also occur.

The hydrotreating plant employs usually two main sections: reaction section and fractionation section. The first one generally includes one or two catalytic reactors and the second one purifies the gasoils from gases like H_2S and NH_3 obtained by the reactions.

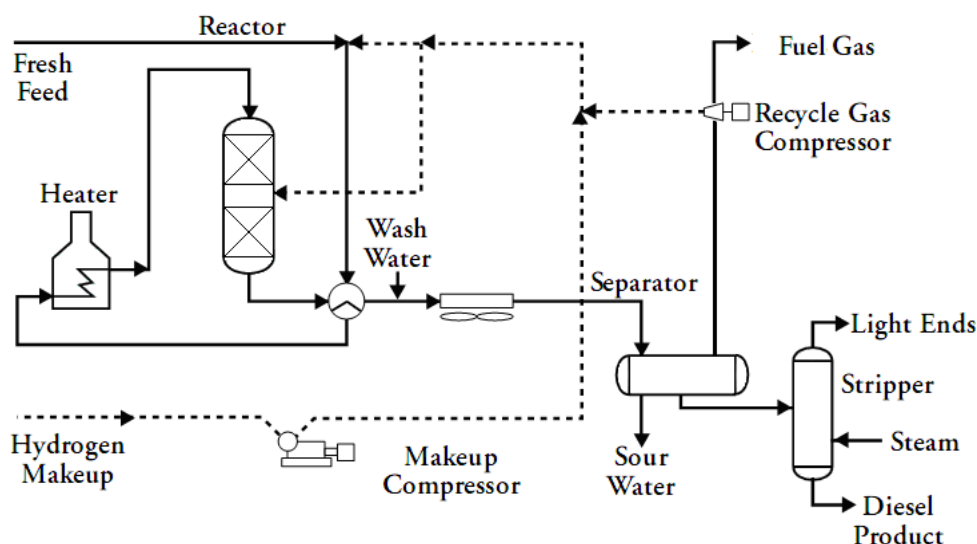


Fig.2. 1 Typical scheme of hydrotreating unit

Fig. 2.1 represents the typical scheme of hydrotreating unit. The liquid fresh feed is preliminarily mixed with makeup hydrogen (coming from the hydrogen production system) and recycle gas (high in hydrogen content) into an accumulator, then it passes through a heat exchanger to be pre-heated before going into the furnace where it reaches the reaction temperature ($330\div 380\text{ }^{\circ}\text{C}$). After that, it goes to the reaction section (with one reactor or two reactors in series) where hydrogenation, desulfurization and denitrification of polyaromatic compounds occur. Catalytic bed inside the reactors is usually divided into different reaction zones and between each couple of them, a flow distribution system is present to guarantee a uniform distribution of the liquid on the catalyst surface.

The reactor effluent flows again through the heat exchanger to be partially cooled before entering the high-pressure separator where the hydrogen-rich gases are separated and recycled to the first stage for mixing both makeup hydrogen and fresh feed. The liquid from the bottom of the separator flows to the stripping column where the light ends, H_2S and NH_3 removal is realized using low-pressure vapor water. Vapor products obtained into the hot accumulator are cooled, condensed and collected into the high-pressure cool accumulator. Thus, gas high in hydrogen content is produced and then sucked up by the recycle compressor and added up together with the feed.

The liquid product from the accumulator flows to the next medium pressure accumulator where the gas phase that it still contains is removed. The two liquid and gas products of the last accumulator are respectively sent to the accumulator of the

stripping column top and to the medium pressure washing column where the high hydrogen gas is cleaned from H₂S by the methyldiethanolamine solution.

The scheme described is a simple hydrotreating plant with one reactor but more the one reactor could be present because they allow obtaining high quality gasoils with a very low sulfur level. This is possible using a typical hydrotreating catalyst both in the first and in the second reactor. In this way the first stage is useful to remove sulfur and nitrogen contents compounds and the second one to realize the hydrogenation.

The major companies like Topsøe, Criterion, Shell, Akzo and UOP use this technology to produce gasoils.

2.2 Hydrotreating reactions

Several classes of reactions occur simultaneously in hydrotreating:

- Hydrogenation (HDA);
- Hydrodesulfurization (HDS);
- Hydrodenitrogenation (HDN);
- Hydrodeoxygenation (HDO);
- Hydrodemetallation (HDM);

Theoretically, these should all be considered to understand the reactivity patterns for commercial feedstock. Nevertheless, due to the limited impact of oxygenated and porphyrinic compounds on the process, usually, the last two reactions are neglected. In fact, the hydrodeoxygenation reactions could be neglected because are involved only in the hydrotreating of particular feedstock (usually not processed due to their high acidity). Furthermore, the hydrodemetallization reactions are not considered because they totally occur over a very thin catalytic layer located in the top of the reactor. Therefore, the rest of the reactor processes feedstock without any remaining metal.

2.2.1 Hydrogenation reactions

Hydrogenation is a class of chemical reactions that results in an addition of hydrogen (often as molecule H₂) usually to unsaturated organic compounds in the presence of a catalyst.

The hydrogenation reaction is exothermic and reversible under typical hydrotreating operating conditions, therefore, although its kinetics is favorite by the temperature increase, complete conversion may not be possible due to equilibrium limitations. It

means that to describe these reactions and their conversion, it is necessary to understand the thermodynamic aspects and the kinetic properties.

Because of the exothermic property, the extent of the reaction at equilibrium decreases with increasing temperature. Thus, temperature increase, to give higher rates in the other reactions, results in lower equilibrium conversions in aromatic hydrogenation.

Considering the generic reaction



the equilibrium constant is

$$K_{eq} = \frac{Y_{AH}}{Y_A P_{H_2}^n} \quad (2.2)$$

and the equilibrium concentration of the aromatic species can be described by

$$\frac{Y_A}{Y_A + Y_{AH}} = \frac{1}{1 + K_a P_{H_2}^n} \quad (2.3)$$

where Y_A and Y_{AH} are the mole fractions of aromatic and hydrogenated aromatics, respectively, K_a is the equilibrium constant, P_{H_2} the hydrogen partial pressure and n the number of hydrogen moles required for hydrogenation.

The analysis of this formula suggests how the conversion depends on the pressure; in fact, the lower equilibrium conversions are especially significant at lower pressure while high pressures favor low equilibrium concentrations of aromatic compounds (high conversions). Especially, this is true when the number of hydrogen moles required to saturate the aromatic rings is high. In term of temperature dependence, increasing the temperature the equilibrium constant decreases and this results in a higher aromatics equilibrium concentration. This is in agreement with the theory because the influence of the temperature on the equilibrium constant can be described by the Van't Hoff equation:

$$K_{eq}(T) = K_0 \exp\left(\frac{\Delta H_r}{RT}\right) \quad (2.4)$$

In this equation, K_0 represents the pre-exponential factor, R the universal gas constant and ΔH_r the reaction enthalpy. Due to the exothermic reaction ΔH_r is lesser than zero, therefore, as said above, increasing of the temperature results in a decreasing of the equilibrium constant.

In the literature (Girgis and Gates, 1991), results for some characteristic aromatic compounds (naphthalene, phenanthrene, and fluorine) show that the hydrogenation

equilibrium constants are lesser than unity at typical hydrotreating temperatures. Consequently, operation at high hydrogen partial pressures is necessary to hydrogenate aromatic hydrocarbons to an appreciable extent. Moreover, for aromatic hydrocarbons containing more than one ring, hydrogenation proceeds via successive steps each of which is a reversible reaction. The equilibrium constant is generally higher for hydrogenation of the first ring, but since more moles of hydrogen are involved in the final ring hydrogenation, the hydrogenation of the final ring is more thermodynamically favored than the hydrogenation of the first one (Korre et al., 1994, Aubert et al., 1988)

Another important aspect is the reactivity of the aromatic compounds. This is widely studied by different authors groups like Girgis and Gates (1991) and Korre et al. (1995) who say the hydrogenation of polyaromatic compounds proceeds in a ring-by-ring manner and no partially hydrogenated compounds are detected.

Usually, the typical polyaromatic compounds present in a gasoil are classified into triaromatic, diaromatic and monoaromatic compounds and, due to the typical temperature range of gasoil (250-360°C), compounds with more than four aromatic rings are negligible.

The polyaromatics reactivity changes as a function of their molecular structure, in particular, it increases with the number of aromatic rings and consequently the order of the reactivity is:



This is not enough to understand the different aromatics reactivity because, inside each macroclass characterized by the same number of aromatic rings, reactivity is higher for higher number of condensed rings. Consequently, in the scale of reactivity the most reactive compounds are anthracene and phenanthrene with three condensed rings, followed by naphthalene while biphenyl, having a molecule with two non-fused aromatic rings, has the same reaction rate of the monoaromatic compounds. Reactivity of monoaromatic compounds is one order lesser than the order of polyaromatics species (Girgis and Gates, 1991).

Moreover, for groups with the same number of condensed aromatic rings, the presence of phenyl substituents in benzene or naphthalene has no significant effect on the reactivity for hydrogenation. Alkyl substituents could enhance hydrogenation but the small effect of single substituents suggests that the enhancement in reactivity resulting from the electrodonating influence of the aryl substituents is probably compensated by increased steric hindrance of adsorption.

Finally, for groups with one or two aromatic rings, hydrogenation of a ring located at the end of the molecule is faster than hydrogenation of an internal ring.

The reactivity increases when the temperature increases due to the Arrhenius law:

$$k(T) = k_0 \exp\left(-\frac{E}{RT}\right) \quad (2.5)$$

where k_0 is the pre-exponential term and E the activation energy.

That means increasing temperature determines opposite contributes from thermodynamic and kinetic aspects. Consequently, varying temperature the predominant effect can be the kinetic effect or the equilibrium effect. For this reason, increasing the temperature inside the typical hydrotreating range, the degree of aromatic saturation obtained with industrial feedstock goes through a maximum. In fact, at lower temperature there is a kinetic control whilst at higher temperature the reaction is equilibrium controlled (Cooper and Donnis, 1996; Ancheyta et al, 2005, Chowdhury et al. 2002).

The limit of the temperature between the kinetic and thermodynamic control depends on the plant pressure and flow-rate. In fact, as shown in the figure 2.2 which represents an example related to a Middle East heavy gas oil (Cooper and Donnis, 1996), pressure enhance shifts that limit to higher temperature and progressively increases the conversion favoring the direct reactions.

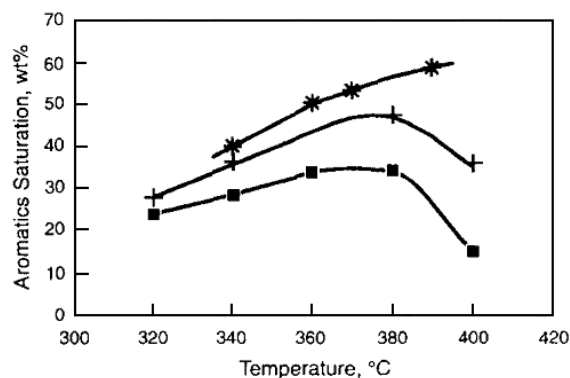


Fig. 2. 2 Aromatic saturation as a function of reactor temperature and pressure on a Middle East heavy gas oil: (□) 4.5 MPa, (+) 6.5 MPa, (*) 12.5 MPa.

2.2.2 Hydrodesulfurization reactions

Sulfur present in gasoil can be divided into non-aromatic and aromatic sulfur. The first group includes sulfides, disulfides and mercaptans (thiols) and the second one thiophenes, benzothiophenes, dibenzothiophenes, benzonaphthothiophenes and benzo[def]dibenzothiophenes, Fig. 2.3.

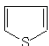
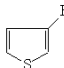
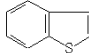
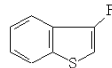
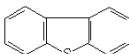
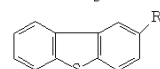
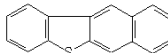
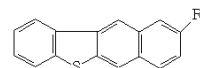
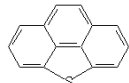
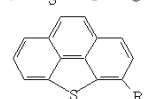
Compound Class	Structure	
Thiols (Mercaptans) Disulfides Sulfides		RSH RSSR' RSR'
Thiophenes		
Benzothiophenes		
Dibenzothiophenes		
Benzoaphthothiophenes		
Benzo[def]dibenzothiophenes		

Fig.2. 3 Classification of sulfur compounds

Because of the temperature range, benzonaphthothiophenes and benzo[*def*]dibenzothiophenes quantities are negligible.

Mercaptans, sulfides and disulfides are so much more reactive than the others sulfur compounds that they can be considered infinitely reactive in high-conversion processes. However, also thiophenes and most of alkylbenzothiophenes exhibit high reactivity, even at the low temperature of 280 °C, and are completely desulfurized at 360 °C. In contrast, alkyl dibenzothiophenes are more resistant to desulfurization and most of them are still present in the desulfurized oil. The three-ring compounds are one order of magnitude less reactive than the two-ring compounds, but the reactivity is similar for compounds having three or more rings. However, the reactivity strongly depends on the alkyl substituents presence and position, in fact, benzothiophene and dibenzothiophene have similar HDS reactivity but they are more reactive than their alkyl-substituted compounds. The reactivity of benzothiophenes decreases with increasing of the methyl groups' number and it depends also on their position; in particular, methyl groups on the thiophene ring at the 2-, 3- and 7- positions significantly reduce the reactivity of the compound (Schuit and Gates, 1973). Houalla et al. (1980) studied the effect of methyl substituents on the reactivity of dibenzothiophene suggesting that if they are at the 4- or 6- position or at 4,6-positions the dibenzothiophenes are refractory compounds due to the steric configuration that hinders the hydrodesulphurization reaction. In the opposite, the methyl substitution at the 3- and 7- positions decreases the reactivity only slightly and methyl groups at 2- and 8- positions do not affect the reactivity.

The different reactivity of these compounds depends on the rate of adsorption on the catalyst surface, which is affected by different molecule inflexibility because of the methyl-substituents position.

Under typical hydrotreating operating conditions employed industrially, the HDS of organosulfur compounds is essentially irreversible. The equilibrium constants decrease with increase of the temperature in agreement with the HDS exothermicity and they reach values much less than one only at temperatures considerably higher than those practically required do.

The kinetics of hydrodesulfurization of diesel feedstock is complex, due to the presence of many kinds of sulfur compounds.

The reaction mechanism of thiophene is not totally clear but the most common idea is that the first reaction is the C-S bond cleavage (hydrogenolysis) to produce butadiene, then the hydrogenation of this intermediate to produce butene and finally the hydrogenation of butene into butane (Fig. 2.4). These results suggest that hydrogenolysis and the hydrogenation take place on different kinds of actives sites (Schuit and Gates, 1973; Van Parijs and Froment, 1986a).

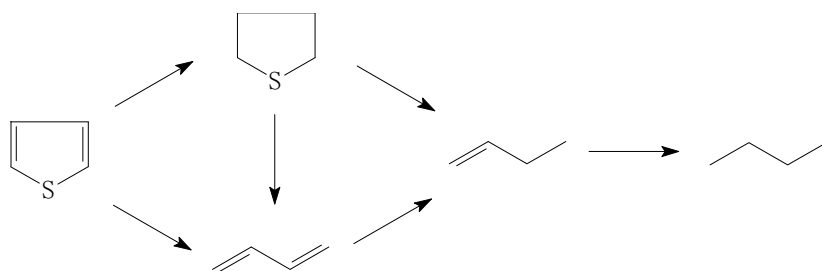


Fig.2. 4 Reaction network of thiophene

The reaction scheme proposed for benzothiophene is a triangular reaction network where, similarly to thiophene mechanism, more than one type of sites is operative for hydrogenolysis and hydrogenation (Van Parijs et al., 1986b). The triangularity of the scheme is due to the production of dihydrobenzothiophene that is a partial hydrogenated product, represents only the intermediate of reaction because it is very reactive and reacts very easily to produce ethylbenzene (Fig. 2.5).

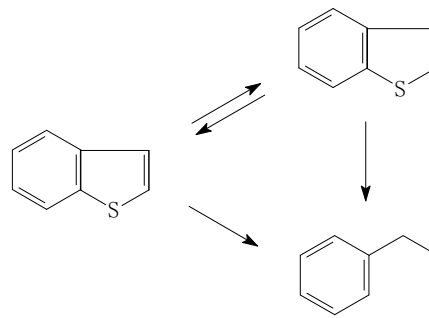


Fig.2. 5 Reaction network of benzothiophenes

For individual sulfur compounds such as thiophene, benzothiophene and dibenzothiophene, the reaction is a very fast hydrogenolysis described like a first-order reaction with respect to the sulfur compounds without any equilibrium limitation.

On the other hand, alkyl-dibenzothiophenic compounds reactions could be characterized by limitations related to the equilibrium depending on the operating temperature. According to the Gates and Topsøe (1997), the alkyl-dibenzothiophenes react through two parallel pathways consisting of a hydrogenolysis (direct desulphurization, DDS route) yielding biphenyl, and a hydrogenation followed by desulphurization (HYD route) yielding first tetrahydrodibenzothiophene (THDBT) and then cyclohexylbenzene.

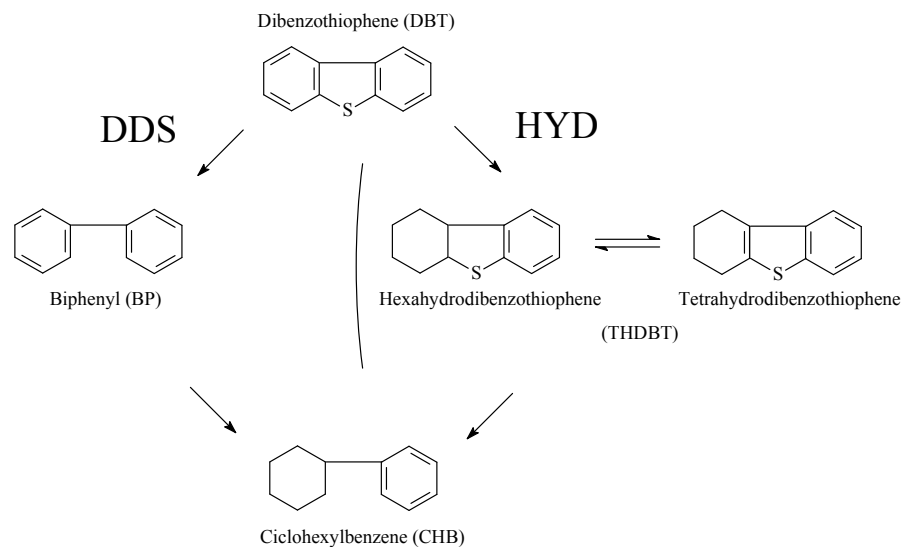


Fig.2. 6 Reaction network for dibenzothiophenes hydrodesulfurization and hydrogenation catalyzed by $\text{CoMo}/\gamma\text{-Al}_2\text{O}_3$ or $\text{NiMo}/\gamma\text{-Al}_2\text{O}_3$

2.2.3 Hydrodenitrogenation reactions

Generally, gasoil contains low levels of nitrogen compounds but they strongly affect the hydrotreating performance. Nitrogen content is dependent on the origin of the crude oil and it changes for different typical feeds of hydrotreating (Tab.2.1)

Hydrocracker Location	Crude origin	Feedstock	Nitrogen content [wppm]
EU	Ural and Nigerian oils	HVGO	1300
Asia	Arabian Light and Medium	LVGO+HVGO	750
Asia	Iranian Heavy	HVGO	1200
Asia	Iranian Heavy	HVGO	1500
Asia	Iranian Heavy	HCGO	3300
South America	Orinoco Belt	HVGO	2800
South America	Orinoco Belt	HCGO	6600
South America	Neuquenean oils and North West	LVGO	1000
Middle East	Iranian Heavy	HVGO	2300

Tab. 2.1 Different nitrogen content in feedstock of different origin

The Fig. 2.7 shows that the nitrogen distribution is different considering a SRGO (Straight Run Gasoil), LCO (Light Cycle Oil) and VGO (Vacuum Gasoil) and it is concentrated in the heavy portions of these fractions

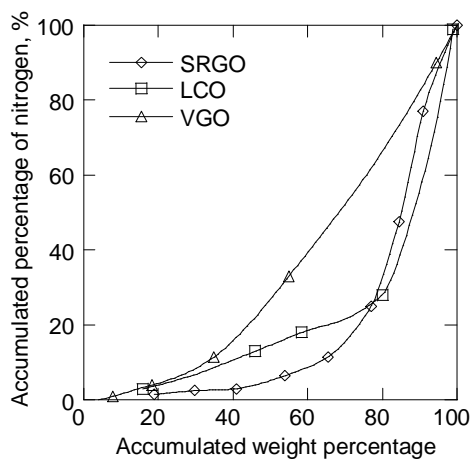
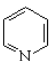
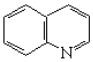
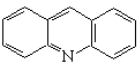
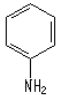
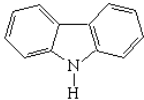


Fig.2. 7 Nitrogen distribution in a SRGO, LCO and VGO

Most nitrogen species present in gasoil are in the form of heterocyclic nitrogen compounds with multiple rings. Non-heterocyclic nitrogen compounds such as

aliphatic amines and nitriles are also present, but in considerably smaller amounts, and they are denitrogenated much more rapidly than the heterocyclic compounds. Consequently, non-heterocyclic organonitrogen compounds are less important to explain the nitrogen-removal chemistry occurring in the hydrotreating.

Nitrogen species can be grouped in two different classes characterized by a different kinetic behavior. As shown in the table 2.2, first group is the basic compounds group where the nitrogen atom belongs to a ring with six carbon atoms. The second group is that of refractory compounds. In this case, the nitrogen atom is included into a five member aromatic ring. In agreement with the literature, the repartition of these compounds is 1/3 for basic compounds, 2/3 for non-basic (neutral) compounds.

Basic Compounds		Neutral Compounds	
Pyridine		Amine $R-NH_2$	Pyrrole
Quinoline		Aniline	Indole
Acridine			Carbazole
			

Tab. 2.2 Classification of nitrogen compounds

In the last group, the lone-pair electrons on the nitrogen atom are localized around the aromatic ring and are unavailable for donation to a Lewis acid.

Aromatic nitrogen compounds removal is rather difficult and it requires a preliminary hydrogenation before denitrification. Studies of hydrodenitrogenation of heterocyclic compounds show that the HDN pathway involves:

- Hydrogenation of the nitrogen ring;
- Cleavage of one C–N bond, forming an amine intermediate;
- Hydrogenolysis of the amine to hydrocarbons and ammonia.

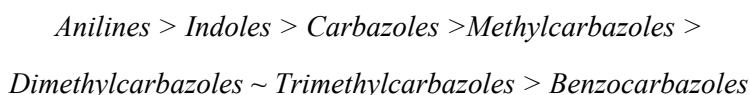
In particular, basic nitrogen group is characterized by a great affinity for the hydrogenation sites of the catalyst that hence are not available for other reactions, with particular reference to the indirect desulfurization (via preliminary hydrogenation) of the most refractory sulfur species.

The requirement that ring hydrogenation should occur before nitrogen removal implies that the position of the equilibrium of the hydrogenation reactions could affect nitrogen-removal rates if the rates of the hydrogenolysis reactions are

significantly lower than the rates of hydrogenation. Although the hydrogenation equilibrium is unfavorable, the effect of higher hydrogen partial pressures is to force the equilibrium considerably toward the hydroprocessing products, and HDN is virtually irreversible under typical reaction conditions. The equilibrium constants are less than unity for ring saturations and become smaller with increasing temperature, as the ring hydrogenations are exothermic. The overall hydrogenation and hydrogenolysis is favorite even at high temperature as 500°C

Usually, the rates of hydrogenation are higher than those ones of C–N bond scission. The steric effects that involve in the C–N scissions are inferred to be nearly equivalent for quinoline, acridine, benz[*c*]acridine, benz[*a*]acridine and dibenz[*c,h*]acridine. Reactions of basic nitrogen compounds with Lewis acids are strongly affected by steric hindrance. The equivalence of the steric effects implies that end-on adsorption through the nitrogen atom does not occur since otherwise the HDN rates for the potentially more hindered compounds, such as benz[*c*]acridine and dibenz[*c,h*]acridine, would be expected to have been orders of magnitude less than those for compounds such as acridine.

Nitrogen molecules are often very low reactive if compared with the corresponding sulfur species. The decreasing order reactivity of nitrogen compounds is:



2.2.4 Hydrodeoxygenation reactions

Oxygen level in crude oils are usually low (< 0.1%), therefore even if hydrodeoxygenation occurs under hydrotreating conditions oxygen removal is generally not a goal of this process.

As reported by Girgis and Gates (1991), in commercial hydrotreating feedstock oxygen compounds belong to two classes, phenol and naphthol derivatives and heterocyclic oxygen compounds like furan and its derivatives. Alcohols, carboxylic acids and ketones are also present, but in smaller amount. As for HDS and HDN, pathways to HDO products can involve oxygen removal either before or after hydrogenation of the aromatic rings. The steps in this reaction are similar to those in the HDS of benzothiophene.

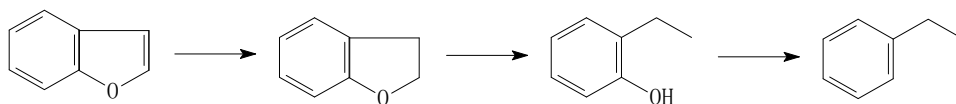


Fig.2. 8 Reaction network of benzofuran (Angelici, 1997)

For the heterocyclic compounds, the reaction mechanism is not completely clear and the Authors propose conflicting mechanisms.

The hydrodeoxygenation reaction is exothermic and, at typical hydrotreating temperatures, it is virtually irreversible. Reactivity of different compounds shows that benzofuran and dibenzofuran are much less reactive than phenols.

2.3 Hydrotreating feeds

The hydrotreating feeds can have different properties as a function of the type of crude oil fed to the refining system. Usually, the hydrotreating is used to process atmospheric feeds straight run gas oil (SRGO), light cycle oil (LCO), and their mixtures. Sometimes the percentage of LCO can be reduced to add a diesel oil coming from a thermal cracking (Visbreaking), VSBGO, as a function of the desired products qualities.

The quality of straight run gasoil, coming from the atmospheric distillation plant, depends on both the characteristics of crude oil and from the characteristics of the distillation. Several classes of hydrocarbons are present in the SRGO like paraffines, naphthenic and aromatics compounds. Their percentages depend on the type of gasoil but, usually, the aromatic content is 20÷30 %v.

Instead light cycle oil contains a higher aromatic content (40-50%v). In this case, short side chains characterize the aromatic compounds. Moreover, usually LCO has lower sulfur content than SRGO, typically it has an order of magnitude of hundredths while SRGO has an order of magnitude of thousandths.

On the contrary, very high sulfur content is present into the VSBGO (about 2%) In addition, it has high polyaromatic content because of the fractionation of heavy compounds.

2.4 Commercial catalysts

The typical hydrotreating catalysts consist of molybdenum supported on a high surface area carrier, usually alumina, promoted by cobalt or nickel. They are quite versatile because exhibit activity for the main hydrotreating reactions like hydrogenation, hydrodesulfurization, hydrodenitrogenation, hydrodemetallation and hydrodeoxygenation. The γ -Al₂O₃ is a predominant support but also silica-alumina and zeolites can be used with aim to enhance rate of hydrocracking reactions. These catalysts are active in the sulfide state, being either pre-sulfided or sulfided on stream with a sulfur containing feed. The operating form contains the slabs of MoS₂, which distribution on the support depends on the Mo loading and sulfiding

temperature. The average pore size is generally between 75 and 300 Å, although a distribution of pore sizes is prevalent. As reported by Topsøe and Clausen (1984), by use of Mössbauer Emission Spectroscopy (MES) and Extended X-ray Absorption Fine Structure (EXAFS), into these slabs structure each molybdenum atom is surrounded with six sulfur atoms forming a trigonal prismatic structure.

In particular, as reported in the Fig. 2.9 drawn from Helveg et al. (2000) using the Scanning Tunneling Microscope (STM), MoS₂ nanostructure is a triangular cluster while the protrusions are arranged with hexagonal symmetry. This is a layered compound, consisting of stacks of S-Mo-S sandwiches held together by Van der Waals interactions. Each sandwich is composed by two hexagonal planes of S atoms and by an intermediate hexagonal plane of Mo atoms, trigonal prismatic coordinated to the S atoms.

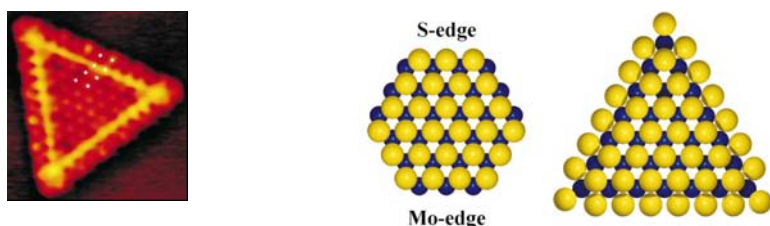


Fig.2. 9 MoS₂ nanostructure

When Co or Ni are added on the MoS₂ structure they do not affect the slab size, it does not appear to appreciably increase the vacancies number, but the vacancies associated with the Co or Ni are more active than those associated with the Mo, leading to the increased promotional activity of the catalyst.

Co or Ni can be present by different configurations:

1. Directly on the alumina like atom
2. Like Co₉S₈
3. Inside the sulfide of molybdenum like Co-Mo-S or Ni-Mo-S

but the last one is the more important phase, firstly because it has a similar structure with MoS₂ and then because it is the main structure to favorite the hydrodesulfurization reactions. In fact, the Co₉S₈ (Ni₃S₂) phase has bland promoting effect on these reactions while the sulfur atoms are present on the alumina surface in small quantities.

The distribution of these phases changes as a function of the Co/Mo (Ni/Mo) ratio for example, when the $\text{Co/Mo} \leq 1$ the Co-Mo-S (Ni-Mo-S) phase is the favorite one, otherwise it is replaced with the Co₉S₈ (Ni₃S₂) phase. That explains why usually the

used Co/Mo (Ni/Mo) ratio is chosen near to the unity to have the maximum reactions rate.

Cobalt or nickel atoms are dislocated on the MoS₂ surface at the edge sites of the slabs. Actually, the Co-Mo-S phase is not a single structure but a combination of different phases where cobalt (or at the same way nickel) changes the basic structure and modifies the electronic density of the slab.

As shown in the Fig.2.10 (Lauritsen et al., 2001, 2004), Co-Mo-S nanoclusters have a hexagonally truncated shape as opposed to the triangular shape of the MoS₂ nanoclusters observed previously. The hexagonal morphology is therefore attributed to the incorporation of cobalt in the MoS₂ structure.



Fig.2. 10 Co-Mo-S nanostructures

Finally, the alumina support is not very important to create the Co-Mo-S or Ni-Mo-S structure but it is very important for the morphology, consistence, stability and dispersion of the structure.

The chemical composition and the physical properties are not the only parameters that influence the catalyst activity. Another important property is the size of the catalyst particles. In fact, the choice of this parameter is related with the necessity to eliminate the diffusion problems. For large particles, a near center part may not be utilized during the reaction but too small particles can be disintegrated and they are not suitable for fixed bed reactors because of large pressure drops. It is very important to select a proper size and shape of particles because they are crucial for the performance of a fixed bed since the activity for catalysts that have the same chemical composition and structure depends on the size and shape of their particles. Typical particles shapes of industrial hydrotreating catalyst are shown in Fig.2.11

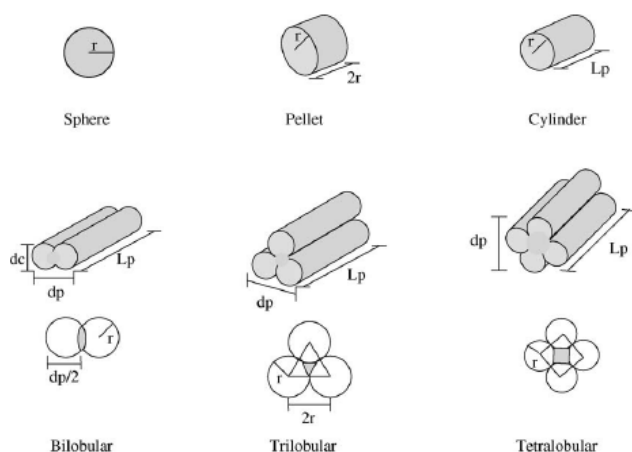


Fig.2. 11 Particle shapes of industrial hydrotreating catalysts. (Ancheyta et al., 2005)

Assuming the same total geometric volume of the 3-lobe commercial sample at equal L_p/d_p ratio of 2.25, the geometrical characteristics (L_p , d_p , r_c) of all shapes were calculated (Macías et al., 2004). It is observed that external area increases with the following trend and radius of cylinder behaves inversely:

$$S_p : \text{sphere} < \text{pellet} < \text{cylinder} < \text{2-lobe} < \text{3-lobe} < \text{4-lobe}$$

$$r_c : \text{4 lobe} < \text{3lobe} < \text{2-lobe} < \text{cylinder} < \text{pellet} < \text{sphere}$$

The lobe-shape particles have higher values of the L_p/d_{peq} ratio, since they exhibit lower d_{peq} .

To be used in the hydrotreating, catalysts are made active by the pre-sulfation procedure because the active phase is not made from oxides but metal sulfides. The presulfiding is realized in gas phase using a H_2/H_2S mixture containing 2-5%w of H_2S or in liquid phase using dimethyl disulfide. The maximum temperature of the procedure does not exceed the hydrotreating temperature. Before sulfiding, catalyst contains oxidized metals like MoO_3 or WO_3 ; NiO or CoO that become molybdenum or tungsten sulfide (MoS_2 or WS_2) characterized by tetravalence of the metal. Instead, nickel and cobalt can form different kinds of sulfides as a function of Ni/Mo and Co/Mo ratios as said before. The activation of the catalyst changes with regard to the catalyst and the producers.

The activation in the gas phase is suggested for some types of catalysts and it consists of:

1. Preliminary catalyst pre-wetting with gasoil which did not undergo cracking;
2. Hydrogen and hydrogen sulfide introduction (fixed flow and fixed time);
3. Activation lasting for some days;

4. Stabilization phase;

On the other hand, a typical activation procedure in liquid phase consists of:

1. Purification with nitrogen at room temperature;
2. Purification with hydrogen;
3. Soaking phase with gasoil and 2.5% of dimethyl disulfide without hydrogen and pressure and Liquid Hourly Space Velocity fixed in advanced;
4. Hydrogen introduction after some hours since soaking phase start;
5. Temperature increase until typical hydrotreating values;
6. Stabilization phase for some hours to complete the catalyst sulfiding;
7. Change of the operating conditions to reach again the initial conditions, paying attention to avoid loading the reactor with products obtained by cracking.

For each step, it is very important to preserve appropriate operating conditions to obtain a correct transformation of the active sites. For example, above 300°C it is opportune to change gradually the temperature to avoid thermal shocks that determine coke depositions and deactivation of the catalyst.

Anyway, even optimizing the operating conditions, during the hydrotreating, the catalyst deactivates through several mechanisms including coke deposition and poisoning with metals, therefore the structure of active sites, obtained during the activation, can change another time.

Usually the deactivation of the catalyst is a combination of coke and metals contribute because deactivation by metals always occurs simultaneously along with that by coke and their effects are related each other. In hydrotreating, catalysts show a fast deactivation during the first few days on stream, after which a long period of almost stable activity is attained. At the end of the run, which can be up to two years of operation, the activity drops again in a fast way and the catalyst needs to be regenerated (Furimsky and Massoth, 1999). The so-called start of run deactivation is due to a rapid initial coke deposition process and the adsorption of poisons from the feed. This process is mainly controlled by the type of the catalyst, the stability of the active sites or the acidity of the support, and by the feed composition. The second deactivation process is mainly due to the blocking of the pore structure by deposited metals and coke. The nature of the metals deposited depends on the origin of the feed, for example, typical poisons are metallic and organo-metallic species such as arsenic, lead, mercury, nickel, phosphorus, silicon, sodium and vanadium. Arsenic is a characteristic hydrotreating poison while V and Ni are the predominant metals for

heavy feeds. Deactivation by metals is irreversible and metal poisoned catalyst can be difficult to regenerate.

Poisoning typically occurs either by chemical destruction of active sites or by blocking access to active sites. The rate of metal deposition varies from metal to metal. For example, in the case of V and Ni, the initial deposition occurs at much higher rate for V than for Ni. This suggests that the formation of V deposits may have an adverse effect on the rate of Ni deposit formation. While the initial coke deposition is rapid before the pseudo-equilibrium level is reached, metal deposits continually increase with time.

The deactivation due to coke deposition is called fouling, its effect is to fill the catalytic pores, and it is the main cause of the initial pore volume loss. In this way, the catalytic hydrotreating can be influenced by restrictive diffusion inside the catalyst especially when the size of reactant molecules approaches the pore diameter.

There are two different kinds of fouling:

- Physical fouling
- Chemical fouling

Physical fouling occurs because of poisons present in the feed. A typical example is the particulate. A possible solution to avoid this poisoning is to insert a filter in the inlet of reactor to keep all kind of particulates in the feed.

Chemical fouling occurs because of the rubber and coke formation. Rubbers are obtained by polymerization of unsaturated molecules and usually they are formed upward the reactor inside the heat exchanger where high content of oxygen and olefins are present. Coke formation occurs in the reactor by condensation reactions of aromatics nucleuses. It is responsible of the catalyst deactivation and the filling of the pores but it can be limited processing the feeds in high partial pressure of hydrogen. Removal of coke is realized by two different kinds of regeneration processes where coke is removed by combustion to convert molybdenum and cobalt sulfides in oxides. This regeneration is not a complete process because the distribution of cobalt is not complete and the regenerated catalyst does not recover the same activity of the fresh catalyst.

2.5 Characteristic operating conditions

Three important operating conditions affect the hydrotreating performances, temperature, pressure and LHSV.

The parameter used to monitor the **temperature** is usually the Weighted Average Bed Temperature (*WABT*) that corresponds to the medium temperature between inlet

and outlet. It is used to simulate an industrial reactor, both with or without quench zones, using an isothermal pilot reactor. Stefanidis et al. (2005) indicate the most common definition of the $WABT$:

$$WABT = \frac{T_{in} + 2T_{out}}{3} \quad (2.6)$$

where T_{in} is the inlet temperature and T_{out} the outlet temperature. It describes the medium temperature inside a single catalytic bed. In cases of reactors with more than one bed in series, the $WABT$ is estimated by the following expression:

$$WABT = \frac{\sum_{i=1}^n WABT_i \cdot m_{cat,i}}{\sum_{i=1}^n m_{cat,i}} \quad (2.7)$$

where $WABT_i$ is the medium temperature for each catalytic bed and $m_{cat,i}$ its mass.

To hold the same conversion, despite of the progressive deactivation of the catalyst, usually the $WABT$ is gradually raised ($0.05^\circ\text{C}/\text{day}$) starting from an initial temperature called Start of Run (SOR) to compensate for the fall in activity due to coke deposits until the maximum permissible temperature (End of Run, EOR) when the catalyst life is over. The inlet temperatures of the catalytic beds should be continually monitored to avoid excessive temperature variations among the several reactor zones.

Although reactor **pressure** is a project variable and not an operating condition, it is a very important parameter in the hydrotreating plant and it should be kept at the design value. Decreasing pressure affects both the quality of the hydrotreated gasoil and the catalyst life. In fact, if the pressure is decreasing and the temperature holds the typical value of hydrotreating a formation of carbon residues occurs because of the condensation reactions of the aromatic nucleus. On the contrary, the coke formation is as much disadvantaged as the hydrogen partial pressure in the reactor is high. The hydrogen consumption depends on both the polyaromatic, sulfur and nitrogen concentrations in the feed and the operating condition in the catalytic reactor. Usually the operating conditions are chosen to minimize the coke formation keeping the high partial pressure in the reactor bottom.

The **LHSV**, defined as the ratio between volumetric flow rate and the catalyst volume in the reactor, represents a fundamental parameter to obtain the desired conversion inside the reactor. Defined the catalyst volume, the LHSV represents the inverse of the residence time of the mixture.

Small variation of LHSV can result in big variation of conversion, should the process being kinetically controlled or controlled by mass transfer.

Other parameters that can affect the hydrotreatment performances are:

- Furnace outlet temperature: its undesired fluctuations affect the temperature in catalytic bed;
- Recycled hydrogen concentration: it affects the activity of the catalyst and it should be kept at high values guaranteeing a long life of catalyst;
- Flow rate and quality of the aminic solution of the washing column
- Temperature of high pressure separator: it should have the value of 200°C such to have a correct balance between gas and liquid phases after the flash;
- Vapor flow and temperature in the stripping column: they should be such to guarantee the H₂S removal from the mixture, avoiding the vaporization of excessive quantity of the product.

2.6 Reactor fluidynamic

The typical reactor of hydrotreating plant is a trickle-bed reactor (TBR). The TBRs can be defined as a fixed bed of catalyst particles, contacted by a cocurrent downward gas-liquid carrying both reactants and products. When the gas and liquid are fed co-currently upward through the catalyst bed, the reactor is called upflow reactor or flooded-bed reactor (FBR). Upflow reactors are often preferred in laboratory studies since complete wetting can be achieved inside them (De Wind et al., 1988), while in trickle-beds an incomplete catalyst wetting has to be accounted for.

Depending on the manner in which the packings are introduced and the gas and liquid distributors are configured, four different flow regimes can be identified in the TBR:

- Trickling flow;
- Pulsing flow;
- Spray flow;
- Bubble flow.

Trickling flow regime appears at relatively low gas and liquid input flow rates. The liquid flows down the column from particle to particle on the packings surface and the gas phase moves in the void space of the flow channel. When the liquid flow rate is very low, a fraction of the packings could be dry but when the liquid rate increases

the partial wetting changes to complete wetting and the packings results in totally covered packings.

Pulsing flow occurs at relatively high gas and liquid flow rate. It is characterized by a formation of slugs that have a higher liquid content than the remainder of the bed.

Spray flow regime occurs when the gas flow rate is high while the liquid flow rate is low. The opposite pattern, observed when the gas flow rate is low and the liquid flow rate is high, is the **Bubble flow**. In this case, the bed is filled with liquid and the gas passes down the bed in the form of bubbles.

The flow maps that define the transitions between different regimes show that the bounds are not clear and they can change under different operating conditions during the experiments. It is even possible to have more than one flows regime in the same reactor when the operation condition are such to be very near the one transition between different regimes (Ng and Chu, 1987). For example, usually industrial processes are carried out in the trickling flow regime but considering a column operating near the trickling-pulsing transition, as the gas phase goes down through the column, its density decreases with decreasing pressure. Since the gas mass flow rate remains the same, the gas velocity increases causing pulsing flow in the bottom while maintaining trickling flow at the top.

Trickle-bed reactors have different advantages for which they are preferred on industrial scale plant (Gianetto and Specchia, 1992):

- Liquid flow approaches mainly piston flow leading to higher reaction conversions;
- Elimination of filtration of the dispersed catalyst;
- Low catalyst loss: important when costly catalysts are used;
- No moving parts;
- Possibility of operating at higher pressure and temperature;
- Larger reactor sizes;
- Lower investment and operating costs;
- Low liquid-solid volume ratio: less occurrence of homogeneous side reactions;
- Possibility of using, in the cocurrent configuration, high flow rate of the phases without flooding;
- Possibility of varying the liquid rate according to catalyst wetting, heat and mass transfer resistances.

The TBR results in an ideal plug-flow reactor when the axial dispersion is negligible allowing reaching the allowed conversion. In fact, because of the reactor big size, in particular the length, and the very small size of the catalyst particles compared to reactor size, the back mixing does not affect the reactor dynamic. Moreover, downward flows are much more widely used than upward flows, because they are characterized by small pressure drops (in upflow, instead, hydrostatic head of the liquid must be overcome) and are rather robust with respect to unit upset because of the reduced liquid hold-up, (Biardi and Baldi, 1999). However, always because of the reduced liquid hold-up, partial wetting of the catalyst is quite likely.

In fact, one of the disadvantages of the trickle-bed reactor is the incomplete and/or ineffective catalyst wetting with low liquid flow rates and reactor diameter/particle size ratio ($< 15-20$) that cause liquid maldistribution.

Three different kinds of liquid maldistribution are possible in the trickling regime:

- Poor liquid distributor design: Although more catalyst particles are wetted by the liquid phase, other pellets are not. Since gas and liquid reactants have to spread out within the catalyst pellets, without a good distribution of liquid phase the unwetted portion part is not used in the reaction.
- Anisotropic medium: the reason of the liquid maldistribution is related to the manner the catalyst is packed and the preferred orientation of the particles. In this case, a substantial fraction of the liquid can be channeled to some preferential pathways while some others remain unwetted.
- Vaporization: it is a typical form of liquid maldistribution in the reactors with high exothermic reactions. As the liquid film flows down the column from particle to particle, vaporization takes place because of the high temperature and particles near to the bottom could be dry.

The liquid maldistribution causes hot spots or even runaway if the heat produced inside the particles cannot be removed because of the lack of liquid, in fact another important disadvantage of the TBR is the difficulty in the recovery of the reaction heat. Moreover, if high exothermic reactions are present, a poor radial mixing and the high intra-particle resistance make the temperature control inside the reactor difficult.

Other typical TBRs disadvantages are:

- Lower catalyst effectiveness due to the large catalyst particle size;
- Limitations on the use of viscous or foaming liquids;

- Risk of increasing pressure drop or obstructing catalyst pores when side reactions lead to fouling products;
- Sensitivity to thermal effects, although this drawback can be limited by recycling part of the outlet liquid or injecting cooled gas.

Most commercial TBRs normally operate adiabatically at high temperatures and high pressures. Kinetics and/or thermodynamics of reactions conducted in TBRs require high temperatures, which in return increase gas expansion and impede the gaseous reactant from dissolving sufficiently into the liquid. Therefore, elevated pressures (up to 30 bar) are necessary to improve the gas solubility and the mass-and heat- transfer rates. Due to complexities associated with transport-kinetics coupling in TBRs, general scale-up and scale-down rules for the quantitative description of transport phenomena in TBRs working under realistic conditions remain elusive (Al-Dahhan et al., 1997).

Chapter 3

Pilot Unit



The study and the optimization of the hydroprocessing process has been carried out using a pilot unit, located in the “Saras Ricerche e Tecnologie” Company, able to simulate the typical industrial hydroprocessing unit. In this Chapter, this pilot scale plant will be described and it will be compared with the industrial scale plant to explain their similes and their differences and to understand how two plants so different for some important characteristics can be considered equivalent units.

Moreover, it will be shown a typical experimental test realized on the pilot unit to get confidence with the difficulties that an experimental section can present and how a correct test must be realized to obtain reliable results and which standard procedures it is necessary to apply to get the results reproducible.

3.1 Pilot unit description

Pilot unit consists of two units, which can work with two different configurations, series and parallel. Each unit results in a feed section followed by a reaction section, a separation section and finally a storage section for the hydrotreated products. One cooling system, fed by a chiller, serves both units.

Parallel and series configurations are different and substantially they represent one-stage and two-stage processes respectively. In the parallel configuration these units work in a totally independent way and for every reactor it is possible to choose the flow rates of gas and liquid, gaseous and liquid inlet feeds, up-flow or down-flow configuration, catalyst, pressure and temperature. On the other hand, in the series configuration, the same gaseous and liquid feeds go through both reactors therefore, they are characterized by the same flow-rate and the same pressure. Unlike, they can have, similarly to the parallel configuration, different kinds of catalyst, different configuration of the flows (down-flow or up-flow) and different temperature profiles.

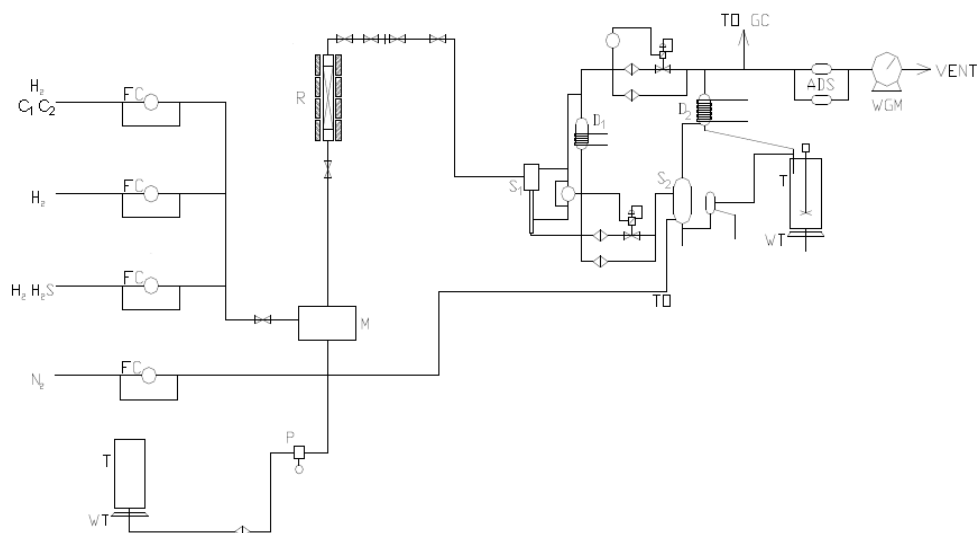


Fig.3. 1 Simplified scheme of hydrotreating pilot unit

Fig. 3.1 describes the simplified scheme of the pilot unit. The outgoing liquid feed, contained within the tank, T , is directed through the dosing pump, P , to the static mixer, M , where it is contacted with the high-hydrogen gas previously compressed. Biphasic mixture is directed to the reaction section where the reactor, R , can work in down-flow or up-flow configuration. Inside the reactor, the reaction occurs under typical hydrotreating operating conditions of temperature, pressure and LHSV and in

the presence of $\text{CoMo}/\text{Al}_2\text{O}_3$ or $\text{NiMo}/\text{Al}_2\text{O}_3$ catalyst as presented in this thesis. The resulting products are directed to the hot high-pressure separator S_1 where a first separation, between liquid and gas, occurs. Outgoing gas is fed to a cold high-pressure separator or demister D_1 where the condensation of liquid drops dragged by gas takes place. This condensed liquid is recombined with the bottom liquid from S_1 while the outgoing off-gas from D_1 goes through a pressure regulation valve, the wet gas meter and finally to the vent.

Instead, liquid exiting from S_1 enters the low-pressure nitrogen stripper S_2 where a nitrogen flow allows the removal of residual light ends, naphtha and H_2S . The bottom stream from the stripper, constituted by gasoil and vacuum gasoil, is finally stored inside the storage tank T , while the overhead goes to the demister D_2 where naphtha is condensed and sent to an appropriate storage tank while the stripping gas and light ends are vented.

A complete scheme of the hydrotreatment pilot unit is reported in the Fig.3.2 where the almost symmetric units are represented. In fact, going into details of explanation of the different sections in the total scheme it will be possible to elucidate that the two sections are the same apart for the differences in the feed storage tanks.

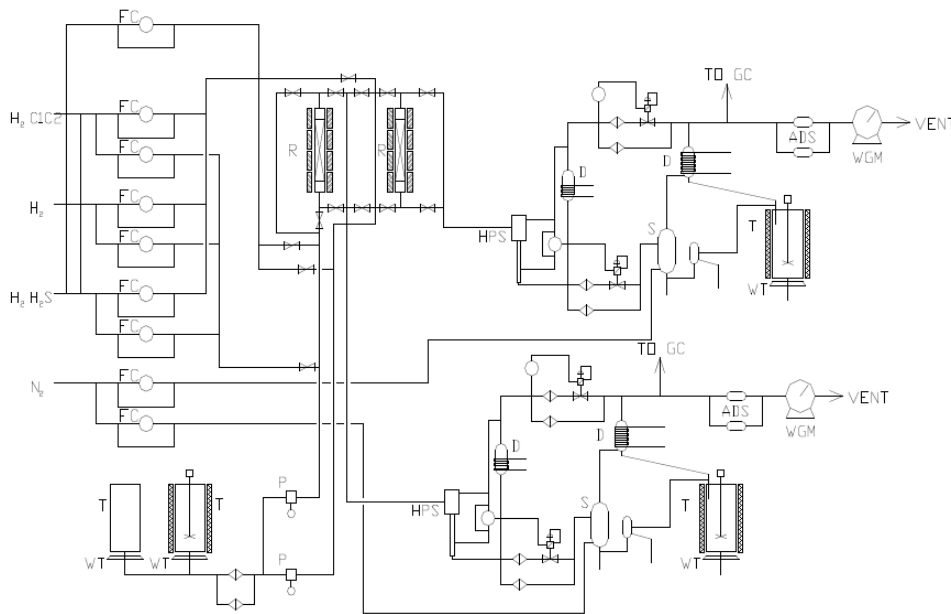


Fig.3. 2 Completed scheme of hydrotreating pilot unit

The different sections

- Gaseous feed section;
- Liquid feed section;
- Reaction section;

- High-pressure separation section;
- Stripping section;
- Treatment, recycle, discharge section
- Products storage section

will be present in detail in the following.

3.1.1 Gaseous feed section

Pilot unit has four different independent lines to feed gaseous phase. The first is the hydrogen line, the second one the H₂S line, the third and the fourth ones are the nitrogen and light ends lines respectively. Nitrogen is used to realize the stripping of the hydrotreated products, do the blanketing of the feed tanks in order to avoid the oxidation of the mixture because of the air and to improve the outflow of liquid directed to the pumps. Light ends may be sent to the reactor to better simulate the real feeds because containing C₁-C₃ components while H₂S may be used to study the inhibitive effect of this gas on the hydrotreatment reactions. Due to the corrosive character of the H₂S, its piping is made of oxidation-resistant materials. Usually the gases are accumulated inside the storage cylinder inside which the maximum pressure is 200 bar and from where they can be sent directly to the plant or subjected to the preliminary compression. In fact, usually they are sent to the compressor with a 25 bar pressure and then compressed to reach the operative pressure. Several manometers are dislocated to verify the internal pressure inside each cylinder and the pressure along the gas lines. The pilot unit is equipped with two *reciprocating compressors* able to increase the pressure until 220 bar. In the parallel configuration, the compressors work independently for each unit, and each reactor can be characterized by a different gas flow and pressure.

The inlet gas to the reactor is monitored by a series of valves and *mass flow controllers* that control the flow rate and verify the pressure of the gas introduced in the plant.

3.1.2 Liquid feed section

The liquid feed section is equipped with two different storage tanks (*T* in the Fig.3.2). One of them is insulated and can be stirred by hand. In fact, the pilot unit is able to simulate both the hydroprocessing of gasoil and the hydrocracking of heavy vacuum gasoil (HVGO). HVGO is nearly solid at ambient temperature, therefore it is necessary to warm up and to stir it to have a liquid mixture as high as possible homogeneous. The heating up is realized using electrical elements located on the walls of the storage tank. This problem does not exist when gasoil is fed to the plant because this feedstock is liquid and it does not give stratification problems being

already homogeneous enough. Therefore, it can be directly sent to the reactor without any stirring. A scale for each tank controls how much feed is contained inside the tank and a level indicator roughly verifies the residue quantity of liquid.

Before reaching the *positive displacement dosing pumps (P)*, the liquid phase goes through a *filter*. The sample points are dislocated up-ward and downward the filters and on the pressure side of the pumps. They are very useful because allow monitoring the obstruction of the filters and the correct work of the pumps. Liquid flow rate is manually modifiable changing the piston stroke or the piston frequency of the *reciprocating dosing pumps*.

3.1.3 Reaction section

The biphasic mixture can be fed to the reactor in up-flow or down-flow manner by the upward and downward valves to the reactor.

The reactor is 760 mm long and has a 19 mm diameter and it is filled with different layers. On the top, a layer of inert material and a glass wool sieve plate to ensure a good flow distribution are present. Moreover, the layer of inert material works to pre-heat the inlet cold mixture, in order to meet everywhere, inside the reaction section, the operative temperature. The catalyst bed is located in the middle part of the reactor to minimize border effects, provide a uniform distribution of the gas and liquid flows and facilitate the hydrogen saturation of the feed. Furthermore, the reaction section is loaded with hydroprocessing commercial catalysts (NiMo/Al₂O₃ or CoMo/Al₂O₃, DN= 1.3 mm) diluted with small inert particles (1:1(v/v) CSi 0.1 mm) to avoid channeling and minimize back mixing. On the bottom, a layer of inert material and a glass wool sieve plate are present mainly to limit the pressure drops due to the catalytic bed.

Further to improve the flow distribution inside the reactor, the catalytic bed is sometimes divided in two or more beds whose number depends on catalyst volume necessary to realize the experimental test. The flow distribution is improved spacing out every pair of beds with a narrow layer of glass wool (5÷10 mm) that carries out the same rule of the flow distributor for the industrial plant. For the same reason, a narrow glass wool layer is located on the top of the first inert material layer as well.

To avoid the drag of the particles because of the liquid exiting from the reactor, the last part of the catalytic bed is equipped with another glass wool layer followed by a grid.

A sketchy representation of the reactor is presented in the Fig.3.3:

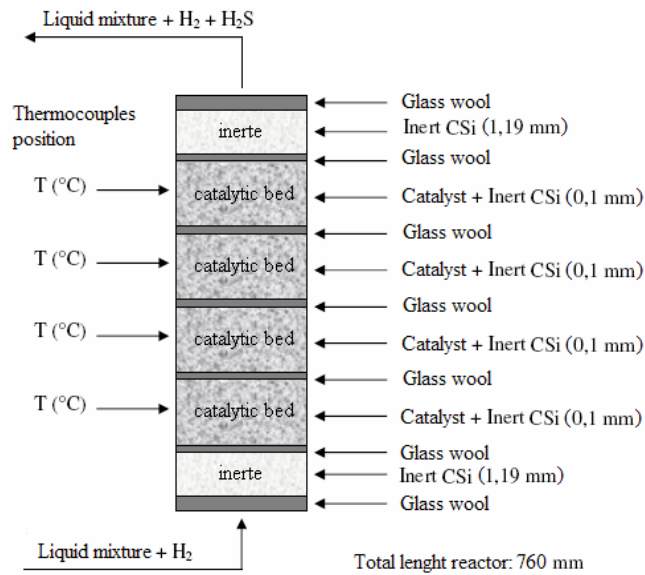


Fig.3. 3 Example of loading scheme for a hydroprocessing reactor

Regarding the thermal profile, the reactor temperature, controlled by four independently heated furnaces, is monitored with a set of four sensors placed in a thermowell located along the axis of the catalytic bed and another set of skin thermocouples (Fig.3.4).

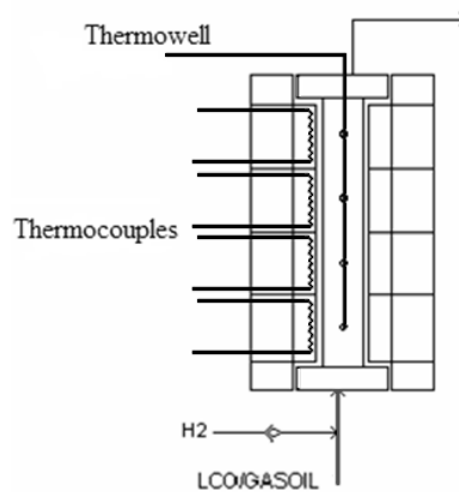


Fig.3. 4 Thermowell and thermocouples location inside the pilot unit reactor

Usually, hydroprocessing reactions produce heat causing an increase of temperature of 3-6°C while the cold inlet feed decreases the temperature only some degrees. With respect to these variations, the manual regulation of set point of the external temperature allows to establish an isothermal profile along the reactor.

The values of internal and external temperatures are reported on the control panel of the pilot unit software. The differences between internal and external temperatures are related to the heat produced during the hydroprocessing reactions. Three different zones can be identified inside the reactor: an *inlet zone*, which is conditioned by the cold feed entering in the reactor, a *reaction zone*, which is the most affected by the heat of the exothermic reactions and an *outlet zone* where the reactions are feeble and the heat produced is lower.

If the reactors work by the series configuration – two-stage gasoil hydroprocessing or heavy gasoil hydrocracking– the outlet mixture from the first reactor goes through the second one to achieve the desired conversion.

3.1.4 High-pressure separation section

As shown in the Fig.3.1, the pilot unit has two separation sections that are used in different ways depending on which reactors configuration is used, series or parallel configuration. When the series configuration is chosen, only one high-pressure separation section is used, on the other hand the parallel configuration needs both sections, one for each reactor. Fig.3.2 shows that the high-pressure separator (HPS) is a tower with a variable diameter, the larger one on the top (internal diameter equal to 73 mm) where the mixture flash occurs followed by a liquid-gas separation and the smaller one on the bottom (internal diameter equal to 21 mm) where the liquid flows out. The liquid level in the bottom is set by the control system used to run the plant. The tuning occurs by a differential pressure transmitter and a PID controller (Proportional Integral Derivative controller), that acts on the opening of a particular valve (called Kammer valve) which is suitable to work at high temperature and pressure. The minimum and the maximum levels are set by a calibration procedure that precedes the pilot unit start-up. It is also possible to manually change the level operating the valves located downward the separator. Even the operative pressure of the separator is adjustable in automatic or manually. Using the automatic mode, pressure is regulated acting on the opening of the control valve present in the gas line after the high-pressure separator. A PID controller measures the pressure and acts the trim of the valve as a function of the difference between the pressure set point and the measured pressure. When problems arise on the control valves or with the differential pressure transmitter, it is possible to change the pressure manually acting on the valves located on the gas and liquid lines downward the separator.

3.1.5 Stripping section

The liquid from the hot high-pressure separator goes through the stripping column that works at a low level of temperature and pressure. Inside the stripper, H_2S and NH_3 are stripped by a countercurrent nitrogen flow; the gas-liquid contact is

improved introducing a metallic grid. Sample points to analyze products are available on the stripper and on the storage tank bottom.

3.1.6 Treatment, recycle and discharge section

The outgoing gases from high-pressure separator and stripper are directed to the adsorption columns where the removal of H_2S occurs. It is also possible to recycle a fraction of the outgoing gases to the liquid fresh feed before the inlet inside the reactor. In this case, it is necessary to channel the gas from the demister D and the separator S to a compressor because the recycled gas pressure must be the same of the fresh gas one.

3.1.7 Product storage section

The storage tanks are insulated (as shown in the Fig.3.2) and equipped with a scale. The product can be heated by an electrical resistance located on the walls of the storage tank that are controlled through the control system. This control system allows monitoring and visualizing of the tanks temperature.

3.2 Pilot unit fluid dynamic

The description of the pilot unit showed that the reactors of the unit are able to work both with the down-flow and up-flow configuration but, as stated in the Paragraph 2.6 with regard to the industrial unit description, up-flow reactors are often preferred in laboratory scale while the trickle-beds are the most common reactors in industrial scale.

One of the main motivations is the incomplete and/or ineffective catalyst wetting if the liquid flow-rates are low and the ratio between reactor diameter and particle size is lesser than 15-20. In fact, all the parts of the catalyst bed are theoretically taking part to obtain the overall conversion because a flowing liquid film surrounds each particle while gas passes through the remaining void space. However, particularly at low velocities, liquid can flow through the bed while gas flows through another part. That means only a fraction of catalyst particles is contacted by liquid and it contributes to the overall conversion. But, the complete wetting is only a necessary condition and not a sufficient one because, even when the catalyst is totally surrounded by the liquid, if part of it is not enough refreshed, part of the catalyst particles may not be used during the reaction.

Moreover, the problem is further worse because in laboratory scale the reactor diameter is so small that it is impossible to introduce a distributor plate like in the industrial reactor. The main consequence is the lower catalyst effectiveness whose

remedy is to change the flow direction; consequently, working using a flooded bed reactor is preferable since the effectiveness of the catalyst wetting is 100%.

Although the up-flow reactor implies higher pressure drops, it has other advantages compared to the down-flow reactor like a higher liquid holdup and better heat transfer performances. They result in a higher efficiency and lifetime of the catalyst. Anyway, the up-flow system, that requires higher energetic consumption, is considered very less extensively and data about this kind of reactor fluid dynamics are limited.

As previously reported, valid motivations exist about why simulating a trickle bed industrial plant using a flooded bed pilot unit instead of a trickle bed one would be preferred. At this point, it is really required to underline that the two units are the same by a fluid dynamic point of view only when both act as ideal plug flow reactors (PFR). This assumption is certainly true in term of the industrial reactor in which the Peclet numbers have always values high enough to guarantee that the axial dispersion effect is negligible. Consequently, the problem exists especially in term of pilot unit in fact, because of the reduced dimensions and especially the limited lengths, the Peclet numbers have magnitude not so high to make the back mixing negligible (cf. Paragraph 5.1.1).

3.3 Experimental test on the pilot unit

The explanation concerning the carrying out of one experimental test on pilot unit is useful to get confidence with the experimental data that represent the input for the model. In fact, it is important to know which difficulties could be present during the experimental test and how an uncorrected realization of the test can affect the quality of the results.

For this reason, the proper test is preceded by a fundamental scheduling phase that includes:

- Choose the feed to process in the pilot unit;
- Verify the feed properties (density, sulfur, nitrogen and aromatic contents, distillation curve);
- Choose the kind of catalyst and evaluate the quantity of it and the inert material to load in the reactor;
- Establish the loading scheme;
- Choose the procedure to activate the catalyst;
- Select the flows configuration (up-flow or down-flow; series or parallel);
- Define the sequence of the different runs, establish the time dedicated to each run, the frequency of sampling and analysis.

When the experimental tests are planned, the loading of the catalyst is ready to be realized. This is a very critical and delicate phase to guarantee a good uniformity of the catalyst in the beds and a good positioning of different layers (inert material, catalyst + inert, glass wool) respect to the thermocouples locating as well. In fact, a correct location of the reactive zones respect to the temperature measurement points better allows monitoring how the reaction is going on related to the differences of temperature existing between the values measured from the internal and external thermocouples.

When the quantity of catalyst has been chosen, it is diluted with fine inert material like carborundum with 0.1 mm diameter, usually using a volumetric ratio between catalyst and inert equal to 1:1. The loading of the catalyst is realized considering the number of active zones chosen in the scheduling phase because the catalyst-inert phase is equitable shared out in all of them. The total reactor volume, considering the volume of the thermowell located along the center of the catalytic bed, is hence known and it is possible to evaluate which fraction of this volume is assigned to the location of the glass wool. The residual volume without catalyst, glass wool and the thermowell is filled up with two layers of inert material; often it is carborundum with size greater than those one used to realize the dilution of catalyst (1.19 mm Ø). After catalyst is loaded, the reactor is connected to the feed lines with flanges. All valves are positioned according the flows configuration (up-flow or down-flow) and the series or parallel scheme selected during the scheduling step. The liquid mixture is loaded into the storage tanks and the cylinders are connected to the gas feeding ramps. Hence, plant and compressors start up is realized. During this phase, different parameters must be monitored. For example, the pressure in the cylinders, the pressure of the compressed air for valves and compressors, the level of the oil into the compressors and pumps, the water level in the *gas flow meter*, in the *chiller* and in the *cooling-tower*.

Before carrying out experiments, it is necessary to realize the leak test verifying the tightness of all the connections of the plant due to the reactors introduction, disassembly and cleaning. The leak test consists into introducing inside the pilot plant a flow of nitrogen exceeding the maximum operating pressure that will be used during the experiments. Usually the connection tightness is verified up to pressures 20-30% exceeding the maximum operative pressure allowed for the experimental tests.

Therefore, a 15 bar/h pressure ramp is planned until the maximum pressure is reached. Then, stopping gaseous feed by contemporary closing the upwards and downwards valves, the system is kept at such pressure for 2 hours. If any loss exists, a pressure drop is measured from the several manometers located in the different part of the system. Maximum admissible value of pressure loss is 0.1 bar/h; if

greater losses are present, it is necessary to localize them using soaped water and depressurizing the system to restore the tightness. When the losses are removed, the leak test is repeated again.

Once verified the absence of leaks from the unit, the catalytic system is activated through liquid presulfiding. The activation of the catalyst changes with regard to the catalyst and the producers but as reported in the Paragraph 2.4 usually the presulfiding is realized using a H_2/H_2S mixture in gas phase or dimethyldisulfide in liquid phase. The oxidized metals become molybdenum or tungsten sulfide characterized by tetra-valence of the metal. Instead, nickel and cobalt can form different kinds of sulfides as a function of Ni/Mo and Co/Mo ratios. The activation phase is always followed by a stabilization phase that depends on the catalyst properties (usually 5 days with gasoil). In fact, the activity and selectivity of a catalyst change during the initial period on stream due to the formation of coke deposits on its surface. After this period, the activity and selectivity remain constant over a long period. During the stabilization phase, gasoils coming from cracking plants are not used in order to avoid the further formation of coke. The operating conditions used during the stabilization phase are almost the same as during the first experiment that will be realized in the pilot unit. When the stabilization phase is complete, the experiments can be carried out. Each experiment has a different time length, depending on how much time is needed to achieve the steady state of the system when a generic operating condition changes. For example, the parameters that usually are changed during the experimental campaign are temperature, pressure, LHSV and quality of the feed. The length of the transitory depends on which of these operating parameters are changed. The unsteady-state due to the change of temperature goes on for few minutes while a variation of pressure needs a longer time to meet the steady state (few hours).

Along each test, achievement of steady state is verified when product characteristics remain constant. Considering the properties of the liquid product, its most representative property is the distillation curve as density is affected by the possible losses of light products, sulfur by the possible presence of H_2S and aromatics are not very sensitive. Anyway, also many other characteristics, such as off-gas flow rate and composition, sulfur level and operating condition concur to the detection of steady state achievement.

It is recommendable to conclude each group of experiments by a repeatability test. This test proposes again the same operating conditions of the first test (directly after the stabilization phase). Unless considerable deactivation of the catalyst occurs, the results of these tests should be comparable. In case they should not be that, the detection of the possible causes (such as sharp temperature variations and consequent coke formation) and the verification of the tests reliability are needed.

Therefore, samples concerning both feed and hydrotreated product are taken and characterized in terms of density, distillation curve, and sulfur, nitrogen and aromatic content to monitor the performances of the system

All through the working of the pilot unit, the main operating parameters are automatically recorded by the process software. Such parameters are pressures and temperatures of the reactors, temperature of the storage tanks and weight of liquid into each storage tank, gas flow-rate and liquid level into the high-pressure separators. Instead, other parameters are only visualized with the analogue indicators and they must be manually recorded at the beginning of the test in case they change significantly.

During the standard running, the plant can work also without any external assistance but a frequent monitoring of the several parameters allows to opportunely verify working anomalies and to attend on the plant without compromising the experiments results.

Day by day, it is opportune to verify the overall mass balance closure

$$\Delta\% = \frac{\left(W_{in} + Q_{in} \cdot \frac{MW_{H_2}}{N} \right) - \left(W_{out} + Q_{out} \cdot \sum \frac{C_i \cdot MW_i}{N} \right)}{\left(W_{in} + Q_{in} \cdot \frac{MW_{H_2}}{N} \right)} \cdot 100 \quad (3.1)$$

where W_{in} and W_{out} are the inlet and outlet hydrocarbons mass flow rates, Q_{in} and Q_{out} are the volumetric flow rates for treat and off-gas expressed in NI/h, N is the molar volume of ideal gases (22.4 NI/mol), C_i are the molar fractions determined in the offgas and MW_i are the corresponding molecular weights. W_{in} is evaluated averaging the mass difference registered on tank T_1 during 24 hours while for W_{out} is the weight average during 3 to 6 hours of the mass of the product. The value for Q_{in} is based on the set point of the gas flow meter while Q_{out} derives from 4 hours average of the determination of the offgas flow rate through the wet gas meter located before the vent.

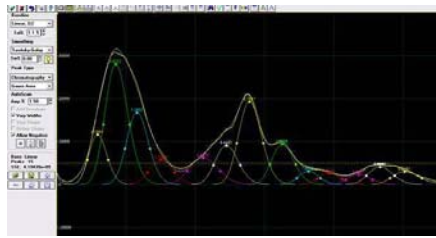
Development of the phenomenological model



In the preceding Chapters, both hydrotreating industrial plant and pilot unit have been described. In fact, a detailed analysis is needed to develop a phenomenological model, based on the constitutive equations and able to simulate such different systems. The final goal is to realize a model to optimize the running of the industrial plant in each situation for all feeds, catalysts, temperature, pressure and LHSV in order to guarantee the full respect of both diesel demand and environmental specifications. This goal can be met by simulation of the pilot unit, developing a model able to totally describe this system but not so much rigorous to introduce an excessive computational complexity.

Chapter 4

Feedstock and product characterization



The phenomenological model development needs a deep knowledge of the real processes and a detailed characterization of the feedstock and products.

Therefore, starting from the state of art concerning the models of hydrotreating, a simplified, but enough detailed, description of a complex mixture, like gasoil, and the definition of a limited number of macro-classes describing the different kinetic behaviors of the hundreds of gasoil compounds has been realized.

4.1. State of art

The objective to realize a model able to completely describe the hydroprocessing process and at the same time enough simple to be solvable without too many computational problems clashes with the complexity of gasoil and the impossibility to describe the kinetic behaviors of all aromatic compounds of such mixture. Each group of authors who have studied the hydroprocessing process met this clash and tried to solve it using different approaches. Some of them have concentrated on the study of single compounds, someone else on the identification of macro-classes characterized by a molecular structure and others on the definition of reactivity classes including compounds with the same kinetic behavior.

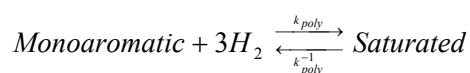
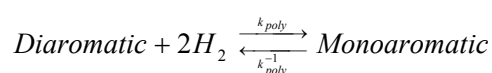
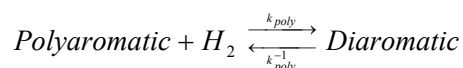
Many authors have devoted themselves on the first kind of approach. For example, Toppinen et al. (1996a, 1996b) have studied the hydrogenation of mono- di and tri-substituted alkylbenzenes while Rautanen et al. (2000, 2001 and 2002) have concentrated on liquid-phase hydrogenation of toluene, naphthalene and tetralin. These studies are undoubtedly important to know the kinetic behavior of several compounds characterized by a different number of aromatic rings but they are not very flexible. In fact, it becomes very complicated to use them for a mixture like gasoil because in this case they should be applied on all aromatics compounds giving an enormous matrix of components unmanageable both in term of mathematical solution and in term of compounds analysis. Moreover, they cannot describe the real behavior of gasoil because they do not consider the competition effects of the different compounds into the mixture. In fact, due to the adsorption on the same catalyst surface, compounds must compete to occupy the active sites while, considering the components one by one, no model can simulate this simultaneous adsorption. Some competition effects can be identified studying at least two components as made by Rautanen (2002), Rautanen et al. (2002) and Lylynkagas et al. (2002) on mixtures of naphthalene, tetralin and toluene. These works show that, while naphthalene inhibits the hydrogenation of toluene and tetralin, they have no effect on the hydrogenation of naphthalene. This is because of the different strength and different adsorption mode that decreases in the following order: naphthalene > tetralin > toluene.

Toppinen et al. (1997) have also studied several binary mixtures, like mixtures of alkylbenzenes, founding that the aromatic compounds react in queues so that the most reactive components start to react immediately while the least reactive components do not practically react until the most reactive components had been completely hydrogenated. This type of reactivity decreases with the increasing number of substituents in the order monosubstituted > disubstituted > trisubstituted.

The relative positions of the substituents affect the reaction rate so that the reactivity decreases in the order ortho > para > meta. These papers give important information, but only as partial description of the competition effect because only few interactions are studied. In fact, the overall situation could be different analyzing very complex mixtures.

Chu and Wang (1982) have developed some more complex models, where they describe industrial feeds containing more than two components. In this case, the kinetics of hydrogenation, hydrodesulfurization and hydrodenitrogenation of polyaromatic compounds are studied simultaneously using the pseudo-first-order rate constants. The relative reactivity has been defined, but little information has been provided in terms of the reciprocal inhibitive effect that can cause an error in the estimation of the aromatic, sulfur and nitrogen compounds of the hydrotreated product.

Anyway, this work represents the first real approach that considers a different kinetic behavior in relation with the molecular structure. A similar approach is proposed in the Choudhury et al. (2002) paper, where different kinetics is related to monoaromatic, diaromatic and triaromatic classes. This is a very important model because the hydrogenation and hydrodesulfurization kinetics are simultaneously described considering a complex real feed like gasoil, a trickle-bed reactor rather than the usual batch system and a real commercial NiMo/Al₂O₃ catalyst. The advantage for this model is the possibility to use the recent analysis methods able to characterize the oil mixture in terms of mono-, di- and polyaromatics, total sulfur content and total nitrogen content because the maximum level of detail it considers is that of macro-classes. In fact, the conversion of aromatics compounds is represented as hydrogenation reaction of each macro-class distinct by a different number of aromatic rings:



Instead, the hydrodesulfurization is represented using only one class to describe the conversion of total sulfur content. Finally, the work does not consider any hydrodenitrification reaction and any nitrogen inhibitive effect.

The results of this work demonstrate that the macro-classes approach is not completely adequate to correctly describe the distribution of hydrotreated products

because the estimation of kinetic parameters is strictly correlated to the feed composition and the polyaromatic content is overestimated. This is due to the existence of different kinetic behaviors inside each molecular class characterized by the same number of aromatic rings that this model cannot represent. For example, biphenyls and naphthalenes into the diaromatic class, or tetralins and cyclohexylbenzenes into the monoaromatic class have different kinetic constants of hydrogenation and dehydrogenation because their reactivity depends on their different condensation level. Moreover, not all aromatic compounds (like alkylbenzenes) are characterized by an equilibrium reaction because some of them present an irreversible kinetics. That causes an over evaluation of the total polyaromatics content because the model consider a limitation of the conversion of these compounds because of the equilibrium. Therefore, such approach does not have all the means to describe the distribution of the components in the hydrotreated products correctly.

This is the main limitation of these methods, because only resorting to a detailed characterization of the feeds the hydrotreating process can be described for all the situations and the environmental regulations can be satisfied.

For this reason, the recent works concentrated on other kinds of methods able to describe the feeds rigorously and to correlate the chemical-physical properties with the reactivity of the components. Most of these methods identify into the complex feedstock a definite number of pseudo-components characterized in terms of average chemical-physical properties of wide boiling fractions. However, they often fail if applied on the hydroprocessing because include into the same class components that have the same properties but different reactivity. Therefore, they are not completely able to describe how the composition of each class changes because they mask the true kinetics and do not describe the real conversion. Quann and Jaffe (1992) developed another method that tries to meet a rigorous description of the feedstock. They realized a method called Structure-Oriented Lumping (SOL) for composition, reactions and properties describing of complex hydrocarbon mixtures. The basic concept of the SOL method is that the hydrocarbon molecules can be described as a vector, with the elements representing structural features sufficient to describe any molecule. This is also a lumped approach but with a major level of detail, considering it describes the molecular structure. The vector is represented as an established sequence of different structural groups and each component is built as a sequence of numbers pointing out the number of each structure. Different molecules can include the same set of structural groups and they are described by the same vector. The structure vector provides a framework to enable rule-based generation of reaction networks and rate equations involving thousands of components and reactions. Since, the SOL provides a foundation for developing molecular

properties- kinetic behavior relationships using different approaches like groups contribution. Anyway, this method has some important disadvantages like the difficulties of determining the chemical reactions pathways (especially in hydrocarbons catalysis where a single molecule can react via parallel pathways) or the kinetic parameters in large sets of molecules.

Another important lumping approach, although applied only on the hydrodesulfurization of alkyl-substituted dibenzothiophenes, has been developed by Froment et al. (1994) to reduce the high number of parameters obtained by the molecular approach using a structural contribution approach instead. The objective is to relate, whenever possible, the reactions involving substituted components to those of non-substituted in terms of the influence of the substituents on the adsorption equilibrium constants and the rate coefficients.

Korre et al. (1994, 1995) have proposed an interesting method to find quantitative structure/reactivity correlations considering that it is reasonable to suggest that the magnitude of the associated reactivity parameters can be defined by structural characteristics. In this case, the method goes beyond the molecular structure integrating it with some information upon the reactivity of the components. In terms of structural arrangement, gasoils are very complex. This complexity is reduced into several classes of compounds undergoing the same reaction, but the reactivity varies with the substituents that affect the electronic character of the group in the Hammett paradigm sense. The identification of these different families issues from a consistent database of reaction pathways, kinetics and mechanisms for catalytic hydrogenation of hydrocarbon compounds with different numbers of aromatic rings. The Langmuir-Hinshelwood-Hougen-Watson (LHHW), describes the reaction networks of these compounds.

The examination of reaction networks of all components reveals the following qualitative trends:

1. The hydrogenation of hydrocarbons proceeded in a ring-by-ring manner;
2. No partially hydrogenated compounds were detected;
3. Hydrogenation reactivity increased with the number of aromatic rings;
 - i. The hydrogenation of isolated single-aromatic-ring group was the slowest;
 - ii. Isolated two-ring-aromatics are intermediate;
 - iii. The hydrogenation of the middle-of-three fused-aromatic rings was fastest;
4. The hydrogenation reactivity depends on the level of condensation;
5. For groups with the same number of fused aromatic rings, hydrogenation reactivity increased with the presence of alkyl substituents and/or naphthenic rings;

6. For molecules with one and two aromatic rings, hydrogenation of the ring located at the end of the molecule was faster than hydrogenation of the ring in the middle.
7. For molecules with three and four aromatic rings, hydrogenation of the ring located at the end of the molecule was lowest than hydrogenation of the ring in the middle.

Based on that presented above, three different saturation categories are identified.

1. The first category, single aromatic ring hydrogenation, was termed **benzenic** hydrogenation (six hydrogen atoms added).
2. Hydrogenation of one out of two fused aromatic rings was the **naphthalenic** hydrogenation class, where four hydrogen atoms were added. Saturation of the terminal of three- or four-fused aromatic ring compounds has also been included in this group.
3. The unique hydrogenation of an aromatic ring fused between aromatic rings defines the **phenanthrenic** hydrogenation category, where two hydrogen atoms are added.

4.2. Definition of the aromatic, sulfur and nitrogen compounds

In the perspective of the development of a phenomenological mathematical model, a poor characterization of feeds and products is inadequate and it is needed to resort to a combination of several experimental methodologies in order to simplify the complexity of a cut like diesel oil.

The important point that emerges from the discussion of the previous Paragraph is that all papers in the literature have primarily studied the hydrogenation and hydrodesulfurization reactions. Therefore, starting from the state of art concerning these reactions, initially the speciation of the aromatic and sulfur compounds will be presented and afterwards the identification of the nitrogen compounds. A separate space will be dedicated to the description of components that take part in the reaction cracking. In fact, they are still the same kind of species identified to describe the previous reactions but the higher level of required detail needs the description of the distribution of the compounds as a function of the alkyl chains length.

4.2.1 Aromatics speciation

Firstly, in this work it has been developed an approach like that presented by Korre et al. (1995) about the classification of aromatic and sulfur compounds to approximate the feeds to the hydroprocessing since a set of molecular classes called lumps and characterized by a definite kinetic behavior has been fixed.

These molecular classes are identified considering some important hypotheses.

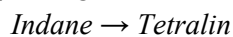
Typically, gasoils are characterized by a boiling point distribution comprised between 230 and 365 °C. Such a boiling curve is compatible with molecular structures with no more than three rings, either aromatic or naphthenic. Instead, in case of vacuum gasoils, structures with four or five aromatic rings are present as well because of the higher range of boiling point. Anyway, the same lumps represent both cases because polycyclic compounds with more than three aromatic rings in the vacuum gasoil are conflated with the corresponding triaromatic structures of gasoil. According to Girgis and Gates (1991), substituents attached to the aromatic structures do not appreciably affect the rate of hydrogenation/ dehydrogenation. Therefore, molecules with identical cyclic structures are included into the same lump.

Finally, according to Korre et al. (1995) and Korre and Klein (1996), for molecules with the same number of aromatic rings the reactivity depends on the number and condensation level of the naphthenic rings attached to the aromatic structure. For this reason, although biphenyls and naphthalenes have both two aromatic rings, they have different reactivity and belong to different lumps. A similar situation exists also inside the triaromatic class but in this case, the different reactivities are neglected. In fact, anthracenes and phenathrenes are considered as the same compounds accepting the error induced by the fact that these molecules have a different level of condensation. Anyway, they are separated from phenylnaphthalenes because these triaromatic structures are included into the diaromatic macro-class.

Moreover, the presence of condensed structures promotes the dehydrogenation reaction, which explains why, in the monoaromatic class, the alkyltetralins undergo dehydrogenation and alkylbenzenes do not. Therefore, they cannot belong to a single molecular lump. Instead, taking the negligibility of the dehydrogenation reaction for the cyclohexylbenzenes, cyclohexyltetralins and phenyldecalines, they can be grouped into a same molecular lump.

Furthermore, within the diaromatic class, the presence of cyclohexylnaphthalene is neglected since this species is typically not present in relevant amounts and hydrogenation of phenylnaphthalene preferentially produces phenyltetralins. Finally, saturates compounds behave as inerts, at least in the explored range of operating conditions and they are considered as a single lump. In fact, the only monoaromatics that can produce them are octahydroanthracenes/phenathrenes and tetralins because the hydrogenation of the others monoaromatic compounds is considered negligible in all operating conditions. For some operating conditions and some catalysts, the constant content of aromatic compounds is observed and in these cases, no hydrogenation of all monoaromatic compounds is considered.

Such hypotheses define a complete scheme of molecular lumps to guarantee a correct description of the hydrogenation but it is still too complicated to characterize feeds and products and to estimate the high number of parameters in the model calibration. Therefore, some other hypotheses are added to simplify further the lumps definition. Firstly, all structures with five member aromatic rings are included in the same lump of their corresponding structures with six member aromatic rings:



This hypothesis does not introduce a large error because the structures with five member aromatic rings are present in very small quantities and they do not affect the quality of results. This is very advantageous because the current experimental methodology cannot distinguish them because they elute at the same time of the corresponding structures with six member aromatic rings.

The second hypothesis is to neglect the partial hydrogenation of the aromatic compounds, for example, dihydrophenanthrene and dihydrophenylnaphthalene. It is justified because any partial hydrogenated product has been observed into the product. In fact, this kind of molecules are instable being characterized by an extremely high reactivity, so they behave like reaction intermediates reacting immediately after they are obtained from the polyaromatic compounds hydrogenation .

The hypotheses reported above suggest which kind of compounds is necessary to consider and which one is possible to neglect without introducing large errors in the feed characterization and to define their reactivity as a function of their structural properties.

In terms of feed characterization, it is clear that this approach requires a level of detail that the recent analysis methods are not able to provide because they can only define the oil mixture in terms of mono-, di- and polyaromatics, total sulfur content and total nitrogen content. For this reason the experimental work, realized with the High Performance Liquid Chromatography (HPLC), is supported by an analytical methodology. The procedure, which closer examination is described in the Appendix, is developed by the SARTEC staff and is able to draw the identification and the concentrations of the subclasses of triaromatic, diaromatic, monoaromatic and saturate compounds (Sassu et al., 2003).

The list of the compounds found by the combination of the experimental analysis and the analytical methodology and their reactivity classes are reported in Table 4.1.

		Number of non- condensed aromatic rings	Number of condensed aromatic ring	Number of non- condensed naphthenic rings	Number of condensed naphthenic rings	Reactivity class
MONO	Alkylbenzene	1	0	0	0	I
	Cyclohexylbenzene	1	0	1	0	I
	Cyclohexyltetralin	1	0	1	1	I
	Tetralin	0	1	0	1	I
	Octahydro- anthracene/phenanthrene	0	1	0	2	I
	Phenyldecaline	1	0	0	2	I
DI	Tetrahydro- anthracene/phenanthrene	0	2	0	1	II
	Cyclohexylnaphthalene	0	2	1	0	II
	Naphthalene	0	2	0	0	II
	Biphenyl	2	0	0	0	I
	Phenyltetralin	2	0	0	1	I
TRI	Anthracene/phenanthrene	0	3	0	0	III
	Phenylnaphthalene	1	2	0	0	II

Table 4.1 Class of reactivity of the aromatic compounds

The table shows that the classification of the gasoil compounds based on the number of aromatic compounds does not coincide with the classification based on the reactivity class. This is justified considering that when the aromatic rings are phenyl-substituents, they do not affect the hydrogenation while the reactivity class of the molecule is the same of the corresponding molecule with the same number of condensed aromatic rings without any phenyl group (for example: phenylnaphthalene). Moreover, compounds with the same number of aromatic rings but a different number and position (condensed and non-condensed) of naphthenic groups have the same behavior because they do not affect the reactivity on the aromatic compounds.

By combination of the information coming from the number of aromatic rings and the class of reactivity, it is possible to draw the scheme reported in the Fig.4.1. As

shown later on, the compounds reported in such scheme will be used as key component to identify the different reactions for each molecular lump.

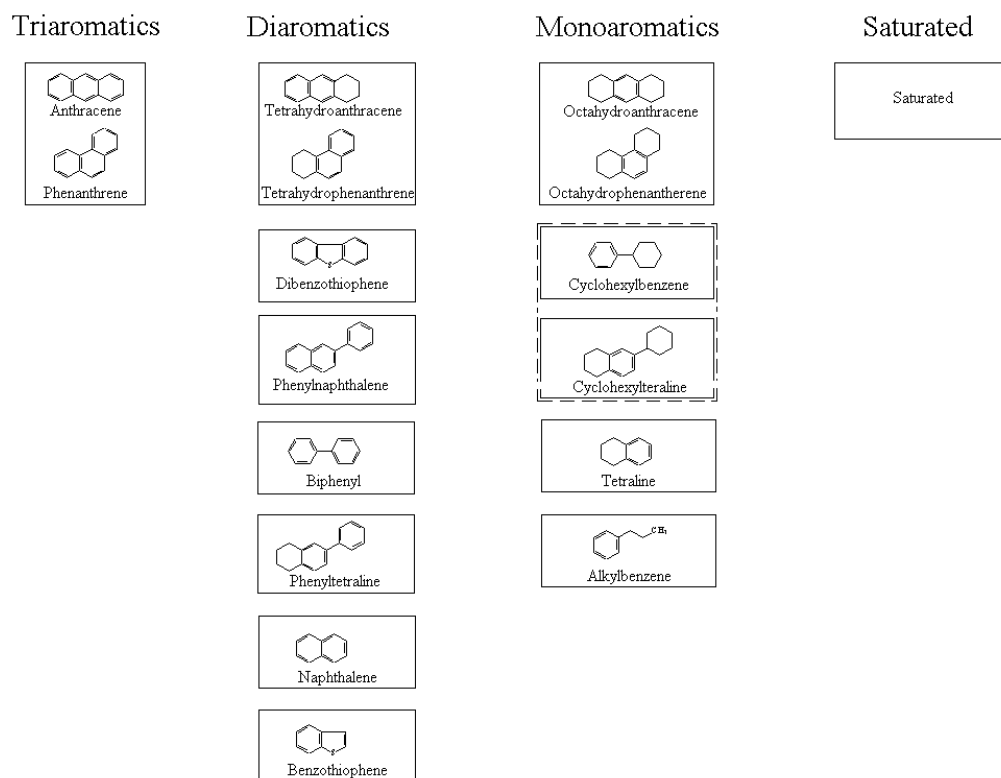


Fig.4. 1 Classification of the aromatic compounds lumps

Fig.4.1 shows that only one subclass is considered describing saturate and triaromatic classes. Saturates are considered as a single lump because they seem to behave as inerts, at least in the explored range of operating conditions. In order to account for the diversity in structure and reactivity of aromatic compounds, four sub classes are identified for the mono-aromatics (i.e. alkylbenzenes, tetralins, cyclohexylbenzenes and octahydrophenanthrenes) and five sub classes were identified for the di-aromatics (i.e. naphthalenes, biphenyls, phenyltetralins, tetrahydrophenanthrenes, phenyl-naphthalenes, benzothiophene and dibenzothiophene).

However, the lumped scheme contains also other two lumps belonging to the sulfur compounds class. They represent the labile sulfur compounds present in the gasoil that react extremely fast to produce aromatic compounds that participate to the hydrogenation scheme. For this reason, they are included in the hydrogenation approach. In particular, they are dibenzothiophene (DBT) and benzothiophene (BT) that react to produce respectively biphenyl and alkylbenzene.

4.2.2 Sulfur compounds speciation

Labile benzothiophene and dibenzothiophene are not the only sulfur compounds present in a gasoil but the other sulfur species are not included in the previous scheme because their amounts are very low and their conversion does not affect the concentration of the total aromatic compounds in the hydrotreated product.

Despite their concentrations (a few couple of hundreds of wppm), such compounds are very important in a gasoil because although they are negligible for the hydrogenation they become significant in terms of hydrodesulfurization. Although hundreds of sulfur compounds are present in a gasoil, most of them can be easily desulfurized under typical hydrotreating operating conditions. The challenge for deep desulfurization consists in the removal of the refractory compounds, mainly alkyldibenzothiophenes, from diesel fuel. In fact, all these compounds represent those one that can allow achieving the very low bound of 10 wppm that the environmental EU regulations impose.

These compounds are characterized by low reactivity, mainly due to the steric configuration that hinders the hydrodesulfurization reaction. In this context, many studies have been devoted to the understanding of the main refractory compounds behavior, i.e. 4 methyl-DBT (Meille et al., 1997, 1999) and 4,6 dimethyl-DBT (Kabe et al., 1993) while little attention has been addressed to the great variety of the other dibenzothiophenes that significantly contribute to the total sulfur level of the final product.

Sulfur species distribution is analyzed using an analytical method developed by SARTEC staff running on a Gas Chromatograph equipped with a PTV injector and a Pulsed Flame Photometric Detector (PFPD) (see the Appendix). By this method, a chromatogram as reported in the Fig. 4.2 is obtained. Sulfur present in the gasoil can be divided into non-aromatic and aromatic sulfur. The first group includes sulfides and mercaptans and in the analytic condition used, it is eluted as a hump extending almost along the entire Gas Chromatograph (GC) profile. Aromatic sulfur includes thiophenes, eluting at approximately 10 minutes, benzothiophenes and dibenzothiophenes.

Anyway, they are almost exclusively alkybenzothiophenes and alkyldibenzothiophenes. Most alkylbenzothiophenes exhibit high reactivity even at low temperature; in contrast, alkyldibenzothiophenes are more resistant to desulfurization (Ma et al., 1994). In fact, already visual inspecting Fig. 4.2 with the GC profile for the sulfur species of a gasoil feed (in particular a SRGO) and a mild hydrotreated product, it is seen that both non-aromatic sulfur, thiophenic and benzothiophenic compounds are completely absent in the product.

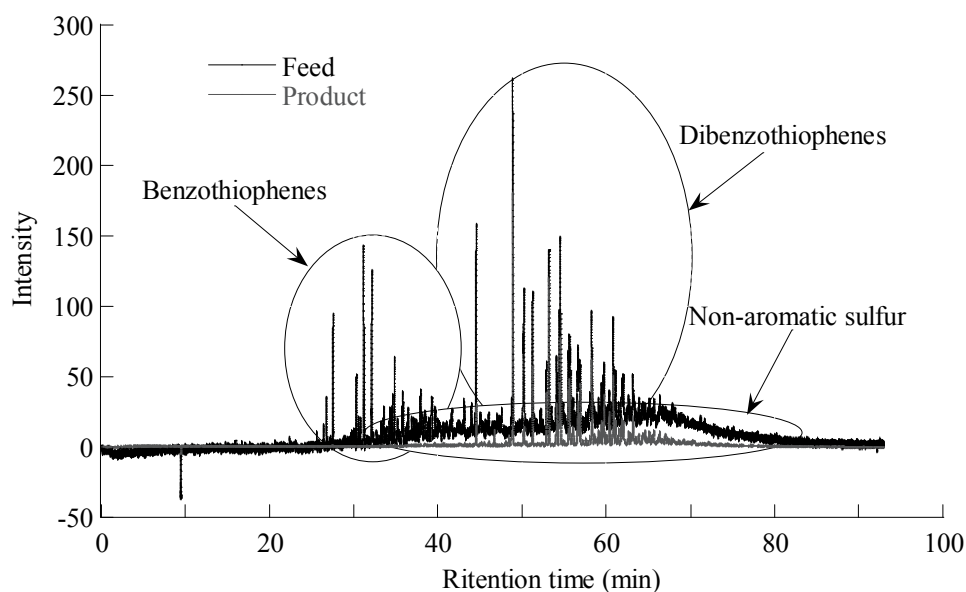


Fig.4. 2 Chromatogram of sulfur compounds obtained from the analytical method PFPD

Instead, the dibenzothiophenes can be “easily” or “hardly” removed according to their HDS reactivity as function of the different types of substituents.

Analyzing the PFPD GC profile (Fig. 4.2), it turned out that the approximately 55 sulfur species present in the hydrotreated products belong to the dibenzothiophenes class. In agreement with Ma et al. (1994), the products characterized by same conversion have been grouped into four lumps. Each group includes the alkyldibenzothiophenes that have the same kinetic behavior found comparing the conversion of each peak between feed and product for different test realized at different operating conditions. These sulfur molecular lumps are called R_1 , R_2 , R_3 and R_4 to indicate the increasing refractory behavior:

- R_1 includes *mild refractory* sulfur compounds;
- R_2 includes *medium refractory* sulfur compounds;
- R_3 includes *refractory sulfur* compounds;
- R_4 includes *strong refractory* sulfur compounds.

In particular, the two last ones are very important because they are characterized by the same kinetic behavior of the 4 methyl-DBT and the 4, 6 dimethyl-DBT, respectively. Because of the position of the methyl groups and their strong steric effect, they represent the main refractory sulfur compounds where the sulfur atom adsorption, in particular by the DDS reaction (cf. Paragraph 2.2.2), on the catalyst surface become very complex. In fact, the increasing refractoriness also justifies the different attitude of the several sulfur lumps respect to the DDS and the HYD

pathways in the hydrodesulfurization mechanism. R_1 mainly react by the DDS route with a fast kinetics, and its conversion is higher than 95% under the typical operating conditions. R_2 also undergoes the DDS route but with a slow kinetics and conversions typically are included between 85 and 95%.

On the other hand, R_3 takes part in both DDS route and HYD route with very slow kinetics and conversions included between 70 and 85%. Finally, R_4 still follows the DDS route but primarily undergoes the HYD route because its components need a first hydrogenation of the aromatic ring. In this case, the kinetics is extremely slow and the conversions are below 70% under the typical operating conditions.

The conversion of the refractory sulfur compounds results in the production of biphenyl and cyclohexylbenzene but previously they were not included in the hydrogenation scheme because their amounts are very low compared with the percentages of the aromatic compounds.

The sulfur characterization reported above is enough to describe the gasoil hydrodesulfurization but it has some problems to describe other feeds like VGO. In fact, in this case, the experimental results show the presence not only of species belonging to the same lumps of gasoil but also of other species present only in the VGO. For example, these naphthothiophenes and benzonaphthothiophenes need to be included into a new lump, since, even if they could have the same reactivity of the compounds in the previous lumps, they could be characterized by a complete different reaction network.

4.2.3 Nitrogen compounds speciation

In terms of nitrogen compounds, typically the nitrogen levels found in diesel fuel feeds range from 20 to 1000 $\mu\text{g/ml}$. In agreement with the literature (Wiwel et.al., 2000), the nitrogen compounds can be divided into different classes:

- Aliphatic amines;
- Anilines;
- Heterocyclic aromatic groups.

Most of them, in particular for heavier feeds, are present as aromatic heterocyclic and can be classified in two different groups. The former is the basic compounds group that includes heterocyclic aromatic compounds where the nitrogen atom belongs to a six member aromatic ring. The latter one is the non-basic, or neutral, compounds group where the nitrogen atom belongs to a five member aromatic group, (cf. Paragraph 2.2.3)

Therefore, pyrrole, indole and carbazole belong to the non-basic group and pyridine, quinoline and acridine to the basic group even if this group includes the aliphatic amines and anilines.

Analysis of nitrogen compounds is rather difficult because of the low concentrations found in a typical feedstock and the cleanup procedures, prior to the gas chromatographic analysis, are rather tedious. For this reason and because of the unavailability at this moment of an experimental methodology that allows classifying the nitrogen compounds, the information about nitrogen speciation required for this work have been taken from the literature. In fact, the SARTEC staff is still realizing an internal method to analyze in detail the concentration of the different nitrogen compounds similarly to the nitrogen compounds speciation. The absence of a specific speciation did not represent an impossible obstacle to realize this work. In fact, the results obtained demonstrated that a simple repartition of nitrogen into only two classes is enough to describe its conversion.

Therefore, as suggested by Sun et al. (2005), it has been assumed that non-basic nitrogen compounds are a significant fraction of the total nitrogen content. Also Laredo et al. (2003) gave some indications to describe the nitrogen compounds indicating that although total nitrogen content is typically higher in LCO than in atmospheric gasoil (AGO), the basic nitrogen content is higher in AGO. They indicate a 1/0.75/2.5 ratio of quinolines, indoles and carbazoles in AGO and 1/2.3/12.2 ratio of anilines, indoles and carbazoles in LCO. In particular, as reported by Bettati et al. (2005) the typical repartition of basic and non-basic compounds in a gasoil is 1/3 and 2/3 respectively.

The last repartition is the simplified speciation used to study the kinetics of hydrodenitrogenation, to find the correct kinetic mechanism and to correctly describe the cross effect of the nitrogen compounds. It is confirmed also experimentally.

4.3. Definition of the compounds for cracking reactions

The components that undergo cracking are the same previously described for the hydrogenation. In this case, however, a different approach is needed because the only lumped scheme is not enough detailed to describe the different kinetic behaviors of the several aromatic classes. An extremely higher level of detail is required because cracking reaction concerns the side chains break in addition to the aromatic rings saturation. Starting considering that on the hydroprocessing catalyst the only kind of cracking reaction is the dealkylation while isomerization and ring-opening are negligible, components belonging to the same molecular lump and with the same behavior with regard to the hydrogenation behaves differently for the cracking. That means that, in terms of cracking, the only information about the concentrations of the several classes is no more useful and the knowledge of the distribution of the different compounds inside the same lump varying the length of

the side alkyl-chains becomes necessary. This classification is far away to be simple. Firstly, this is due to the analytical limitations already discussed for the hydrogenation. Secondly, the variety of the available alkyl structures is innumerable and it is impossible to know all the components present in the feedstock and their distribution. Therefore, considering the bibliographical references regarding the basic structure of the crude oil products (Quann and Jaffe, 1992), an important hypothesis is made considering a strong asymmetry for the alkyl components. In this way, it is assumed that each compound is characterized by only one side chain or, in case of more chains, one of them is predominant and is the only one that undergoes cracking. This assumption is analytically strengthened by results coming from the ^{13}C NMR. (Carbon Nuclear Magnetic Resonance) that demonstrate the only existence of one alkyl-chain.

Within a such consideration, the deconvolution by HPLC, still used to have information about the total concentrations of the several molecular lumps, is jointly applied with the simulated distillation (SimDis) analyzer to obtain the distribution of molecular weights (therefore the distribution of side chain lengths) finding the compounds population for each lump. In the specific instance, the curve of the boiling point distribution obtained from the simulated distillation is really well approximate by the cumulative gamma distribution (Fig.4.3). This allows us to know for each temperature the quantitative percent mass that boiled below such temperature

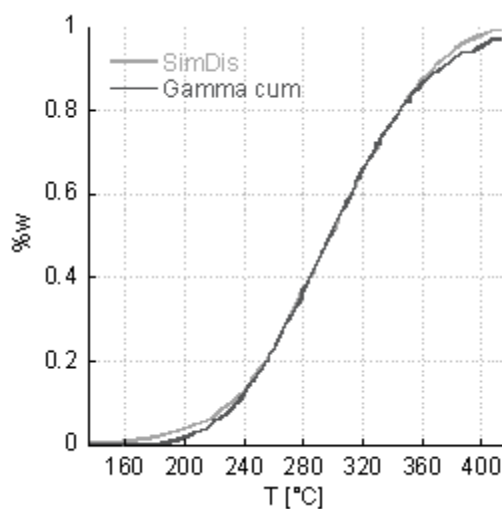


Fig.4. 3 Approximation of experimental SimDis curve by the cumulative gamma distribution.

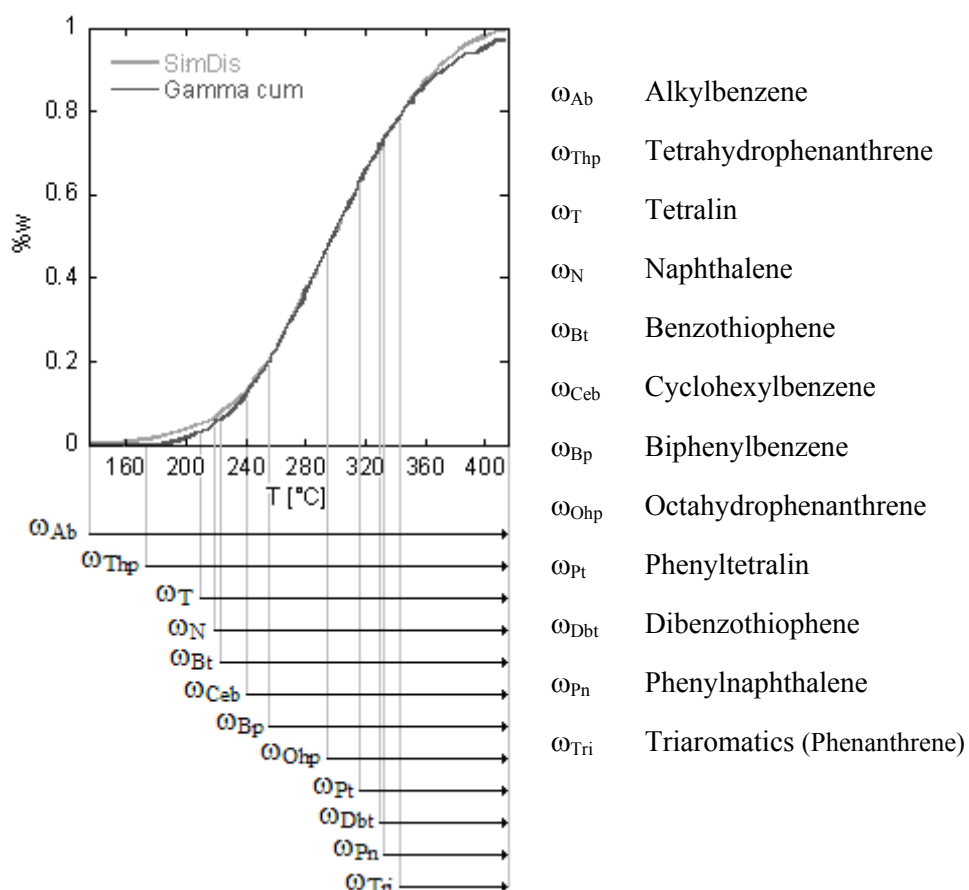


Fig.4. 4 Identification of intervals along the temperature range in the SimDis curve

The distributions of the hydrogenation molecular classes is found supposing that each lump's distribution starts from the temperature of the base component, which does not have any side chain, and extends as far as the end of the SimDis curve.

In this way, as shown in the Fig.4.4, it is possible to identify a series of intervals along the temperature range in the SimDis curve, each one characterized by a range of temperature and molecular weight. It contains the lumps with at least one component characterized by that value of boiling point typical of such interval.

By this procedure, the molecular lumps existing in each interval are individualized and for each class the number of carbon atoms and the corresponding molecular weight is identified. This is made considering that, depending on the structure, components with the same boiling point could have different molecular weight. At this moment, the nature of the compounds inside each temperature range is known but their concentrations remain unknown. Hence, using the repartition of the aromatic compounds in the several molecular lumps in agreement with the

deconvolution, it is supposed to split up the total concentration of each interval (known by SimDis) among all classes present in such interval. In this way, for each molecular lump the distribution of the different components belonging to the different intervals of temperature is found (Fig.4.5).

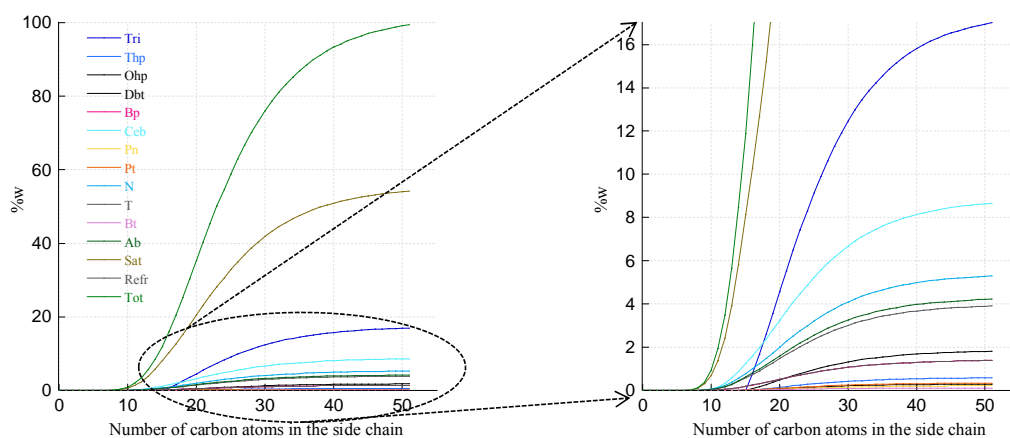


Fig.4. 5 Cumulative distributions of the different molecular lumps.

This approach, in spite of the simplification only considering the compounds with one side chain, allows us to obtain about 600 components distributed in the several molecular lumps that have known concentrations.

Chapter 5

Model formulation



The motivations of this work, presented in the beginning of this thesis, led the refineries, also in consideration of the varying quality of the feedstock, to optimize the hydroprocessing operating conditions. This goal can be best achieved by the use of a suitable mathematical model that has the property to be a phenomenological model that needs a deep knowledge of the process.

5.1 Hypotheses of the model

Since industrial hydroprocessing typically occurs within trickle bed reactor, the system behaves as a plug flow without axial dispersion with negligible mass transfer resistances. While, the experiments utilized to develop the model, has been carried out in the pilot unit located in the SARTEC Company using a flooded-bed reactor. In this case, the presence of gas and liquid phases could induce an appreciable back mixing and it becomes needed to verify which the effect of the axial dispersion is. Furthermore, the limiting step among the superficial reaction and the mass transfer terms should be identify to describe the reactor with a homogeneous or heterogeneous model.

5.1.1 Axial dispersion influence

Trickle-bed reactor in the industrial plant and flooded-bed reactor in the pilot unit have different fluid dynamics. Even so, the pilot unit correctly simulates the real plant when both of them have reactors that behave like an ideal plug-flow reactor. Consequently, it is needed to know what importance the axial dispersion plays to rightly develop the model and to verify if it is negligible.

Usually, the magnitude order of the Peclet number in an industrial plant is about 10^3 , while it becomes about 10 for the pilot unit. Therefore, in the real scale Peclet number is high enough to be sure that the axial dispersion is negligible. Instead, in the pilot unit, the effect of the back mixing could be important and it is necessary to increase the Peclet number reducing the axial dispersion.

An important parameter that improves the ideal plug-flow character of the reactor is the particles size. In fact, as the particles size decreases, the axial dispersion coefficient decreases as well and the magnitude of Peclet numbers changes from few tens to few hundred. One way to satisfy the requirement of small particles is to dilute the large catalyst particles whit fine inert particles. Thus, the hydrodynamics are dictated by the packing of the small inert particles, whereas the catalytic phenomena are governed by the catalyst particles. This is, in fact, a decoupling of hydrodynamic and kinetic behaviors.

It is not certain that this shrewdness is enough to guarantee the ideal behavior of the reactor. For this reason, in the following, it will be presented the approach used to determine which kind of model it is best to use, ideal plug-flow or plug-flow with axial dispersion.

Firstly, some reflections should be made *a priori* considering the little size of the reactor, without any valuation of the dispersion coefficient. They allow us to understand why it is simple to neglect the axial dispersion in a typical reactor of the

industrial plant but it is impossible to do immediately the same for the small-scale reactor.

In fact, reactor dimensions have effect on residence time distribution of reactant considering the reduction of reactor diameter. As the diameter is reduced, the wall effect increases and the overall characteristics of the packing can no longer be considered the same as in the unperturbed packing. In fact, the bed void near the wall deviates from the statistical fluctuations inside the bed and reaches value of unity very close to the wall while the surface area per unit volume is equal to zero. Both bed void and specific area affect the local fluid velocity and contribute to deviate from the ideal plug flow the reactor (Sie, 1991).

Actually, the most important effect that causes a greater deviation from plug flow is the reduction of reactor length that enhances the back mixing that superimposes on the overall flow an additional transfer that decreases the conversion and increases the reactant concentration. In fact, assuming that the equivalent height of the mixing stage remains the same, a reduction of the reactor length presupposes that the reactor has a lesser number of mixing stages and a greater distribution of the residence time. In order to establish if in the pilot unit the term of axial dispersion is negligible or not, it is possible to use a rule called Mears criterion (Mears, 1971). This criterion has been derived by comparison between the ideal plug-flow model analytical solution and the plug-flow model with axial dispersion approximate solution. The last one is obtained by perturbation solutions considering first order reactions subsequently generalized for n -order reactions. When Peclet is high, it is sufficiently accurate terminating the series after the first two terms because for plug flow all terms after the one are negligible. Imposing that the effluent concentrations resulting from the plug flow model and the axial dispersion model are equal, the ratio between the reactors lengths needed to obtain the same conversion has been calculated. Mears criterion assumes that in order the deviations can be considered negligible, the lengths ratio must be smaller than 5% that is $Pe > 20n \ln(1-X)^{-1}$. In such formula, n represents the order of the reaction and X the conversion.

Gierman (1988) considered the above criterion to be rather severe arguing that the accuracy of temperature definition in practical cases is lesser than 1°C and only seldom it is possible to derive rate constants to accuracy greater than 10%. Consequently, Sie proposed a somewhat more relaxed one where $Pe > 8n \ln(1-X)^{-1}$. It is clear that such magnitude of the error does not justify the use of a conservative criterion like Mears one. The Mears and Sie criterions have been applied to verify the negligibility of the axial dispersion in our model. The conversions in Table 5.1 refer to the refractory sulfur compounds present in the gasoil because, due to their low quantity and reactivity, they represent the main compounds on which the axial dispersion may have the greatest effect.

X	Pe _{reatt}	Pe by Sie	Pe by Mears
0.97	54.67	28.05	70.13
0.993	77.38	39.69	99.24
0.9993	113.34	58.12	145.29
0.9999	143.85	73.68	184.21

Table 5.1 Results of the Mears and Sie criteria application

As reported in the Table 5.1, the model obeys the Sie criterion but not the Mears one because the number of Peclet obtained from the model for different value of conversions is higher than that one calculated with the first method and lower than that one calculated with the second method. Anyway, this is enough to demonstrate that the axial dispersion is negligible and the reactor behaves as ideal plug-flow.

Anyway, several correlations are available in the literature to estimate the axial dispersion coefficient for both trickle-bed and flooded-bed reactors.

As indicated by Piché et al. (2002), many correlations are present in the literature (Tab. 5.2):

Authors	Correlation	Specifications
Ebach and White	$\frac{D_{ax}\rho_L}{\mu_L} = 13.5 \left(\frac{\rho_L d U_L}{h_T \mu_L} \right)^{1.06}$	$\frac{\rho_L d U_L}{h_T \mu_L} < 100$
Liles and Geankoplis	$D_{ax} = 0.261 d^{0.73} \left(\frac{U_L}{h_T} \right)^{0.93}$	$2 < \frac{\rho_L d U_L}{h_T \mu_L} < 500$
Hochman and Effron	$\frac{U_L d}{h_T D_{ax}} = 0.042 \left(\frac{\rho_L d U_L}{\mu_L (1-\varepsilon)} \right)^{0.5}$	$4 < \frac{\rho_L d U_L}{\mu_L} < 80$
Buffham and Rathor	$\frac{U_L d}{h_T D_{ax}} = 0.45 \left(\frac{U_L^2}{h_T^2 g d} \right)^{0.27}$	$1.5 < \frac{1000 U_L^2}{h_T^2 g d} < 20$
Kobayashi et al.	$\frac{U_L d_h}{h_T D_{ax}} = 60 \left(\frac{\rho_L d_h U_L}{h_T \mu_L} \right)^{0.63} \left(\frac{d_h^3 g \rho_L^2}{\mu_L^2} \right)^{-0.73}$	$1 < \frac{\rho_L d_h U_L}{h_T \mu_L} < 100$
Fu and Tan	$\frac{U_L d}{h_T D_{ax}} = \frac{1.4 \times 10^{-4}}{d^{0.75} \varepsilon} \left(\frac{9\pi(1-\varepsilon)^2}{16\varepsilon^3} \right)^{0.25}$	$\frac{\rho_L d U_L}{\mu_L} < 4$
Tsamatsoulis and Papayannakos	$\frac{U_L}{a_G h_T D_{ax}} = 2.14 a_G^{-0.72} \varepsilon^{-0.85}$	$0.08 < \frac{\rho_L U_L}{a_G \mu_L} < 8$
Cassanello et al.	$\frac{U_L d}{D_{ax}} = 2.3 \left(\frac{\rho_L d U_L}{\mu_L} \right)^{0.33} \left(\frac{d^3 g \rho_L^2}{\mu_L^2} \right)^{-0.19}$	$5 < \frac{\rho_L d U_L}{\mu_L} < 50$

$$\text{Michell and Furzer} \quad \frac{U_L d}{h_T D_{ax}} = \left(\frac{\rho_L d U_L}{h_T \mu_L} \right)^{0.7} \left(\frac{d^3 g \rho_L^2}{\mu_L^2} \right)^{-0.32} \quad 80 < \frac{\rho_L d U_L}{h_T \mu_L} < 8000$$

Tab.5.2 Summary of important published correlations predicting liquid axial dispersion coefficients.

Most of them are more appropriate for down-flow TBR reactor and especially Fu and Tan or Tsamatsoulis and Papayannakos expressions are better to describe the axial dispersion coefficient concerning a flooded bed reactor. The application of these correlations allows estimating the magnitude order of the axial dispersion and value if the reactor behavior is like an ideal plug-flow.

5.1.2 Mass Transfer Resistances

The fluid dynamic of the pilot unit is also affected by the mass transfer contribute. In fact, flooded-bed reactor is a heterogeneous reactor where different mass transfer resistances are present between the different phases. However, in the model, the reactor is described like a homogeneous reactor because the superficial reaction is assumed as limiting step and no mass transfer resistances are considered. Therefore, it is necessary to analyze if the transfer term of hydrogen from gas to liquid, the diffusion resistance through the external film around the catalyst particles and the resistance inside the catalyst pores are negligible. On this point, the three-phase reactor can be described like a series of three different zones represented by gaseous, liquid and solid phase respectively. Therefore, the global coefficient of the mass transfer (k_G) multiplied by the total surface area is defined as

$$a_l k_G = \frac{I}{\frac{I}{a_l k_l} + \frac{I}{a_s k_s} + \frac{I}{a_q k_q}} \quad (5.1)$$

where k_l is the gas-liquid mass transfer coefficient, k_s is the liquid-solid mass transfer coefficient, k_q represents the intra particle mass transfer (IPMT) and a_l , a_s , a_q are their surface areas. The choice of the correlations to value these coefficients depends on the flow regime inside the reactor. Both in the pilot unit and in the industrial plant the process is carried out with an excess of hydrogen to reduce the already limited resistance to the mass transfer between the gas and the liquid phase and to maximize the difference of the hydrogen between these phases. In this way, the liquid phase is saturated of hydrogen and both resistances, gas-liquid and liquid-solid become negligible. Anyway, if k_l value is needed, there are different correlations between the flooded-bed reactor in the pilot unit and the trickle-bed in

the industrial plant because of the different effect of liquid rate into these different systems. The only correlation that will be reported concerns the flooded bed reactor. In truth, few correlations exist in the literature to estimate the gas-liquid coefficient for a flooded-bed reactor; the main one is the Specchia et al. (1978) correlation:

$$Sh = \frac{k_l \cdot a \cdot D_R}{D_{AL}} = \left[2.14 \cdot \left(\frac{\rho_l \cdot u_0^l \cdot D_R}{\mu_l} \right)^{0.5} + 0.99 \right] \cdot \left(\frac{\mu_l}{\rho_l \cdot D_{AL}} \right)^{0.33} \quad (5.2)$$

where the parameters are:

- A Surface area between gas and liquid [m^2/m^3];
- D_{AL} Molecular diffusivity in liquid [m^2/s];
- k_L Liquid mass transfer coefficient [m/s];
- D_R Reactor diameter [m];
- ρ_L Density of liquid [kg/m^3];
- u_0^l Superficial velocity of the gas [m/s];
- μ_l Viscosity of liquid [$\text{kg}/(\text{m}\cdot\text{s})$];

Comparison of the gas-liquid mass transfer and the kinetic terms shows that hydrogen transfer between gaseous and liquid phase occurs faster than reaction because hydrogen diffusivity is very high, therefore the k_l coefficient can be considered negligible. Moreover, assuming that gas-liquid mass transfer is the limiting step, the increase of the hydrogen flow should determine an increase of the conversion but the choice to carry out the process in excess of hydrogen excludes *a priori* this possibility.

The estimation of the liquid-solid transfer coefficient is still characterized by different correlations between flooded-bed and trickle-bed reactor. For example, Goto and Smith (1975) proposed the formula of Evans and Gerald (1953) valid for a multiphase up-flow reactor:

$$\frac{k_s}{u_L} \left(\frac{\mu}{\rho D} \right)^{\frac{2}{3}} = 1.48 \cdot \left(\frac{\rho u_L d_p}{\mu} \right)^{-0.52} \quad (5.3)$$

and the Van Krevelen and Krekels (1948) correlations for trickle-bed regime:

$$\frac{k_s}{Da_t} = 1.8 \left(\frac{G_L}{\mu a_t} \right)^{\frac{1}{2}} \left(\frac{\mu}{\rho D} \right)^{\frac{1}{3}} \quad (5.4)$$

In both correlations, k_s is a function of the molecular diffusivity (D), the density of the liquid (ρ), the viscosity (μ), the superficial velocity (u_0) and the diameter of the catalyst particles. As suggested by Goto and Smith (1975), the liquid-solid mass

transfer is greater in the trickle bed than in the liquid-full bed, at the same flow rate, for the larger particles. This is probably due to the larger linear velocities in trickle beds where part of the volume is occupied by gas.

Finally, the intra-particle mass transfer is estimated applying the Glueckauf lumping approach supposing that the catalyst trilobe behaves like a catalyst of cylindrical shape:

$$k_q = \frac{D_{eff}}{4R} \quad (5.5)$$

where R is the radius of the catalyst particle and $D_{eff} = D_{mol} \frac{\varepsilon}{\tau} (1-\lambda)^4$ is the effective diffusivity (Spry and Sawyer, 1975). In the correlation of effective diffusivity, D_{mol} is the molecular diffusivity, ε the catalytic particle porosity and τ the tortuosity. The term $(1-\lambda)^4$ takes in account solid matter can be deposited during catalyst life and it involves a reduction of the pore radius provoking a substantial lessening of the effective diffusivity.

Under the typical operating conditions, even in the pilot unit, the velocity of the fluid phase is sufficiently high to make the liquid-solid mass transfer negligible. Instead, the intra particle mass transfer can be sometimes important. Usually, this is not a problem using the actual catalysts because its contribute is negligible and the homogenous and heterogeneous systems behave in the same way, but for the catalysts of new generation, characterized by a greater reactivity, the weight of the internal mass transfer could be more important. In this case, the behavior of the multiphase system can differ from the homogenous one and the aging of the catalyst could increase the differences between these systems. This is because k_q depends on geometry of catalytic particles and on the value of effective diffusivity (D_{eff}). Moreover, it could decrease during the life of the catalyst because of solid matter deposition in the catalyst pores.

If the system is controlled by the IPMT, an increase of the LHSV determines an increase of conversion in spite of the effect of the residence time reduction. Usually it has been observed that the increment of the flow rate causes the decrement of the aromatic conversion and this excludes that the intra particle mass transfer represents the limiting step.

From the foregoing discussion it is clear that the assumption to describe a homogeneous reactor instead that a heterogeneous one is correct until the mass transfer resistances are lesser than the kinetic term.

This study is realized for several values of LHSV, and taking in consideration the reaction from biphenyl to cyclohexylbenzenes. For each LHSV it has been made a comparison between the pseudo-homogenous and the heterogeneous system based

on an increasing of the kinetic constant and a variation of intra-particle mass transfer coefficient (k_q).

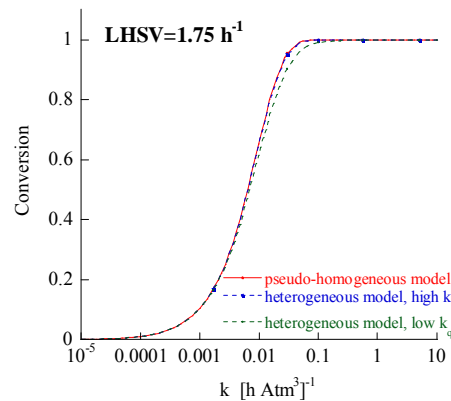


Fig.5. 1 . Influence of IPMT for low LHSV (1,75 h⁻¹); Feed: SRGO+LCO; Pressure: 90 bar

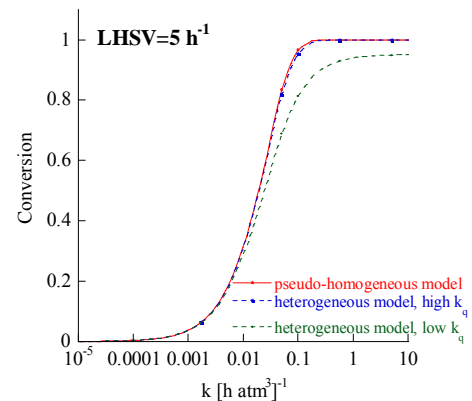


Fig.5. 2 Influence of the IPMT for high LHSV (5 h⁻¹); Feed: SRGO+LCO; Pressure: 90 bar

At each value of LHSV, the results demonstrate that the increase of the kinetic constant causes a deviation of the behavior between heterogeneous and homogenous systems (Fig.5.1 and 5.2). The effect is as more pronounced as lower is the value of k_q since the transition from a kinetic regime to a transfer regime occurs for gradually smaller kinetic constants. For low values of LHSV, the effect is not very marked, because of the increment of the kinetic constant, the heterogeneous and homogenous systems catch up unitary biphenyl conversion whether for values of kinetic constant for which a kinetic regime exists or for values that determine the transition to internal mass transfer regime. The justification is that the biphenyls participate to an irreversible reaction that, in these operative conditions, has a sufficiently long residence-time to guarantee the total conversion of all reagents in products. As the LHSV grows up, the residence-time diminishes, in the homogenous system, the overall rate of process coincides with the reaction rate and so the conversion is complete. Unlike that, in the heterogeneous system, the overall rate of process is the sum of the reaction rate and of the mass transfer one. Increasing the kinetic constant, the rate of reaction is limited by the rate of mass transfer and the transition from a kinetic regime to a regime of mass transfer resistances occurs. In this case, internal mass transfer becomes the controlling phenomenon and opposes such a resistance that the overall rate of process is not ever sufficiently high to compete with the feed crossing of the reactor. Therefore, the feed leaves the reactor before the reaction is complete.

5.1.3 Other hypotheses

There are some other hypotheses in the development of the model.

1. The models have been realized with the assumption of the density variation negligibility between feed and product. In fact, in the pilot unit the density has been measured both in the inlet and in the outlet of the reactor and just a variation of 2% has been observed.
2. The process is carried out with an excess of hydrogen. This allows us to reduce the partial pressure of hydrogen sulfide that represents one of the main products coming out from the hydrodesulfurization reaction.
3. The model is valid for stationary-state because the experimental data from the pilot unit describe this plant in stationary conditions
4. No inefficiency is present and the catalyst is assumed thoroughly wetted by the fluid phase.
5. Evaporation and condensation of the reactants do not occur.
6. In agreement with the plug-flow model, none concentration gradient exists in the radial direction.

5.2 Mathematical model development

The model has been developed starting from the rigorous expressions, then the previous hypotheses have been applied and it is simplified

Rigorous heterogeneous model

Mass balance in the gas phase, i is H_2 or H_2S :

$$D_{0e}^G \frac{\partial^2 C_i^G}{\partial x^2} - u_0^G \frac{\partial C_i^G}{\partial x} - K_L a_L (C_i^G - C_i^l) = 0 \quad (5.6)$$

Mass balances in the liquid phase, i is H_2 or H_2S and j a generic aromatic, sulfur or nitrogen compound:

$$D_{0e}^L \frac{\partial^2 C_i^L}{\partial x^2} - u_0^L \frac{\partial C_i^L}{\partial x} - K_S a_S (C_i^L - C_i^S) + K_L a_L (C_i^G - C_i^L) = 0 \quad (5.7)$$

$$D_{0e}^L \frac{\partial^2 C_j^L}{\partial x^2} - u_0^L \frac{\partial C_j^L}{\partial x} - K_S a_S (C_j^L - C_j^S) = 0 \quad (5.8)$$

Mass balances in the solid phase, i is H_2 or H_2S and j a generic aromatic, sulfur or nitrogen compound:

$$K_S a_S (C_j^L - C_j^S) - \sum_k v_{kj} \rho_{app} r_k = 0$$

$$K_S a_S (C_j^L - C_j^S) - \sum_j v_{ij} \rho_{app} r_j = 0$$
(5.9)

where:

a_L	Surface area between gas and liquid per volume unit [m^2 / m^3]
a_S	Surface area between liquid and solid per volume unit [m^2 / m^3]
C_i	Concentration [kmol / m^3]
D_{0e}^G	Axial dispersion in the gas phase [m^2 / s]
D_{0e}^L	Axial dispersion in the liquid phase [m^2 / s]
K_S	Transfer coefficient from bulk liquid to catalyst particles [s^{-1}]
K_G	Overall transfer coefficient from gas to liquid [$\text{kmol} / (\text{m}^2 \text{s})$]
r_j	Reaction rate [$\text{kg}_j / (\text{kg}_{\text{cat}} \cdot \text{s})$]
u_0^G	Gas superficial velocity [m / s]
u_0^L	Liquid superficial velocity [m / s]
z	Axial coordinate [m]
ρ_{app}	Apparent density of catalyst [catalyst mass/total volume]

The rigorous heterogeneous model may be simplified considering only two phases: a solid phase and a pseudo-homogeneous fluid phase including gaseous and liquid phases. This is the model typically used when the mass transfer become important because however the mass transfer between gas and liquid is always negligible.

Simplified heterogeneous model

$$D_{0e} \frac{\partial^2 \omega_i}{\partial x^2} - u_0 \frac{\partial \omega_i}{\partial x} - a_s K_G (\omega_i - \omega_{is}) = 0$$
(5.10)

$$a_s K_G (\omega_i - \omega_{is}) - \sum_j v_{ij} \rho_{app} r_j = 0$$
(5.11)

As said before, during this work none last generation catalyst has been used, therefore the mass transfer resistances are negligible and therefore it is possible to use a homogeneous model without introducing any error significantly important.

Homogeneous Model

$$D_{0e} \frac{\partial^2 \omega_i}{\partial x^2} - u_0 \frac{\partial \omega_i}{\partial x} - \sum_j v_{ij} \rho_{app} r_j = 0$$
(5.12)

where ω_i is the weight fraction of the i -th lump, x the longitudinal coordinate, u_0 the liquid surface velocity, D_{0e} the axial dispersion coefficient estimated through the correlation developed by Goto and Smith (1975), ε_s the volume bed fraction occupied by the catalyst (experimentally determined), ν_{ij} the stoichiometric coefficient for the i -th lump in the j -th reaction. r_j are the reaction rates, they will be made explicit in the following Chapters.

It is possible to observe that although the back mixing is negligible compared to the other mass balance terms, the model has been written introducing the axial dispersion coefficient. This is because in the numerical solution the use of the plug-flow model with axial dispersion avoids numerical problems typical of the ideal plug flow model especially if the dynamic model is considered.

No thermal balance is introduced to describe the pilot unit model because, as said in the Chapter 3, it is isotherm and the thermal balance is unnecessary. Such balance becomes essential to extend the model to the industrial plant. In fact, it is an adiabatic system characterized by strong temperature increment range (30-40°C) because of the high exothermicity of the hydrogenation and hydrodesulfurization reactions. For this reason, the thermal balance will be presented:

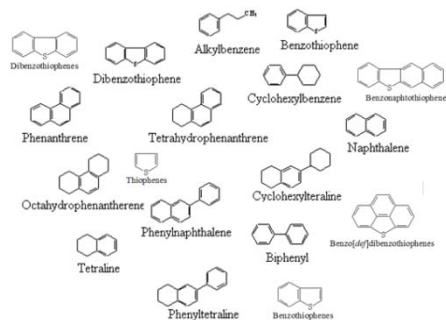
$$k_{eff} \frac{\partial^2 T}{\partial x^2} - u_0 \rho C_p \frac{\partial T}{\partial x} - \sum_j \Delta H_{reaz} r_j = 0 \quad (5.13)$$

where k_{eff} is the effective conductivity, T is the temperature, ρ the density of the mixture, C_p the specific heat and ΔH_{reaz} the enthalpy of the different reactions.

The estimation of the ΔH_{reaz} will be presented after the kinetic terms will be defined. In the following Chapters, several model applications will be presented, but only after a detailed explanation of hydrogenation, hydrodesulfurization and hydrodenitrogenation kinetics and mechanisms will be given in Chapter 6 to understand better the foundations of this work.

Chapter 6

Hydrogenation and hydrodesulfurization kinetics



Once feedstock and product are characterized qualitatively and quantitatively, the kinetic scheme to describe the hydrogenation, hydrodesulfurization, hydrodenitrogenation and cracking reactions can be introduced. In agreement with the literature, as reported in the Chapter 4, firstly hydrogenation and hydrodesulfurization reaction mechanisms will be presented neglecting the inhibitive effect of the other species like H_2S and especially nitrogen compounds.

6.1. Hydrogenation reactions

6.1.1 Mechanism of hydrogenation of the aromatic compounds

In the Chapter 4, the aromatic compounds have been identified and they have been classified in 11 different molecular lumps. It is needed now to know how these components are related each other and through which mechanism they react on the catalyst surface. The hydrogenation mechanisms are at this point well known in the literature because many authors (e.g. Sapre and Gates, 1982) have studied the typical hydrogenation products and their reaction networks. From here, starting from the bibliographic references, this thesis considers these previous works finding the hydrogenation kinetic scheme needed to develop its phenomenological model.

Considering the complexity of the gasoil, some authors concentrated on some characteristic compounds of the feedstock studying their products and their reaction networks in suitable solvents like cyclohexane, heptane, isooctane, and few other. For example, Toppinen et al. (1996a, 1996b) focus their attention on the alkylbenzenes study. Their work belongs to that group of works that suggest the formation of a complex during the first hydrogenation while other models suggest that the hydrogenation of aromatic compounds proceeds through sequential additions of adsorbed hydrogen atoms (Lindfors et al., 1993). They studied the reactivity of the different alkylbenzenes and the modeling of the hydrogenation kinetics proposing the reaction mechanism realizing experiments into a batch reactor. However, in this thesis, as reported in Fig.6.1, the alkylbenzenes, formed by the benzothiophenes hydrogenation, do not react because of the negligence of this reaction on the catalyst and operating conditions used in the hydroprocessing plant.

Instead, Rautanen et al. (2002) and Korre et al. (1995) studied naphthalene and tetralin conversion. In particular, the second group of Authors studied the *naphthalene* \leftrightarrow *tetralin* reaction proposing that tetralin represents the main hydrogenated product coming from naphthalene. Instead, tetralin undergoes the hydrogenation to produce *cis*- and *trans*-decaline but, when the equilibrium concentration is reached, it takes part in the dehydrogenation reaction producing again naphthalene. In agreement with their results, the kinetic scheme proposed here will consider the existence of the equilibrium reaction between naphthalene and tetralin (Fig.6.1). Similarly, the same kinetic network will be considered to describe the behavior of the phenylnaphthalene. In fact, although this belongs to the triaromatic class, it behaves like diaromatic compounds (cf. Paragraph 4.2) and it has the same reactivity of naphthalene (Girgis and Gates, 1991) and its main product is phenyltetralin that reacts to form cyclohexyltetraline. This monoaromatic

compound however does not react under the hydroprocessing operating condition to produce its corresponding saturate compounds.

Korre et al. (1995) studied also the reaction of phenanthrene and anthracene suggesting that their main products are dihydrophenanthrene, tetrahydrophenanthrene (sym and asym), octahydrophenanthrene and perhydrophenanthrene. They are related by equilibrium reactions and di- and tetrahydrophenanthrene represent the primary products while octahydrophenanthrene is the secondary product. Perhydrophenanthrene is usually present only with low yields. Considering their reaction network and that reported in the Paragraph 4.2 about the partial hydrogenated product, the scheme on the Fig.6.1 does not consider the existence of dihydrophenanthrene. In this case, phenanthrene reacts to produce initially tetrahydrophenanthrene and then octahydrophenanthrene. The last one reacts also producing perhydrophenanthrene that is included in the generic lump defined for all saturates compounds.

Finally, Sapre and Gates (1982) have studied biphenyls suggesting that biphenyl is the product coming from the dibenzothiophene reaction and it reacts to form cyclohexylbenzene. Cyclohexylbenzene could subsequently react forming bicyclohexyl but usually under the typical hydroprocessing operating conditions and by the typical commercial catalyst, this reaction is negligible (Fig.6.1).

Consequently the considerations made above for the different aromatic compounds added to those proposed in terms of reactivity in the previous Chapter, a lumped scheme for the hydrogenation reactions is presented. It includes:

- 1 lump of triaromatic compounds
- 5 lumps of diaromatic compounds
- 2 lumps of labile sulfur compounds
- 4 lumps of monoaromatic compounds
- 1 lump of sulfur compound

related by the reactions shown in Fig.6.1:

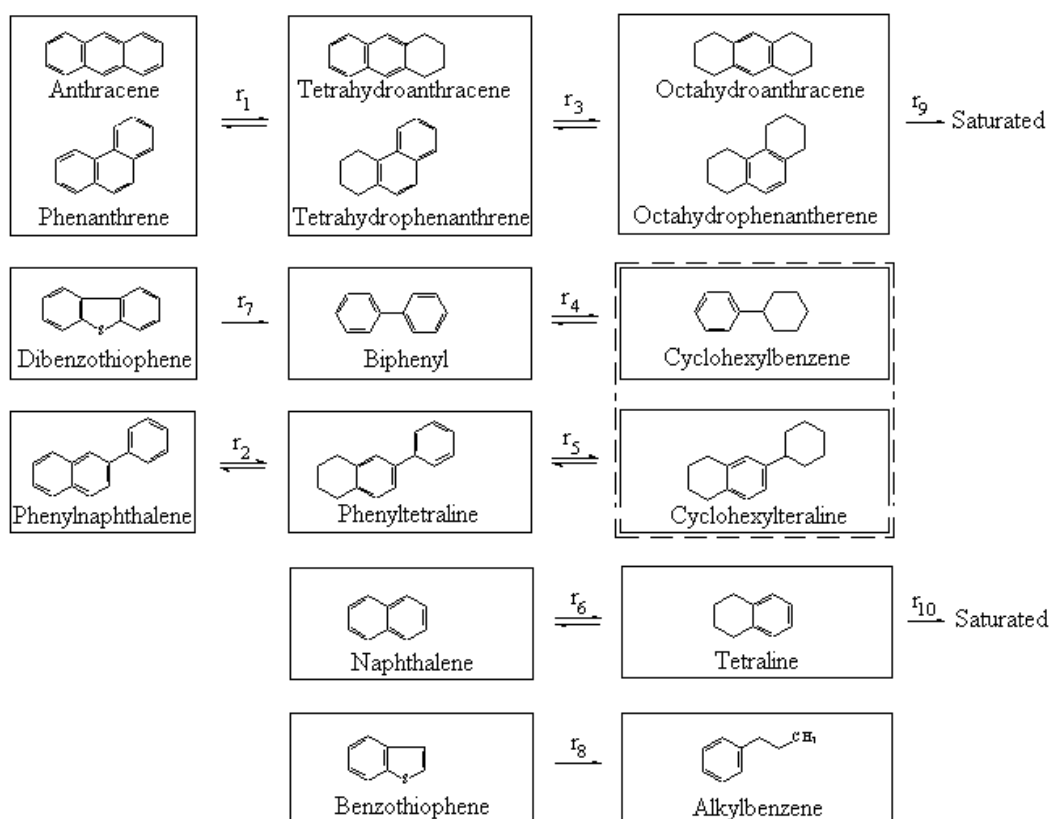


Fig.6. 1 Lumping scheme of the aromatic compounds

Observing the kinetic scheme it is possible to deduce how many parameters the kinetic model has:

- 8 direct kinetic constants;
- 8 inverse kinetic constants for the hydrogenation reactions;
- 2 kinetic constants for the desulfurization of labile sulfur compounds;
- 13+1 adsorption constants, one for the hydrogen and for each lump that adsorbs on the catalyst active sites.

However, by some considerations the number of the parameters can be reduced without introducing excessive approximation such as to invalidate the model.

Firstly, in the conditions used during the hydroprocessing, the dehydrogenation of the saturated compounds is negligible. Moreover, as reported by Sapre and Gates (1981), the hydrogenation of alkylbenzenes and cyclohexylbenzenes is slow and it is not taken in consideration. In agreement with the considerations made about the relation between reactivity and structure and neglecting the effect of the alkyl and phenyl substituents, the kinetic constant of the r_2 (phenyl naphthalene \leftrightarrow phenyltetralin), r_3 (tetrahydrophenanthrene \leftrightarrow octahydrophenanthrene) and r_6

(naphthalene \leftrightarrow tetralin) are considered equal. In the same way r_4 (biphenyl \leftrightarrow cyclohexylbenzene) and r_5 (phenyltetralin \leftrightarrow cyclohexyltetralin) for the diaromatic compounds and r_9 (octahydrophenanthrene \leftrightarrow saturated) and r_{10} (tetralin \leftrightarrow saturated) for the monoaromatic compounds. In fact, during the hydrogenation of the phenylnaphthalene, tetrahydrophenanthrene and naphthalene and during that of the octahydrophenanthrene and tetralin the saturation of one condensed aromatic ring occurs. Instead, during the hydrogenation of biphenyl and phenyltetralin the hydrogenation of the naphthenic ring takes place.

In this way, the number of parameters becomes seven, 4 direct kinetic constants and 3 inverse kinetic constants and therefore three equilibrium constants. Biphenyl and phenyltetralin do not have any equilibrium constants under the hydroprocessing conditions.

Concerning the adsorption constants, they are related to the polarity of the molecules and the number of aromatic rings. Typical values of the adsorption constants for a CoMo/Al₂O₃ catalyst have been proposed by Korre et al. (1996) and reported in the Table 6.1.

	K [L/mol]
4 rings/pyrene	38.5
4 rings/chrysene	38.5
3-ring/lump	17.5
2-ring/lump	7.7
1-ring/lump	7.4
Saturates	3.9

Tab.6.1 Lumps adsorption constants (Korre et al., 1994)

In fact, in agreement with the literature (Korre et al. 1994) the adsorption constants can be grouped in four groups corresponding to triaromatic, diaromatic, monoaromatic and saturate classes. It is assumed that the benzothiophenic and dibenzothiophenic compounds have the same adsorption constants equal to the diaromatic compounds.

6.1.2 Hydrogenation kinetics

In Chapter 4, when the state of art has been presented, it has been underlined the importance to develop a model able to consider the simultaneous presence of different compounds in the gasoil and able to describe not only the conversion of each of them but also their competitive reactions. To meet this goal in a wide range of operating conditions, for different catalysts and for different feeds (with different distributions of the aromatic compounds in the several lumps), Langmuir-

Hinshelwood kinetics is chosen to describe the hydrogenation reaction. In fact, according with Girgis and Gates (1991) and Stanislaus and Cooper (1994) this kind of expression results the best one to describe the conversion of the aromatic compounds by hydrogenation.

For each lump, this kinetics is found considering different hypotheses:

- Hydrogen and hydrocarbons adsorption occur in different active sites;
- Hydrogen adsorption is supposed as molecular adsorption;
- The different classes are not adsorbed with the same easiness and they compete to occupy the active sites of the catalyst.

Considering for example the triaromatic conversion the procedure to obtain such kinetics is presented:

- 1) $T + \pi \leftrightarrow T\pi$ *Adsorption of triaromatic compound on the site π*
- 2) $H_2 + \gamma \leftrightarrow H_2\gamma$ *Adsorption of hydrogen molecule on the site γ*
- 3) $T\pi + 2H_2\gamma \rightarrow D\pi + 2\gamma$ *Reaction between triaromatic and hydrogen adsorbed*
- 4) $D\pi \leftrightarrow D + \pi$ *Desorption of the diaromatic compound*

where π and γ represent the active sites where the aromatic molecules and hydrogen adsorption occur respectively.

All adsorption and desorption steps are equilibrium steps while the reaction is assumed as limiting step:

$$r_1 = k_1 C_T C_\pi - k_1' C_{T\pi} = 0 \quad (6.1)$$

$$r_2 = k_2 P_{H_2} C_\gamma - k_2' C_{H_2\gamma} = 0 \quad (6.2)$$

$$r = k C_{T\pi} C_{H_2\gamma} - k' C_{D\pi} C_\gamma^2 \quad (6.3)$$

$$r_4 = k_4 C_{D\pi} - k_4' C_T C_\pi = 0 \quad (6.4)$$

Therefore using the equilibrium steps to calculate the intermediates of reaction concentrations and writing the balances on the active sites π and γ the Langmuir-Hinshelwood kinetics for the triaromatic hydrogenation is found:

$$r = \frac{k \frac{k_1}{k_1'} \left(\frac{k_2}{k_2'} \right)^2 C_T P_{H_2}^2 - k' \frac{k_4'}{k_4} C_D}{\left(1 + \frac{k_1}{k_1'} C_T + \frac{k_4'}{k_4} C_D \right) \cdot \left(1 + \frac{k_2}{k_2'} P_{H_2} \right)^2} \quad (6.5)$$

In the formula, k and k' are the hydrogenation and dehydrogenation rate constants and P_{H_2} the partial hydrogen pressure. Moreover, each ratio between the direct and the indirect adsorption constant defines the equilibrium adsorption constant

indicated by K . In particular $\frac{k_2}{k_2'} = K_2 = K_{H_2}$ represents the equilibrium adsorption

constant of the hydrogen molecule:

$$r = \frac{kK_1K_{H_2}^2 C_T P_{H_2}^2 - k'K_4 C_D}{(1 + K_1 C_T + K_4 C_D) \cdot (1 + K_{H_2} P_{H_2})^2} \quad (6.6)$$

The denominator of the expression 6.6 is characterized by a product of two different terms coming from the different active sites for the aromatic and the hydrogen molecules. Since they do not have to compete for the occupation of the available active sites and only the term on the left of the denominator needs to describe the competition between the aromatic compounds. Moreover, it emphasizes the strong dependence of the reaction rate from the hydrogen partial pressure.

Some other important considerations can be made about this kinetics:

1. This kind of kinetics is very important because shows that all steps of the hydrogenation, affect the reaction rate by their kinetic parameters but it is not needed to calibrate all these parameters defining an apparent direct kinetic constant and an apparent indirect kinetic constant;
2. By this approach, one reaction at a time is considered and the only competition that appears in the denominator is that between triaromatic and diaromatic compounds (equation 6.6). In truth, many reactions occur at the same time and many compounds simultaneously adsorb on the catalyst surface, therefore the first part of the denominator needs to be extended to describe how they compete to occupy the active sites. The nature of reactions taking place on the same active site is different: hydrogenation, hydrodesulfurization and hydrodenitrogenation reactions can occur. Neglecting, at this moment, the hydrodenitrogenation reaction in agreement with what said in the beginning of the Chapter, the competition between aromatic and sulfur compounds is considered.

Consequently, the kinetic expression will be written as:

$$r = \frac{k^* C_T P_{H_2}^2 - k'^* C_D}{\left(1 + \sum_i K_i C_i\right) \cdot (1 + K_{H_2} P_{H_2})^2} \quad (6.7)$$

where

- $k^* = kK_1K_{H_2}^2$ and $k'^* = k'K_4$
- $\sum_i K_i C_i = K_{sat} C_{sat} + K_{mono} C_{mono} + K_{di} C_{di} + K_{tri} C_{tri} + \sum_j K_{dj} R_j$.

In the last formula, C_{sat} , C_{mono} , C_{di} and C_{tri} represent the concentrations of saturates, monoaromatic, diaromatic and triaromatic classes, while K_{sat} , K_{mono} , K_{di} and K_{tri} their equilibrium adsorption constants. R_j represents a j -th class of refractory sulfur compounds. The presence of this term will be explained in detail afterwards (cf., Paragraph 6.2).

A last hypothesis is made in the derivation of the kinetic expression that is the active sites on the catalyst surface are fully occupied. This is a useful hypothesis because allow neglecting the term 1 into the sum in the denominator simplifying the kinetic expression and the parameters estimation. In fact, even if the values of the adsorption constants are not known for different kinds of catalysts than CoMo/Al₂O₃ one, it is possible to assume the same ratios among the different lumps adsorption constants and the saturates one coming from Korre et al. (1996). In this way the ratios are known and the saturates adsorption constant could be included into the kinetic parameters in the numerator in despite of its absolute value. Therefore, the final kinetics becomes:

$$r = \frac{k^* C_T P_{H_2}^2 - k'^* C_D}{\left(\sum_i K_i C_i \right) \cdot \left(1 + K_{H_2} P_{H_2} \right)^2} \quad (6.8)$$

The approach reported above can be applied on each lump considering the variation of the number of hydrogen molecules involved in the reaction. In this way, omitting the asterisks although the constants remain apparent constants the expression 6.8 is generalized in the following expression:

$$r_j = \frac{k_j C_j P_{H_2}^n - k_j^{-1} C_k}{\left(\sum_i K_i C_i \right) \cdot \left(1 + K_{H_2} P_{H_2} \right)^n} \quad (6.9)$$

where, k_j and k_j^{-1} are the hydrogenation and dehydrogenation rate constants for the j -th lump, K_i the equilibrium adsorption constant of i -th class which competes on the catalyst surface and n the number of hydrogen molecules employed in the hydrogenation.

The kinetics shown in the expression 6.9 represents the final kinetics introduced in the phenomenological hydrogenation model.

6.2 Mechanism and kinetics of hydrodesulfurization of sulfur compounds

Although hundreds of sulfur compounds are typically present in a gasoil, as reported in the previous Chapter (cf. Paragraph 4.2), most of them totally react under the hydrotreatment operating conditions. Hence, they are called labile sulfur compounds and their conversion is described by a first order reaction characterized by a high kinetic constant that describes a quasi- instantaneous reaction. For that reason, the study of hydrodesulfurization reaction focuses on the refractory sulfur compounds conversion primarily justified by the necessity to produce ultra low sulfur diesel. As already said in Chapter 4, they are almost dibenzothiophenes classifiable in four molecular lumps.

The study of their reaction mechanism reported in this thesis, briefly mentioned in the Chapters 2 and 4, is principally based on the work proposed by Gates and Topsøe (1997).

These Authors propose a parallel reaction scheme indicating competitive hydrodesulfurization and hydrogenolysis. The hydrodesulfurization, called also indirect desulfurization, consists in a step by step process beginning with the prehydrogenation followed by the removal of the sulfur atom. Instead, the hydrogenolysis is the direct cleavage of C-S bonds. These two mechanisms have been found by the identification of the hydrodesulfurization products. In fact, two aromatic compounds are the main products of this reaction, biphenyls (BP) and cyclohexylbenzene (CHB) and they are independently obtain through these pathways because under the hydrodesulfurization conditions, biphenyl is not converted readily into cyclohexylbenzene (Van Parijs et al., 1986a, 1986b). As reported in the Fig.6.2, biphenyls are the result of the direct desulfurization that consists in the production of a molecule of H_2S by break of the C-S bond without any hydrogenation of the aromatic rings. On the other hands, cyclohexylbenzenes form by the first hydrogenation of one of the aromatic rings in the alkydibenzothiophene (that produces tetrahydrodibenzothiophene, thDBT) followed by the removal of the sulfur atom.

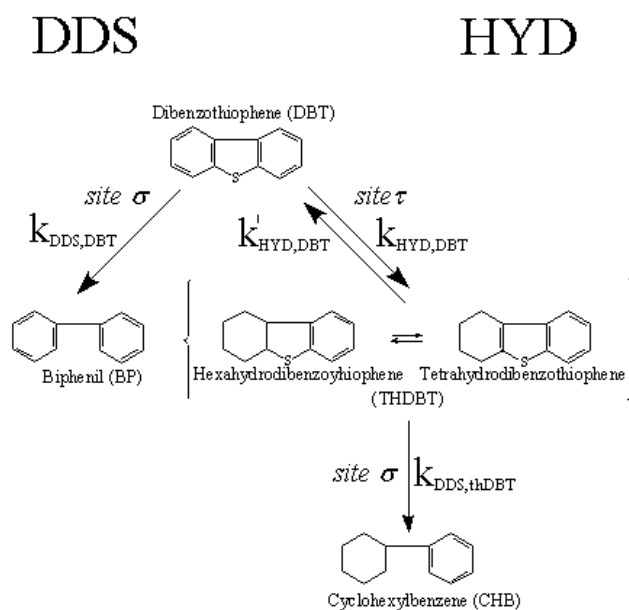


Fig.6. 2 Reaction network for dibenzothiophenes hydrodesulfurization

The most important thing to underline about this network scheme is that the active sites, where the two routes occur, are different. In fact, the direct HDS is assumed to take place on the vacancies of the MoS_2 structure of the catalyst (Erby et al., 2005), called σ , while in the HYD route, the hydrogenation reaction occurs on another site, type π and the hydrogenolysis again on the σ -site (Edvinsson et al., 1993). The existence of two different types of active sites is also proposed from Bataille et al. (2000) and Mijoin et al. (2001) who state that HYD is predominant on the Mo catalyst whereas on the $\text{NiMo}/\text{Al}_2\text{O}_3$ or $\text{CoMo}/\text{Al}_2\text{O}_3$ catalyst the DDS becomes the main pathway. Therefore, the promoter of the catalyst (Ni or Co) does not have the same effect on both reactions because they occur in different parts of the catalyst. In fact, the DDS/HYD selectivity depends on the distribution of intermediates that are formed in the desulfurization and the nature of the catalytic centers on which they adsorb:

- The basic behavior of the anions in the vicinity of the vacancy and the acidity of the SH groups resulting of the heterocyclic dissociation of hydrogen on the vacancy-sulfur anion catalytic pairs;
- The availability and reactivity of hydrogen on the catalytic center.

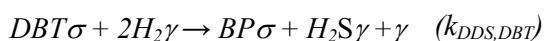
Promoted catalyst is more basic than unpromoted catalyst and therefore it is more reactive in C-S bond cleavage. Because the direct desulfurization occurs by the sulfur atom adsorption, another important factor affects the DDS rate: the steric hindrance of the alkyl-groups that instead do not affect the HYD route.

On the basis on the reaction mechanism shown above, the hydrodesulfurization kinetics is found. Analogously to the hydrogenation reaction, the hypothesis of sites totally occupied is satisfied and they are distinguished from that of hydrogen because their absorption occurred in different active sites. It means the kinetic mechanism is obtained considering three different active sites.

Each pathway of the hydrodesulfurization is described using Langmuir-Hinshelwood kinetics:

Direct desulfurization (DDS):

It occurs on the σ -sites and the different alkylic structures of the various sulfur species strongly affect the adsorption on these sites.



Using the same approach presented in the Paragraph 6.1.2 the DDS kinetics is found:

$$r_{DDS,i} = \frac{k_{DDS} \frac{k_{1,i}}{k'_{1,i}} \left(\frac{k_{2,i}}{k'_{2,i}} \right)^2 C_{DBT} P_{H_2}^2}{\left(1 + \frac{k_{1,i}}{k'_{1,i}} C_{DBT} + \frac{k_{4,i}}{k'_{4,i}} C_{BP} \right) \cdot \left(1 + \frac{k_2}{k'_2} P_{H_2} + \frac{k_5}{k'_5} P_{H_2S} \right)^2} \quad (6.10)$$

The term of the H_2S is removed from the denominator because the amount of the hydrogen sulfide is considered negligible respect to the excess of hydrogen.

In the first part of the denominator, it is reported the competition between the alkyldibenzothiophene and its product but this term should be generalize to describe the competition between all alkyldibenzothiophenes belonging to all four molecular lumps. It is not needed to consider the competition with the aromatic compounds because the hydrodesulfurization occurs on σ -sites but the aromatic hydrogenation occurs on π -sites. Moreover, the term related to biphenyl is taken equal to zero because its adsorption on the σ -site is negligible.

Therefore using the nomenclature mentioned in the Chapter 4 to indicate the refractory sulfur compounds and considering only one adsorption constant for all of them (because of the difficulty to find the real values in the literature) the competition can be described as $K_{refr} (R_1 + R_2 + R_3 + R_4)$. K_{refr} is the adsorption equilibrium constant of the refractory sulfur compounds. In fact, refractory sulfur compounds have a different adsorption constant than labile sulfur and diaromatic compounds because of the steric effect of the alkyl-groups in such groups. For this reason, the several lumps of sulfur should be characterized by different values of K_{refr} because they have a different affinity to the active sites as a function of the alkyl-groups position. Koltai et al. (2002) studied the competitive experiments between 4,6-dmDBT and the aromatics by the kinetic model development of the inhibition between them and they found the ratio of the adsorption equilibrium constants between several compounds and 4,6-dmDBT. For example, they indicated that the ratio between phenanthrene and 4,6-dmDBT is 0.14, therefore knowing the value of the phenanthrene adsorption constant, that of the refractory sulfur compounds has been determined. Unfortunately, few information are available in the literature to determine the other adsorption constants for the remaining sulfur lumps and few data are available to estimate them directly by the model. So, the value of the 4,6dmDBT has been used as constant value of the other three lumps as well being fully aware of the error introduced in the model. This assumption can justify why in the following expression apparent kinetic constants changes for each lump because, although the real kinetic constant is the same for all classes, it includes the different adsorption constants.

Hence, the kinetic expression is generalized:

$$r_{DDS,i} = \frac{k_{DDS,i} C_{DBT} P_{H_2}^2}{(1 + K_{refr} (R_1 + R_2 + R_3 + R_4)) \cdot (1 + K_{H_2} P_{H_2})^2} \quad (6.11)$$

the subscript i represents the i -th lump of the refractory sulfur compounds.

Indirect desulfurization (HYD):

- Hydrogenation of alkylDBT:

The first reaction is the hydrogenation of the alkylDBT and the position of the different alkyl-groups does not affect the adsorption rate. This reaction occurs on the same active sites where the aromatic hydrogenation takes place.





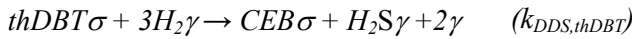
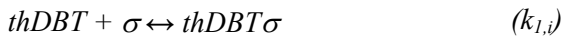
That means it is required to consider the competition not only between all refractory sulfur compounds but also between the aromatic compounds:

$$r_{HYD,DBT} = \frac{k_{HYD,DBT} C_{DBT} P_{H_2}^2 - k'_{HYD,DBT} C_{thDBT}}{\left(\sum_i K_i C_i + K_{di} \sum_{i=1}^4 R_i \right) \left(1 + K_{H_2} P_{H_2} \right)^2} \quad (6.12)$$

In this case, refractory sulfur compounds have the same affinity with other diaromatic compounds to the active sites. In fact, their adsorption on the π -sites is not affected by the presence of the methyl-groups. In agreement to the hypotheses made in terms of hydrogenation, all compounds characterized by the same aromatic structure have the same affinity to the catalyst apart from the side chains presence.

- Hydrogenolysis of thDBT:

The tetrahydrodibenzothiophene is the intermediate of hydrodesulfurization reaction. It undergoes the direct removal of the sulfur atom and similarly to the hydrogenolysis of DBT it adsorbs on the σ -sites.



The kinetics is reported in the expression 6.12

$$r_{DDS,thDBT} = \frac{k_{DDS,thDBT} C_{thDBT} P_{H_2}^3}{\left(1 + K_{refr} (R_1 + R_2 + R_3 + R_4) \right) \cdot \left(1 + K_{H_2} P_{H_2} \right)^3} \quad (6.13)$$

The two kinetic expressions are combined and the complete HYD kinetics is obtained:

$$r_{HYD} = \frac{k_{HYD,DBT} k_{DDS,thDBT} C_{DBT} P_{H_2}^5}{\left(P_{H_2}^3 k_{DDS,thDBT} \left(\sum_i K_i C_i + K_{di} \sum_{i=1}^4 R_i \right) (1 + K_{H_2} P_{H_2})^2 + k'_{HYD,DBT} \left(1 + K_{refr} \sum_{i=1}^4 R_i \right) \cdot (1 + K_{H_2} P_{H_2})^3 \right)} \quad (6.14)$$

where is still $\sum_i K_i C_i = K_{sat} C_{sat} + K_{mono} C_{mono} + K_{di} C_{di} + K_{tri} C_{tri}$.

$$r_{HYD} = \frac{k_{HYD,DBT} C_{DBT} P_{H_2}^5}{\left(P_{H_2}^3 \left(\sum_i K_i C_i + K_{di} \sum_{i=1}^4 R_i \right) (1 + K_{H_2} P_{H_2})^2 + k_{HYD} \left(1 + K_{refr} \sum_{i=1}^4 R_i \right) \cdot (1 + K_{H_2} P_{H_2})^3 \right)} \quad (6.15)$$

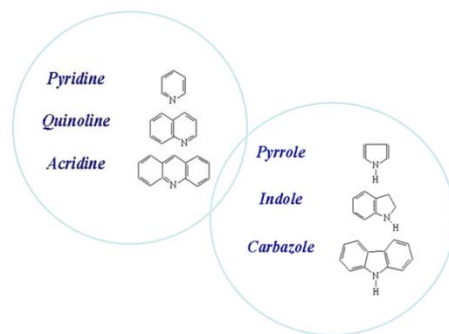
The r_{HYD} kinetics reported in the expression 6.14 can be simplified considering the ratio between the hydrogenation inverse kinetic constant and the hydrogenolysis direct kinetic constant rather than their absolute values. Therefore, a fictitious variable called $k_{HYD}^* = k'_{HYD,DBT} / k_{DDS,thDBT}$ is defined and the equation 6.15 is obtained.

Finally, the total hydrodesulfurization kinetics is the sum of the two pathways contributes.

Depending on the ratios between the different steps contributions in the HYD reaction, the expression 6.15 may be more or less similar to the expression 6.13 form.

Chapter 7

Hydrodenitrogenation kinetics



Although no reference has been presented before on the importance of nitrogen and although it does not have a restrictive bound in terms of environmental specification, it is very important for the reliability of the model. That is because its reaction can strongly affect the other reaction in the hydroprocessing plant and the model cannot disregard the nitrogen cross effect. This is a very innovative aspect of this thesis respect to the literature and then it is worth a specific Chapter.

7.1 Introduction and state of art

Hydrodenitrogenation is one of the reactions considered in the hydrotreatment, though no environmental constraint exists to limit the amount of nitrogen in gasoils. However, the removal of nitrogen is essential to the other reactions of the hydroprocessing and in particular for the hydrodesulfurization reaction. In fact, nitrogen compounds can strongly inhibit this reaction through competitive adsorption. Moreover, the presence of these species, even at low concentrations may limit the catalytic activity and needs the use of higher pressure and temperature to obtain desired conversion of sulfur compounds. Although the competitive adsorption has been recognized since the '50 years, little information is available about the nitrogen inhibitive effect. Several authors have studied the hydrodenitrogenation reaction but most of them have focused on the combined study of hydrodenitrogenation and hydrodesulfurization to study the cross effect of the nitrogen compounds on the sulfur compounds removal.

All authors agree distinguishing all nitrogen compounds in basic and non-basic compounds. They have been studied the nitrogen compounds reactivity and the different inhibitive effect to the sulfur compounds and on different kinds of catalysts.

Laredo et al. (2001 and 2004) studied the inhibition effects of nitrogen compounds on the hydrodesulfurization of dibenzothiophene on CoMo/Al₂O₃ focus on both basic and non-basic compounds like quinoline, indole, carbazole and their mixtures. They claim that inhibiting effect of non-basic nitrogen compounds is comparable to that of basic nitrogen compounds. The inhibiting effect increases in the order Carbazole < Quinoline < Indole and is very strong, even at low concentrations of nitrogen.

Kwak et al. (2001) reported the poisoning effect of carbazole and quinoline on the sulfided NiMoP/Al₂O₃ in the desulfurization of dibenzothiophene, 4-methyldibenzothiophene and 4,6- dimethyldibenzothiophene. The desulfurization of 4-mDBT and 4,6-dmDBT is affected by the presence of the nitrogen compounds even at low concentrations, while the conversion of dibenzothiophene remains nearly unaffected unless the concentration is high. Moreover, quinoline exhibits a stronger poisoning effect than carbazole.

Zeuthen et al. (2001) reported that carbazoles are the predominant N-compounds and they are the basic N-compounds that have the major inhibiting effect on the HDS of diesel fuels.

La Vopa and Satterfield (1988) studied the poisoning of thiophene hydrodesulfurization by nitrogen compounds on a NiMo/Al₂O₃ catalyst. They claimed that the adsorption strength of the inhibitors ammonia < aniline < pyridine < piperidine < quinoline is in agreement with the poisoning of the hydroprocessing catalyst, in particular they reported 5-20 times larger adsorption constants for quinoline than for alkyl aniline in the hydrodesulfurization of thiophene.

Also Furimsky et al. (1999) found out that nitrogen compounds are the most common poisons of the catalyst because of their strong adsorption on the active sites. They studied widely the effect of the nitrogen compounds on catalyst deactivation and their inhibitive effect on the hydrodesulfurization reaction, mentioning many other works concerning this topic.

Moreover, many authors focused on a specific compound proposing their reaction mechanisms to study how the nitrogen compounds conversion occurs. Many works concern the basic compounds, like quinoline (Gultekin et al., 1989; Jian and Prins, 1998a, 1998b; Satterfield and Smith, 1986; Gioia and Lee, 1986; Machida et al., 1999, Prins et al., 1997), acridine (Rabarihoela-Rakotovao et al., 2004) aniline (Prins et al., 1997, Machida et al., 1999), pyridine (Machida et al. 1999). Others are related to the non-basic compounds like carbazole (Nagai et al., 2000; Laredo et al., 2004) and indole (Bunch et al., 2000; Kim et al., 2000).

7.2 Mechanisms of hydrodenitrogenation

Most of nitrogen present in a gasoil is in the form of heterocyclic compounds containing basic or non-basic ring structures.

Non-basic compounds represent the main fraction of the total nitrogen species, about two-thirds of the total nitrogen content in crude oil (Bunch et al., 2000) but the basic compounds are the strongest inhibitors even at a concentration as low as 5 wppm (Laredo et al., 2002). However, strong inhibition of HDS reactions by non-basic compounds has been observed. On the other hands, Sun et al. (2005) affirm that non-basic compounds are more difficult to remove than basic compounds. The difference in their reactivity is attributed to the weaker adsorption strength of non-basic compounds compared to basic species.

Anyway, as reported by Prins et al. (1997), because of the aromaticity of the nitrogen-containing ring in polycyclic aromatics, the nitrogen atom can only be removed after hydrogenation of this ring. In particular, because of the position of the nitrogen atom, basic compounds have a very strong affinity to the hydrogenation active sites.

Unlike hydrogenation and hydrodesulfurization, the hydrodenitrogenation mechanism is not simple to identify and the information available in the literature

about kinetic and adsorption parameters are limited. For this reason, it is not immediate finding the nitrogen compounds kinetics and often they are very complex. In fact, the mechanisms are rather tangled and some nitrogen compounds may produce others nitrogen moieties. This is what happens in the first step of non-basic compounds reaction that usually forms basic nitrogen species (Ho et al., 1991). Hydrodenitrogenation kinetics are found focusing on the quinoline and indole for the basic and non-basic compounds respectively, because they are the main nitrogen compounds present in a cut like gasoil. Their kinetic mechanisms are derived studying the major products coming from their conversion.

Hydrodenitrogenation of quinoline takes place via two parallel pathways. In fact, the major intermediates of reaction are 1,2,3,4-tetrahydroquinoline, obtained by hydrogenation of the aromatic ring containing nitrogen atom and 5,6,7,8-tetrahydroquinoline coming from the saturation of the other aromatic ring. They produce decahydroquinoline but while the final product of the first route is propylbenzene in the second one propylcyclohexane is obtained. For both pathways, the nitrogen atom removal produces ammonia (Fig.7.1).

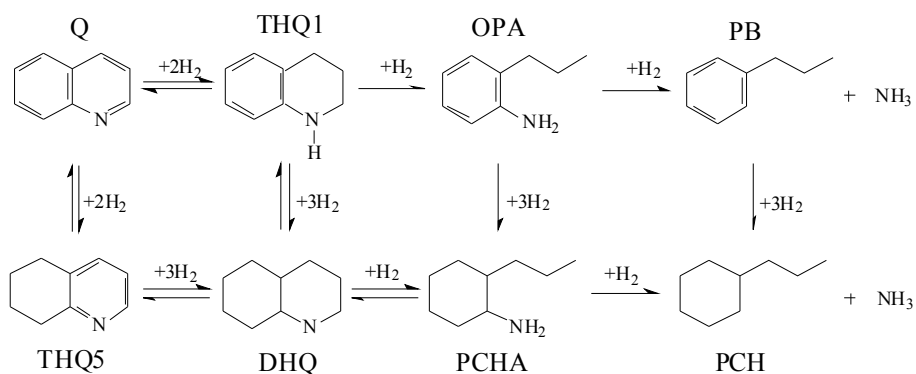


Fig.7. 1 Quinoline HDN complete reaction network

The hydrodenitrogenation of indole starts out with the hydrogenation of the heterocyclic ring in a reversible step that leads to indoline formation. This reaction is characterized by the thermodynamic equilibrium under most operating conditions. Starting from indoline, two different routes may occur. The former concerns the five member heterocyclic atom and leads to the o-ethylaniline formation. The last one is the hydrogenation of the six-member aromatic ring and produces in the beginning octahydroindole and then o-ethylcyclohexylamine. The major final products of this reaction network are ethylbenzene and ethylcyclohexane. In this case also ammonia production occurs.

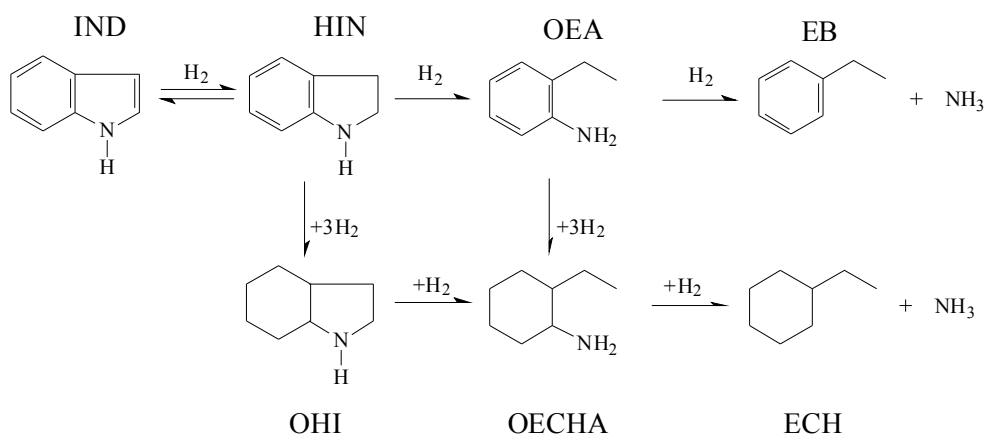


Fig.7. 2 Indole HDN complete reaction network

Both networks show clearly that basic and non-basic compounds conversion needs to undergo first a hydrogenation reaction. In fact, because of the nitrogen atom position its removal from heterocyclic compounds requires the hydrogenation of the ring containing the nitrogen atom before hydrogenolysis of the C-N bond occur. This is required to reduce the relatively large energy of the carbon-nitrogen bonds in such rings and thus permit more facile carbon-nitrogen bond scission (Girgis and Gates, 1991).

Moreover, the first hydrogenation is an equilibrium reaction and the position of this equilibrium can affect nitrogen-removal rates if the rates of the hydrogenolysis reactions are significantly lower than the rates of hydrogenation. Unfavorable hydrogenation equilibrium would result in low concentrations of hydrogenated nitrogen compounds undergoing hydrogenolysis; high hydrogen partial pressures can be used to increase the equilibrium concentrations of saturated hetero-ring compounds to obtain larger HDN rates (Girgis and Gates, 1991).

In addition, Fig.7.1 and Fig.7.2 show that the hydrodenitrogenation network is more complicated than hydrogenation and hydrodesulfurization mechanism. Each reaction step in these networks could be described by a Langmuir-Hinshelwood kinetics, therefore, the total kinetics should be rather complex. Moreover, the situation is further complicated because the first hydrogenation reaction for the non-basic compounds leads to the formation of basic compounds (Laredo et al., 2002). For example, indole is a non-basic compound while indoline is a basic one, pyrrole is non-basic and pyrrolidine is basic, etc. Hence, for each step, it is needed to account the nature of the compounds and the different adsorption strength over the catalyst surface. Literature provides some information about the selectivity of the two pathways. About the quinoline HDN, Jian and Prins (1998a, 1998b) suggest that the concentration of the intermediate DHQ is slightly lower and that of OPA

considerably higher in the presence than in the absence of H_2S . Instead, as reported by Machida et al. (1999), 1,2,3,4-THQ and OPA are the main hydrogenated intermediates when H_2S is present while DHQ without hydrogen sulfide. Consequently, even though the hydrogen sulfide influence is neglected in this work, considering its presence, it has been decided to consider, in agreement with the literature, that the favorite pathway in the quinoline HDN is that in which the hydrogenation of the heterocyclic ring occurs (Fig.7.3):

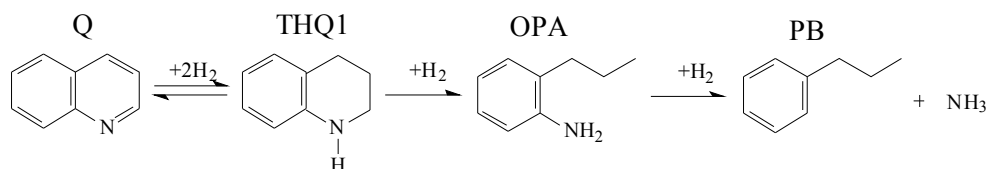


Fig.7. 3 Quinoline HDN simplified reaction network

About indole, Bunch et al. (2000) indicate that the reaction temperature, hydrogen partial pressure and the feed hydrogen sulfide concentration affect the question as to which route is favorite one in the network. The hydrogenolysis reaction to produce OEA is favored by increasing the temperature. Moreover, H_2S and sulfur compounds enhance the hydrogenolysis reaction and inhibit the hydrogenation one. Therefore, similarly to the quinoline, the pathway without hydrogenation of the aromatic ring is chosen as favorite route (Fig.7.4):

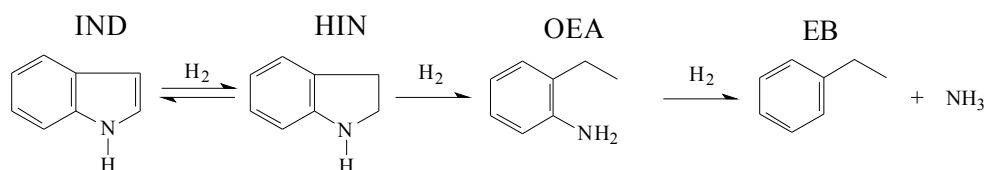


Fig.7. 4 Indole HDN simplified reaction network

7.3 Kinetics of hydrodenitrogenation

The simplified pathways reported in the previous Paragraph are those used to find the hydrodenitrogenation kinetics for all compounds belonging to basic and non-basic compounds. In agreement with the approaches used to find the hydrogenation and the hydrodesulfurization reaction, also to derivate the hydrodenitrogenation kinetics the Langmuir-Hinshelwood kinetics has been chosen.

Quinoline and indole reactions involve a different number of hydrogen molecules, 4 for the former and 3 for the last one, but their schemes are the same including a first hydrogenation that is the equilibrium reaction followed by a hydrogenation and a

hydrogenolysis. To further simplify the mechanism and the achievement of the kinetics and to reduce the number of model parameters to estimate, the first hydrogenation is considered separately and the last two reactions are considered together. Therefore, two steps for the quinoline conversion and indole conversion are obtained involving 2+2 and 1+2 hydrogen molecules respectively. The rate expression for each reaction step is the Langmuir-Hinshelwood kinetics deduced assuming the reaction as limiting step and the other ones in equilibrium. The total kinetics is derived combining each step's expressions.

The treatment may be exposed in generic terms for both types of compounds indicating with n the generic number of hydrogen molecules in the first step and m that one for the last step. The HDN reactions are schematized as



- R represents the reactant, quinoline or indole;
- In represents the intermediate, 1,2,3,4-tetrahydroquinoline or indoline;
- P represents the product, propylbenzene or ethylbenzene

Reversible hydrogenation reaction

This reaction is very important because of the position of the nitrogen atom that does not allow the direct removal. That is the reason why nitrogen compounds, in particular the basic species, have on the contrary a very strong affinity to the π -sites. In fact, hydrogenation step of HDN occurs over the same active sites where hydrogenation and indirect hydrodesulfurization occur.

Therefore, the nitrogen compounds must compete with all compounds present in gasoil to occupy the active sites of the catalyst. This competition is described in the expression afterwards reported:

$$r = \frac{k_1 C_R P_{H_2}^n - k_1' C_{In}}{\left(1 + \sum_i K_i C_i + K_{di} \sum_{i=1}^4 R_i + K_B^\tau C_B + K_{NB}^\tau C_{NB}\right) \left(1 + K_{H_2} P_{H_2}\right)^n} \quad (7.2)$$

The first part of the denominator is characterized by the presence of:

- Aromatic compounds $\left[\sum_i K_i C_i \right]$;
- Sulfur compounds $\left[K_{di} \sum_{i=1}^4 R_i \right]$;

- Nitrogen compounds $\left[K_B^\tau C_B + K_{NB}^\tau C_{NB} \right]$

where the different affinity of these compounds to the catalyst surface is represented by different values of their adsorption constants. In particular, K_B^τ and K_{NB}^τ are the nitrogen adsorption constants over the π -sites, different from those over σ -sites. Moreover, in the formula k_I and k_I' are the direct and indirect kinetic constants, C_B and C_{NB} the concentrations of the basic and non-basic compounds respectively.

Hydrogenolysis reaction

The hydrogenolysis is not an equilibrium reaction and it occurs only after hydrogenation step reduces the activation energy of the C-N bond cleavage. This step occurs on the same active sites where the direct desulfurization occurs after the intermediate of the previous reaction desorbs from the π -sites and adsorbs on the σ -sites. In this case, nitrogen compounds do not compete with the aromatic compounds but only with the refractory sulfur compounds. For this reason, the denominator of the hydrogenolysis step is simpler than that of hydrogenation step. Still considering the reaction 7.1, the following kinetic expression has been derived:

$$r = \frac{k_2 C_{In} P_{H_2}^m}{\left(1 + K_{refr} \sum_{i=1}^4 R_i + K_B^\sigma C_B + K_{NB}^\sigma C_{NB} \right) \left(1 + K_{H_2} P_{H_2} \right)^m} \quad (7.3)$$

where, k_2 is the hydrogenolysis direct kinetic constant, C_B and C_{NB} still the concentrations of the basic and non-basic compounds and K_B^σ and K_{NB}^σ their adsorption constants over the σ -sites.

Once the Langmuir-Hinshelwood kinetics of every step has been found, the total kinetics is derived as their combination.

$$r_{HDN} = \frac{k_1 k_2 C_R P_{H_2}^{n+m}}{\left(Den^\sigma + Den^\tau \right)} \quad (7.4)$$

The equation above is reported in a compact form which terms are made explicit below:

$$Den^\sigma = k_i' \left(1 + Den_S^\sigma + Den_N^\sigma \right) \left(1 + K_{H_2} P_{H_2} \right)^m \quad (7.5a)$$

$$Den^\tau = k_2 P_{H_2}^m \left(1 + Den_A^\tau + Den_S^\tau + Den_N^\tau \right) \left(1 + K_{H_2} P_{H_2} \right)^n \quad (7.5b)$$

$$Den_S^\sigma = K_{refr} \sum_{i=1}^4 R_i \quad (7.5c) \quad Den_A^\tau = \sum_i K_i C_i \quad (7.5d)$$

$$Den_N^\sigma = K_B^\sigma C_B + K_{NB}^\sigma C_{NB} \quad (7.5e) \quad Den_N^\tau = K_B^\tau C_B + K_{NB}^\tau C_{NB} \quad (7.5f)$$

$$Den_S^\tau = K_{di} \sum_{i=1}^4 R_i \quad (7.5g)$$

The terms in the denominator are the same for both nitrogen classes. Using this nomenclature, the generic expression 7.4 may be written explicitly for basic and non-basic compounds generalizing the expression of quinoline and indole for all compounds belonging to their classes:

Basic compounds:

$$r_{HDN}^B = \frac{k_1^B k_2^B C_B P_{H_2}^4}{(Den_B^\sigma + Den_B^\tau)} \quad (7.6)$$

Non-basic compounds:

$$r_{HDN}^N = \frac{k_1^{NB} k_2^{NB} C_{NB} P_{H_2}^3}{(Den_{NB}^\sigma + Den_{NB}^\tau)} \quad (7.7)$$

where

$$Den_B^\sigma = k_1'^B (1 + Den_S^\sigma + Den_N^\sigma) (1 + K_{H_2} P_{H_2})^2 \quad (7.8a)$$

$$Den_B^\tau = k_2^B P_{H_2}^2 (1 + Den_A^\tau + Den_S^\tau + Den_N^\tau) (1 + K_{H_2} P_{H_2})^2 \quad (7.8b)$$

$$Den_{NB}^\sigma = k_1'^{NB} (1 + Den_S^\sigma + Den_N^\sigma) (1 + K_{H_2} P_{H_2})^2 \quad (7.8c)$$

$$Den_{NB}^\tau = k_2^{NB} P_{H_2}^2 (1 + Den_A^\tau + Den_S^\tau + Den_N^\tau) (1 + K_{H_2} P_{H_2})^2 \quad (7.8d)$$

The equations 7.6 and 7.7 are detailed enough to correctly describe the hydrodenitrogenation reaction and the competition between the several compounds of gasoil. Many HDN parameters are present in the equations, some of them are found in the literature. For example, Koltai et al. (2002) indicate that the ratio between the adsorption equilibrium constants over σ -sites (K_B^σ and K_{NB}^σ) and 4,6dm-DBT are 34.18 and 10.01, respectively. Because of the knowledge of constant value of the refractory sulfur compounds, K_B^σ and K_{NB}^σ are also known. On the contrary, the remaining parameters should be estimated. Six of them are the kinetic constants for both classes of nitrogen compounds -

$k_1^B, k_2^B, k_1^{Bt}, k_1^{NB}, k_2^{NB}, k_1^{NBt}$ -and the last two are the equilibrium adsorption constants over the π -sites - K_B^τ, K_{NB}^τ . In order to limit the parameter number of the model, consenting to know the ratio between the hydrogenation inverse kinetic constant and the hydrogenolysis direct kinetic constant rather than their absolute values the kinetics are still further simplified. Therefore, for each nitrogen lump, this ratio is used as a fictitious variable called k^* as reported in the expressions 7.9 and 7.10:

Basic compounds:

$$r_{HDN}^B = \frac{k_1^B C_B P_{H_2}^4}{\left(k_B^* (1 + Den_S^\sigma + Den_N^\sigma) (1 + K_{H_2} P_{H_2})^2 + P_{H_2}^2 (1 + Den_A^\tau + Den_S^\tau + Den_N^\tau) (1 + K_{H_2} P_{H_2})^2 \right)} \quad (7.9)$$

Non-Basic compounds:

$$r_{HDN}^N = \frac{k_1^{NB} C_{NB} P_{H_2}^3}{\left(k_{NB}^* (1 + Den_S^\sigma + Den_N^\sigma) (1 + K_{H_2} P_{H_2})^2 + P_{H_2}^2 (1 + Den_A^\tau + Den_S^\tau + Den_N^\tau) (1 + K_{H_2} P_{H_2})^2 \right)} \quad (7.10)$$

In this way, the number of parameters directly related to the HDN is reduced to six. They add to the hydrogenation and hydrodesulfurization parameters, some among them are present in the hydrodenitrogenation kinetics as well (HDA and HDS equilibrium adsorption constants).

7.4 Inhibition effect of the nitrogen compounds

Hydrogenation and hydrodesulfurization have been discussed in Chapter 6 but studying the hydrodenitrogenation, the competition between all these reactions is emerged, this because they occur on the same active sites of the catalyst, they must compete to occupy the available vacancies in order to adsorb and react. This competition has been already accounted in the HDN kinetics but right now it is clear that even the HDA and HDS need to be changed to consider the cross effect of the nitrogen compounds. Nevertheless, although what just said, sometimes the nitrogen inhibition could be negligible. The negligibility of the inhibition effect is related to the concentrations of the several compounds of gasoil. This is the motivation why the nitrogen conversion never affects the hydrogenation reaction. In fact, considering a typical feedstock of the hydroprocessing plant (SRGO or LCO or their mixture), it is possible to observe that, while the order of magnitude of the aromatic

compounds is some percent, in terms of sulfur and nitrogen compounds it is hundred of wppm. Consequently, the concentration of nitrogen is always lesser than aromatic concentration and they do not feel the effect of inhibition effect.

Instead, the nitrogen conversion can become very important to correctly describe the hydrodesulfurization because in this case the sulfur and the nitrogen compounds contents are comparable. Therefore, they have to compete to adsorb on the catalyst surface and this competition is still more important when the level of nitrogen and sulfur compounds are very low. In fact as suggested by Laredo et al. (2003), the inhibition behavior of these compounds is highly non-linear, showing strong inhibition at concentrations as low as 28 wppm (as nitrogen compounds). They also say that the coverage of active sites by nitrogen compounds is established on the early stages of the reaction and remains nearly constant throughout the experiment. This shows that their inhibiting behavior is due to a strong initial adsorption of the nitrogen compound and a slow kinetics of desorption, rather than to the hydrogenation of the non-basic species to basic ones.

The results reported in the next Chapter show a good prediction of the experimental data even without nitrogen effect because the feedstock are characterized by the same high level of sulfur and nitrogen species. In fact, in this case, although the inhibition effect exists, it is felt very low and the model behaves well both considering or not the nitrogen presence, the error introduced is negligible.

Anyway, in general competition between aromatic, sulfur and nitrogen compounds exists and the kinetic expressions 6.8 and 6.14 should be generalized introducing the cross effect of the nitrogen compounds on the hydrogenation and hydrodesulfurization reactions.

Hydrogenation reaction:

$$r = \frac{k^* C_T P_{H_2}^2 - k^* C_D}{\left(1 + \sum_i K_i C_i + K_{di} \sum_{i=1}^4 R_i + K_B^\tau C_B + K_{NB}^\tau C_{NB}\right) \cdot (1 + K_{H_2} P_{H_2})^2} \quad (7.11)$$

Hydrodesulfurization reaction:

$$r = \frac{k_{DDS,thDBT} C_{thDBT} P_{H_2}^3}{\left(1 + K_{refr} \sum_{i=1}^4 R_i + K_B^\sigma C_B + K_{NB}^\sigma C_{NB}\right) \cdot (1 + K_{H_2} P_{H_2})^3} + \frac{k_{HYD,DBT} C_{DBT} P_{H_2}^5}{\left(P_{H_2}^3 \left(\sum_i K_i C_i + K_{di} \sum_{i=1}^4 R_i + K_B^\tau C_B + K_{NB}^\tau C_{NB}\right) (1 + K_{H_2} P_{H_2})^2 + k_{HYD} \left(1 + K_{refr} \sum_{i=1}^4 R_i + K_B^\sigma C_B + K_{NB}^\sigma C_{NB}\right) \cdot (1 + K_{H_2} P_{H_2})^3\right)} \quad (7.12)$$

It is very important to underline how the competition between the different compounds is described for HDA and HDS in the same manner used in the Paragraph 7.3 to describe HDN reaction.

In fact, summarizing:

Hydrogenation reaction occurs only over π -sites of the catalyst;

- Hydrodesulfurization has two pathways:
 - DDS that occurs only over σ -sites;
 - HYD that occurs firstly on the π -sites and then on the σ -sites;
- Hydrodenitrogenation that occurs firstly on the π -sites and then on the σ -sites;

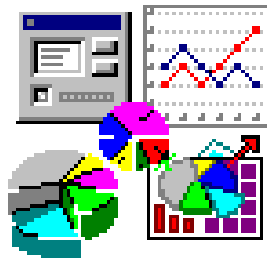
Therefore, over π -sites HDA, HDS and HDN simultaneously occur and over σ -sites only HDS and HDN occur.

To correctly describe the hydrogenation reaction all compounds are considered, the refractory sulfur compounds adsorb by the diaromatic adsorption constant and nitrogen compounds by K_B^τ, K_{NB}^τ .

Instead, the direct desulfurization just considers the competition of sulfur and nitrogen by the constants $K_{refr}, K_B^\tau, K_{NB}^\tau$ while the indirect desulfurization considers in part this same competition and in part the same competition of the hydrogenation. The results considering inhibition effect of the nitrogen compounds will be presented in next Chapter.

Chapter 8

Model results



In this Chapter, it will be presented how the model has been applied with different operating conditions and catalysts in order to verify its behavior with real feeds. The results show the model ability to interpret experimental data for different catalysts, operating conditions and feeds. Finally, the application to a real industrial reactor will be presented.

8.1. Introduction

In the thesis Introduction, it has been stated that two motivations, often conflicting, are the objectives of the hydroprocessing optimization. The conflict is due to the attempts to satisfy environmental specifications processing the remaining low quality oils on one side, and to satisfy the day-by-day increasing gasoil demand on the other one.

In the specific instance, the goal of the model formulation to simulate the hydrotreatment is to optimize the operating plant conditions, to be able to satisfy the two conflicting objectives exposed above whichever the crude oil is processed in the refinery.

Therefore, the goal of the model is to optimize the hydroprocessing operating conditions like flow rate, temperature and pressure (only during design phase) as a function of feed properties.

For this reason, many experiments have been carried out using different feedstock and operating conditions. Different types of catalysts have been also used. Afterwards the experimental campaign is reported (Table 8.1) along with the specific purpose of each test. In fact, some of these experiments have been used to define the HDA, HDS and HDN kinetics and to calibrate the kinetic and equilibrium parameters. The remaining has been used to demonstrate the reliability of the model. As shown in the Table 8.1, the model realization consisted of a combination of a kinetic study and the parameters estimation.

	<i>Catalyst</i>	<i>Feed and modality</i>	<i>Operating conditions</i>	<i>Purpose</i>
<i>Set#1</i>	<i>cat 1</i>	<i>SRGO/LCO HT</i>	<i>T = 330 °C P = 30 – 90 bar LHSV = 1.5 – 2.0 h⁻¹</i>	<i>HDA kinetics definition and tuning of the parameters, HDS kinetics definition</i>
<i>Set#2</i>	<i>cat 1</i>	<i>SRGO HT</i>	<i>T = 330 °C P = 45 – 90 bar LHSV = 1.1 – 1.8 h⁻¹</i>	<i>Test HDA kinetics, HDS kinetics definition</i>
<i>Set#3</i>	<i>cat 1</i>	<i>LCO HT</i>	<i>T = 330 – 365 °C P = 30 – 90 bar LHSV = 1.7 – 2.4 h⁻¹</i>	<i>HDA kinetics definition, tuning of the parameters as a function of the temperature</i>
<i>Set#4</i>	<i>cat 2</i>	<i>SRGO HT</i>	<i>T = 330 °C P = 30 – 90 bar LHSV = 1.5 – 2.0 h⁻¹</i>	<i>HDA kinetics definition and tuning of the parameters, HDS kinetics definition HDN kinetics definition and tuning of the parameters</i>
<i>Set#5</i>	<i>cat 2</i>	<i>SRGO HT</i>	<i>T = 330 – 380 °C P = 75 – 90 bar</i>	<i>Test HDA and HDS kinetic, HDN kinetics definition and</i>

Set#6	cat 2	SRGO HT	$LHSV = 1.0 - 2.0 h^{-1}$	<i>tuning of the parameters</i>
			$T = 330 - 365 \text{ }^{\circ}\text{C}$	<i>Test HDA and HDS kinetic</i>
Set#7	cat 2	SRGO/LCO HT	$P = 60 - 90 \text{ bar}$	<i>HDN kinetics definition and</i>
			$LHSV = 1.5 h^{-1}$	<i>tuning of the parameters</i>
			$T = 350 - 380 \text{ }^{\circ}\text{C}$	<i>Tuning of the parameters</i>
Set#8	cat 2	VGO HT	$P = 90 \text{ bar}$	<i>and test HDA kinetics</i>
			$LHSV = 1.5 h^{-1}$	
Set#9	cat 2	VGO MHC	$T = 365 \text{ }^{\circ}\text{C}$	<i>Test HDA and HDS kinetic</i>
			$P = 75 - 90 \text{ bar}$	
			$LHSV = 1.0 - 1.5 h^{-1}$	
			$T = 390 \text{ }^{\circ}\text{C}$	<i>Test HDA and HDS kinetic</i>
			$P = 90 \text{ bar}$	<i>and HC</i>
			$LHSV = 1.0 - 1.5 h^{-1}$	

Table 8.1 Pilot unit experimental campaign for the model calibration and verification

In Table 8.1, the first kind of catalyst (cat 1) used in the tests (NiMo/Al₂O₃, Set#1, Set#2, Set#3) is a catalyst of second-last generation, particularly suitable for the model calibration because over that the hydrogenation of monoaromatic compounds results negligible and the total aromatic content is almost constant. This catalyst has been used for the hydroprocessing of SRGO, LCO and their mixtures in order to have availability of several lumps concentrations to properly consider their competitive adsorption. The second catalyst (cat 2) is a new generation catalyst that realizes a deep hydrogenation, with particular reference to the hydrogenation of monoaromatic compounds. Four tests have been carried out (Set#4, Set#5, Set#6, Set#7) using this catalyst to realize the hydrotreatment of gasoil and gasoil-LCO mixture while other two (Set#8 and Set#9) are carried out to realize the hydrotreatment and the hydrocracking of VGO (Vacuum Gas Oil).

In the next Paragraphs, the results in term of aromatic, sulfur and nitrogen compounds will be presented, specifying each time if the considered test is a calibration test or a prediction test. The parameters estimation has been carried out initially considering only one level of temperature equal to 330°C. At this level, the hydroprocessing is not very excessive and the concentrations of aromatics and above all sulfur are very high. However, even if it is known that this temperature level cannot satisfy the objectives of this work and does not represent the operating condition chosen in the industrial reality, its choice for the parameters estimation is not casual. In fact, this is the condition where the reversible reactions are controlled by the direct reaction, otherwise for higher values of temperature, the reactions are controlled by the equilibrium and the calibration of the direct and indirect kinetic constants becomes impossible. Moreover, different levels of pressure have been consider because varying this parameter the transition from the kinetic control to the equilibrium control moves to higher temperature. That means, at 330°C, for low levels of pressure, the reactions are close to the equilibrium and for high levels they

are totally controlled by the direct reaction. Therefore, 330°C is a good choice to estimate both equilibrium and kinetic constants.

Once these parameters have been derived for this level of temperature, the equations 2.4 and 2.5 have been used to find the equilibrium and the kinetic constants for different levels of temperature (cf. Paragraph 2.2.1). Therefore, some of the tests for higher levels of temperature have been performed to estimate the activation energies while the adsorption constants have been found directly in the literature. The typical values of the heats of reaction are reported in the Fig.8.1

Reaction	Δh_{reaz} [kcal/mol]	Δh_{reaz} [kcal/mol _{H₂}]
Phenanthrene → Tetrahydrophenanthrene	-31.9	-15.95
Tetrahydrophenanthrene → Octahydrophenanthrene	-31.2	-15.6
Dibenzothiophene → Biphenyl		-11
Biphenyl → Cyclohexylbenzene	-51.7	-17.23
Phenyl-naphthalene → Phenyltetralin		-16.7
Phenyltetralin → Cyclohexyltetralin		-17.23
Naphthalene → Tetralin	-34	-16.7
Benzothiophene → Alkylbenzene	-22.48	-7.49
Indole → Indoline	-13	
Quinoline → 1,2,3,4-Tetrahydroquinoline	-30	

References for the table:

- Korre et al. (1994)
- Girgis and Gates (1991)
- The ΔH of phenyl-naphthalene is the same of naphthalene
- The ΔH of phenyltetralin is the same of biphenyl
- Jaffe (1974)
- Furimsky et al. 1999
- The ΔH of benzothiophene is calculated by the Hess law because of the difficulties to find the value in the literature

		References
Olefine Saturation	-27+/-30 [kcal/mole _{H₂}]	Jaffe 1974
Aromatic Saturation	-14.5+/-16.5 [kcal/mole _{H₂}]	Jaffe 1974/Stanislaus and Cooper 1994
Cracking	-7+/-10 [kcal/mole _{H₂}]	Jaffe 1974
Hydrodesulfurization	-11+/-22 [kcal/mole _{H₂}]	Schuit and Gates 1973

Fig.8. 1 Typical values of heats of reaction for hydrogenation, hydrodesulfurization and hydrodenitrogenation

8.2 Preliminary remarks

In the previous Chapters, the importance of nitrogen inhibition effect has been underlined; especially over refractory compounds desulphurization reactions. The cross effect study represents one of the most important evolutions for this work even to deduct the kinetics for the different hydroprocessing reactions. However, in

agreement with the literature, initially this work neglected the effect of nitrogen on the sulfur compounds conversion. For this reason when the tests with the first kind of catalyst have been realized none experimental analysis has been made to estimate the total nitrogen content. Therefore, only the tests corresponding to the catalyst 2 considered simultaneously hydrodesulfurization and hydrodenitrogenation. Anyway, almost all tests led with the pilot unit have been realized using feeding gasoils and operating conditions for which the competition effect between nitrogen and sulfur was not so strong. Only one among the following reported tests represents a run during which the inhibition effect was significant (Set#6).

However, both the experimental and in model results show that the sulfur concentration in hydrotreated products is very low only when nitrogen is almost fully removed. On the contrary, whenever the nitrogen concentration at the outlet remains high, then the sulfur never reaches low values of concentration. This demonstrates that the competition effect exists and it should be taken into account.

Finally, the model has been applied to an industrial reactor too. This test is significant as far as the competition effect is concerned with, because it shows the model inability to predict correctly sulfur without considering also the nitrogen. On the other hand, it demonstrated that including inhibition effect it is again possible to describe in the right way both the content and the distribution of sulfur compounds in the hydrotreated products. Such results will be presented in terms of macroclasses in the end of this Chapter. None reference to the refinery, the industrial reactor description, the operating conditions used will be reported due to confidential agreement.

8.3 Hydrogenation results for a low level of temperature: catalyst 1 (cat 1)

8.3.1 Calibration test (Set #1)

The test used for the calibration of the model over the first catalyst (NiMo/Al₂O₃, trilobe, DN 1.3 mm) has been realized processing a mixture of straight run gasoil and light cycle oil. The feed properties are synthetically shown in the Table 8.2.

Proprieties	S.I. Unit	Value	Method
Density	kg/m ³	862.1	ASTM D4052-96
Sulfur	wppm	2325	ISO 14596 ASTM D5453-04
Monoaromatics	%w	18.1	EN 12916-2000

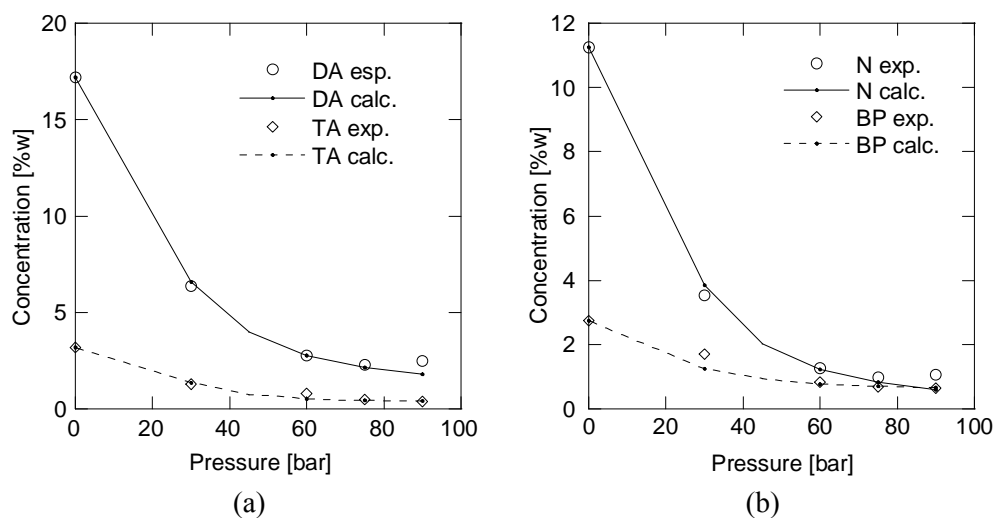
Diaromatics	%w	17.2
Triaromatics	%w	3.3
Total Aromatics	%w	38.6

Table 8.2 Properties of the mixture (SRGO+LCO) used in Set#1

A volume of catalyst equal to 50 cm³ has been diluted with a same volume of an inert material (carborundum, 0.1 mm) and the mixture has been divided in two catalytic beds, separated with narrow layers of glass wool (cf. Paragraph 3.1.3). In the top and in the bottom of the reactor another inert material is still present (CSi 1.19 mm).

The operating temperature of 330°C has been defined in order to work in kinetic regime, reducing at the same time the hydrogenation of the monoaromatic compounds. This temperature has been kept constant during all the sequence of the runs. The pressure has been changed from 30 to 90 bar in order to observe the dehydrogenation reaction effect. The value of LHSV has been kept approximately close to 1.7 h⁻¹ while the gas flow-rate has been chosen in order to have a ratio between the hydrogen and the gasoil ratio (H₂/Oil) equal to 200 NI/l.

Some results of this test are reported in the Fig.8.2, compared to the experimental data. The feed weight fraction of the aromatic compounds is reported next to zero of the abscissa.



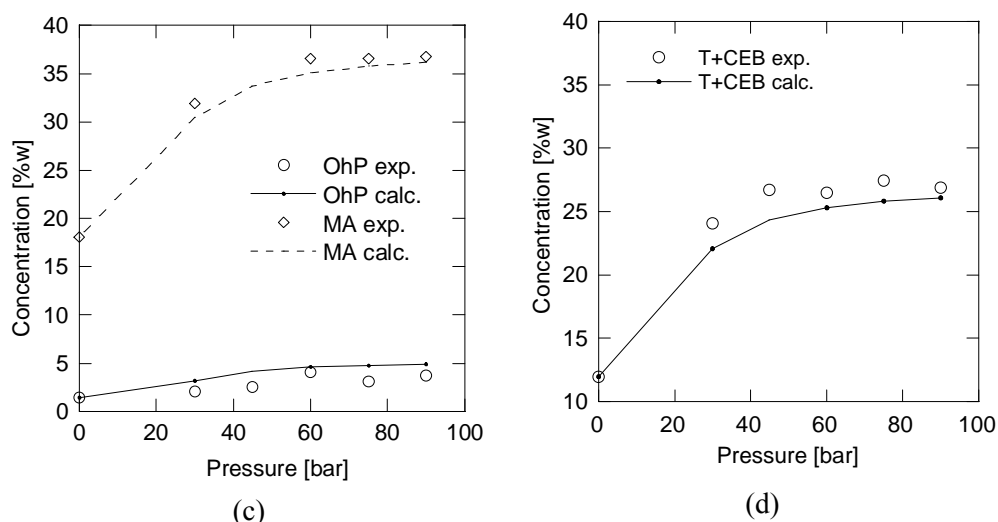


Fig. 8. 2 Hydrogenation: Comparison between experimental data and model results (Set#1)

The Fig.8.2a shows a very good agreement between the experimental data and the model results in terms of diaromatic and triaromatic compounds, ranging the pressure. Moreover, the model is able to consider the moderated variations of the LHSV. The content of the macro-classes is calculated as a sum of the concentrations of the several lumps identified in the Paragraph 6.1.1. Therefore, a detailed analysis of the Fig.8.2b, Fig.8.2c and Fig.8.2d, for the main molecular lumps, should be very useful to understand better the results for the monoaromatic, diaromatic and triaromatic macro-classes. For example, in the Fig. 8.2b it is possible to observe how the slight overestimation of the diaromatics conversion at 90 bar (4.5%) is imputable to the slight overvaluation of the naphthalenes conversion (4%). Concerning the monoaromatic class, in the Fig. 8.2d cyclohexylbenzenes and tetralins are shown. The differences between experimental and calculated values are mainly related to the limitations of the deconvolution in the repartition of the monoaromatic lumps. That causes a 2% as percentage error in the description of monoaromatic compounds in the hydrotreated products.

There are two aspects important to consider in the comparison between the experimental data and the model results. Firstly, the concentrations of monoaromatic, diaromatic and triaromatic compounds are experimentally determined by the EN12916 method that intrinsically introduces an error. Secondly, the estimation of the lumps concentrations is affected also by the error inherent to the deconvolution method (cf. Appendix).

The first kind of error may be accounted knowing the reproducibility and repeatability values associated to the macro-classes because of the method (Table 8.3):

	Range [%w]	Experimental concentration [%w]	Repeatability	Reproducibility
MA	4 ÷ 40	18	± 0.9	± 2.2
	4 ÷ 40	36	± 1.3	± 3.4
DA	0 ÷ 20	17	± 2.0	± 6.0
	0 ÷ 20	3	± 0.6	± 1.5
TA	0 ÷ 6	3	± 0.4	± 2.1
	0 ÷ 6	0.5	± 0.1	± 0.5
Total	4 ÷ 65	40	± 1.5	± 5.4
aromatics	4 ÷ 65	30	± 1.1	± 4.2

Table 8.3 precision parameters of the EN12916 method

For the second one it is not very simple to find a solution and, as reported in the Appendix, a methodology able to objectively describe the position and the area of the peaks overlapped in the chromatogram is going to be realized.

8.3.2 1st Validation test (Set #2)

For the model validation, another experimental test has been used. It is independent respect to the calibration test, in order to verify the model for a feed different from the previous one in terms of aromatic and sulfur content). In this case, the feed is a straight run gasoil with low sulfur content. The characteristics of the feed are reported in the Table 8.4

Proprieties	S.I. Unit	Value	Method
Density	kg/m ³	846.7	ASTM D4052-96
Sulfur	wppm	1548	ISO 14596
			ASTM D5453-04
Monoaromatics	%w	16.4	EN 12916-2000
Diaromatics	%w	11.8	
Triaromatics	%w	3.5	
Total Aromatics	%w	31.7	

Table 8.4 Properties of feed (SRGO) used in Set#2

No fraction of LCO is present in this feed and it is different to the feed of the Set#1. In fact, a comparison between Table 8.2 and Table 8.4 shows a difference in the total aromatic content, 38.6% for the mixture and 31.7% for gasoil. They are

especially related to the diaromatic compounds (17.2% for the mixture and 11.8% for gasoil) while monoaromatics and triaromatics are almost the same. The operating conditions of Set#2 have been chosen equal to Set#1, in order to use the same parameters. The results are reported in the Fig.8.3. They show that, although this test is a simple prediction and although the distribution in the feed is completely different, the model is able to correctly describe the concentration of the polyaromatic compounds in the hydrotreated products (Fig.8.3a). Similarly, to the Fig.8.2, the concentrations of some diaromatic (naphthalene, biphenyls, tetrahydrophenanthrenes, Fig.8.3b and Fig.8.3d) and monoaromatic compounds (octahydrophenanthrenes and tetralin, Fig 8.3c and Fig.8.3d) are reported as a function of the pressure. All figures show that a good agreement between the experimental and calculated concentrations of the lumps exists.

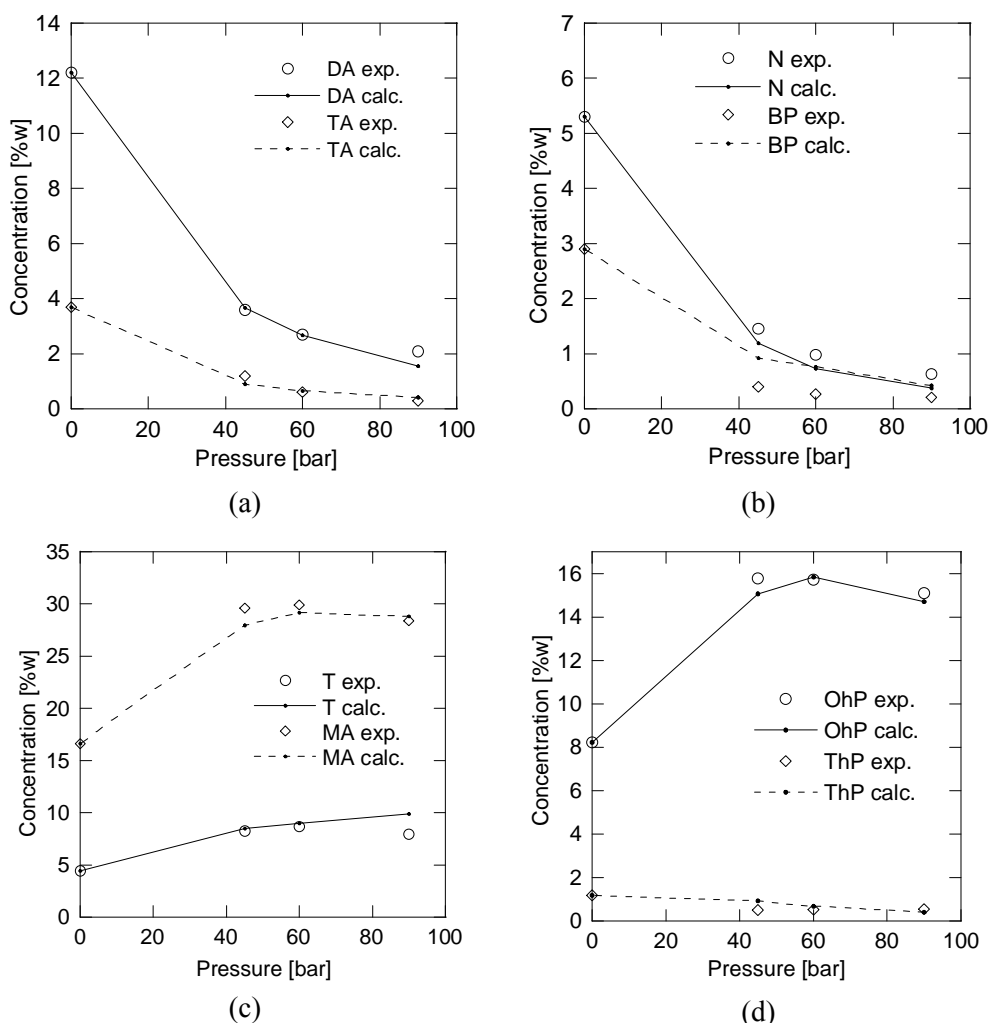


Fig. 8. 3 Hydrogenation: Comparison between experimental data and model results (Set#2)

8.3.3 2nd Validation test (Set #3)

The second validation test has been realized using pure LCO characterized by a high level of aromatic components (59%w) and in particular high concentration of triaromatic species (8.4%w). The Table 8.5 shows the properties of the feed, particular attention should be dedicated to the density that is higher than the other tests because of the high percentage of aromatic compounds.

Proprieties	S.I. Unit	Value	Method
Density	kg/m ³	901.7	ASTM D4052-96
Sulfur	wppm	2440	ISO 14596 ASTM D5453-04
Monoaromatics	%w	27.7	
Diaromatics	%w	22.9	
Triaromatics	%w	8.4	EN 12916-2000
Total Aromatics	%w	59.0	

Table 8.5 Properties of feed (LCO) used in Set#3

Concerning the operating conditions, the same range of Set#1 and Set#2 pressures has been used while the LHSV has been changed into a wider range (1.7 - 2.6 h⁻¹). The temperature level is 327°C, very close to the previous test. Therefore neglecting these few degrees, the equilibrium and the kinetic constants have been used without any parameter adjustment for a direct prediction of the experimental data. The comparison between experimental and model data for such level of temperature is reported in the Fig.8.4.

A good prediction is obtained in terms of triaromatics and diaromatics in Fig.8.4a, while some small discrepancies are shown for monoaromatics in Fig.8.4c. Also analyzing in detail the diaromatic prediction, a small deviation exists between experimental and model data in terms of naphthalenes and biphenyls. Anyway, the reasons are attributable to the limitation of the monoaromatic speciation by the deconvolution method. The Fig.8.4a deserves particular attention because allows to observe how increasing the pressure from 60 to 75 bar and increasing the LHSV from 1.7 to 2.6 h⁻¹, the conversion of tri- and diaromatic compounds significantly decreases. That implies that the effect of LHSV increase (or the reduction of the permanence time inside the reactor) is more important than the effect of the pressure. Moreover, Fig.8.4a shows as such effect is evident both in the experimental and in the model trends.

Anyway, overall, this test with the test of the Set#2 demonstrates a very reliability of the model. In fact, the model is able to predict the composition of the hydrotreated

products for different situations in terms of processed feeds and operating conditions. In particular, it is very able to feel the change of the flow rate and pressure into a typical range for the hydroprocessing plant.

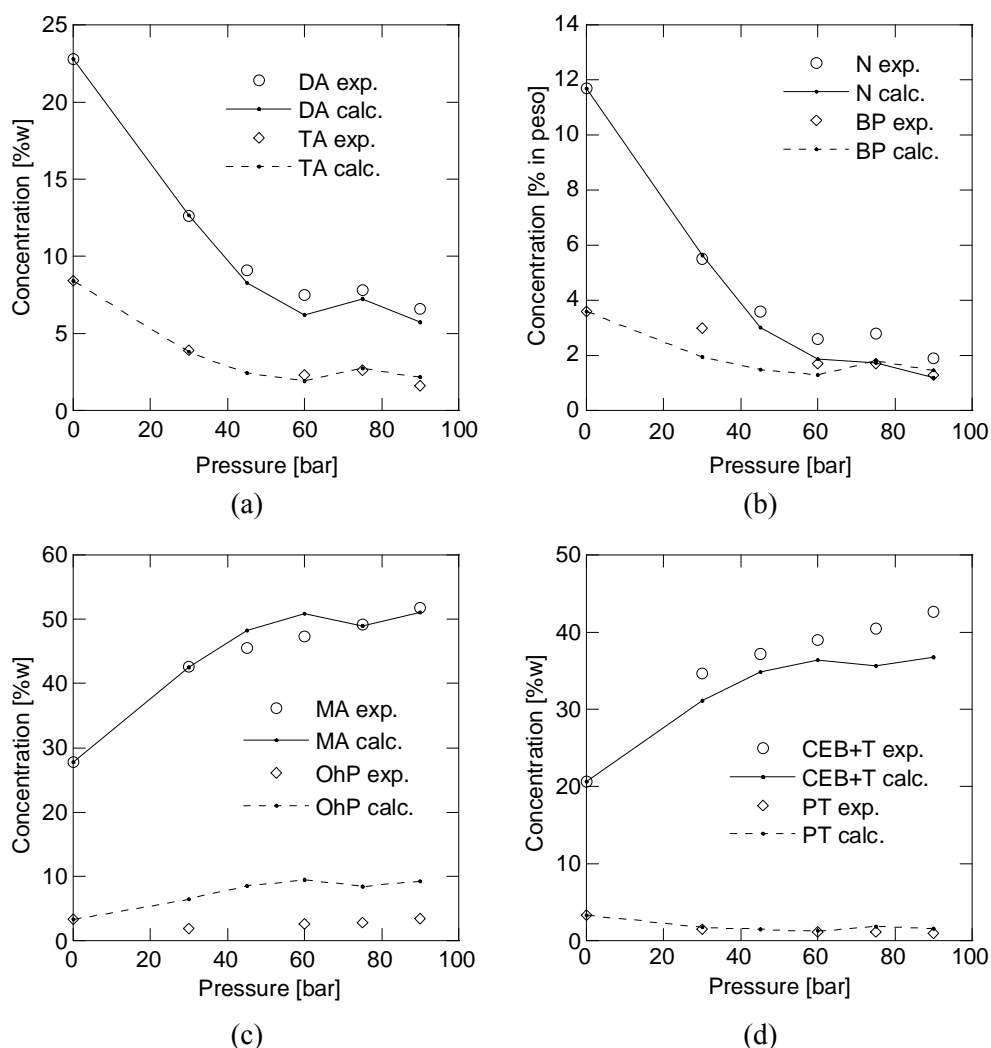


Fig. 8. 4 Hydrogenation: Comparison between experimental data and model results (Set#3)

As mentioned above, despite many assumptions made in order to develop the model reducing the number of parameters, the model is applicable in a wide range of applications and even much more important in a typical range wherein the industrial hydroprocessing is carried out. Indeed, in the tests used for the validation, both content and distribution of aromatic compounds have been modified and some main operating parameters such as pressure and LHSV have been modified.

8.4 Hydrogenation results for a low level of temperature: catalyst 2 (cat 2)

8.4.1 Calibration test (Set #4)

The test related to Set#4 has been initially realized to verify the HDA and HDS kinetics found using the catalyst 1. However, it is very important because allowed to apply the model over new generation catalyst still belonging to the NiMo/Al₂O₃ catalyst type. The new generation catalysts are more reactive, for this reason, the Set#4 has been also used to calibrate the new kinetic constants greater than those of the catalyst 1. While, the same values of equilibrium constants obtained by the catalyst 1 were used.

In this set the feed is a pure straight run gasoil (whose properties are listed in Table 8.6) and the operating conditions change in a range of pressure of 30-90 bar, a range of LHSV of 1.4-1.8 h⁻¹ and a temperature level of 330 °C.

Proprieties	S.I. Unit	Value	Method
Density	kg/m ³	866.4	ASTM D4052-96
Sulfur	wppm	10018	ISO 14596 ASTM D5453-04
Nitrogen	wppm	275.9	ASTM D4629-02
Monoaromatics	%w	16.7	
Diaromatics	%w	10.8	EN 12916-2000
Triaromatics	%w	2.0	
Total Aromatics	%w	29.5	

Table 8.6 Properties of feed (SRGO) used in Set#4

Comparison between results from the model and experimental data, especially in terms of diaromatics and triaromatics shows a good agreement among them (Fig.8.5a). Figure 8.5c shows a good description of the monoaromatics concentration and Fig.8.5b and Fig.8.5d show that the model correctly behaves respect to the individual lumps, both those belonging to the diaromatic class (naphthalenes and biphenyls) and those belonging to monoaromatics class (octahydrophenanthrenes and tetralins +cyclohexylbenzenes). Again, the model gives a good description of the experimental results both at low pressure (30-45 bar) and at high pressure levels (75-90 bar). This is very important because demonstrates

the ability of the model to correctly describe the reactions when they are controlled by the kinetics and when they are controlled by the equilibrium.

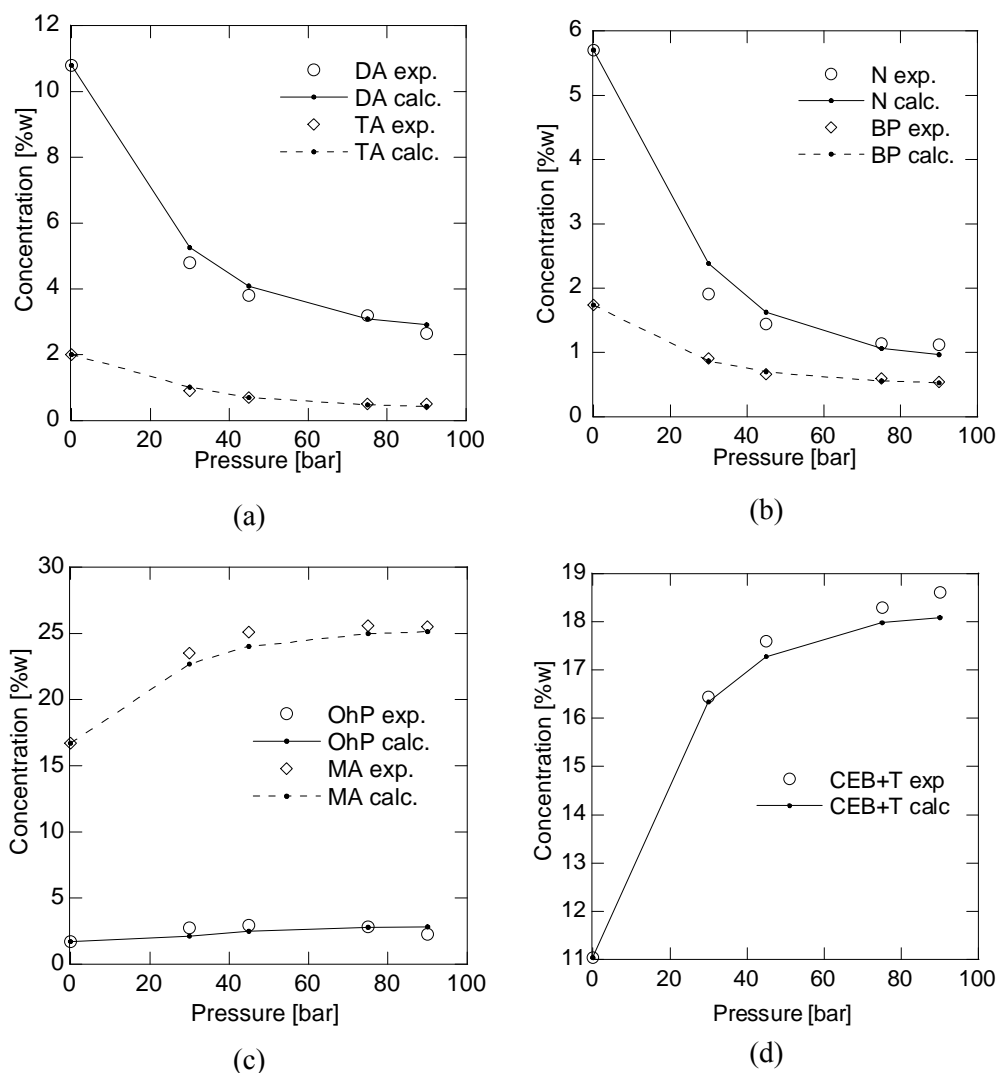


Fig. 8. 5 Hydrogenation: Comparison between experimental data and model results (Set#4)

8.4.2 1st Validation test (Set #5)

The first validation test with catalyst 2 has been realized using a SRGO similarly to the calibration test. These gasoils have only few differences in the properties and they concern in particular the nitrogen compounds. The characteristics of the SRGO for the Set#5 are reported in the Table 8.7.

Proprieties	S.I. Unit	Value	Method
Density	kg/m ³	864.6	ASTM D4052-96
Sulfur	wppm	10577	ISO 14596 ASTM D5453-04
Nitrogen	wppm	232.5	ASTM D4629-02
Monoaromatics	%w	16.6	
Diaromatics	%w	10.4	EN 12916-2000
Triaromatics	%w	1.8	
Total Aromatics	%w	28.8	

Table 8.7 Properties of feed (SRGO) used in Set#5

The experiment has been carried out at one level of pressure equal to 75 bar and for different levels of temperature. Only one run has been realized at low temperature of 330°C but this allows verifying the parameters estimated in the calibration test, both equilibrium and kinetic constants. The results are reported in the form of table because referred only to one run. It is a direct prediction but the model results are close to the experimental data. Indeed, diaromatics and triaromatics are well predicted in the hydrotreated product. Moreover, a good prediction of biphenyl, naphthalenes, octahydrophenanthrenes and tetralin+ cyclohexylbenzenes is obtained.

	Feed [%w]	Experimental Data [%w]	Model Results [%w]
MONO	16.60	23.7	23.703
DI	10.40	3.5	3.797
TRI	1.80	0.5	0.573
Biphenyl	1.496	0.596	0.625
Naphthalenes	5.72	1.540	1.466
Octahydrophenanthrenes	1.617	2.421	2.421
CEB+T	11.213	17.403	17.384

Table 8.8 Comparison between experimental data and model results (Set#5)

8.4.3 2nd Validation test (Set #6)

The second test used for the validation of the model using the catalyst 2 is one of the most important. It has been planned ad hoc to verify the behavior of the model when the results are pretty close to the real properties required for a gasoil. In fact, the feed of this run is still a SRGO but its properties are significantly different from the

SRGO used in the calibration and in the first validation tests. Feed characterization is shown in the Table 8.9.

Proprieties	S.I. Unit	Value	Method
Density	kg/m ³	874.5	ASTM D4052-96
Sulfur	wppm	8166	ISO 14596 ASTM D5453-04
Nitrogen	wppm	176	ASTM D4629-02
Monoaromatics	%w	18.7	
Diaromatics	%w	10.5	
Triaromatics	%w	2	EN 12916-2000
Total Aromatics	%w	31.8	

Table 8.9 Properties of feed (SRGO) used in Set#6

By a comparison between this Table and the Tables 8.6 and 8.7, it is possible to observe that while the total aromatic concentration is almost the same of the previous feedstock, the total sulfur and nitrogen content are significantly different. The set has been again realized at 330°C for two several levels of pressure, 60 and 90 bar. Both runs are at a same value of LHSV=1.5h⁻¹ and the model has been used only to predict the product distribution without any new parameters adjustment. Results are shown in the Table 8.10.

Feed		90 bar		60 bar	
[%w]		Experimental	Model	Experimental	Model
		Data	Results	Data	Results
		[%w]	[%w]	[%w]	[%w]
MONO	18.70	23.40	27.20	25.90	26.60
DI	10.50	2.10	2.40	2.80	3.09
TRI	2.00	0.20	0.41	0.40	0.54

Table 8.10 Comparison between experimental data and model results (Set#6)

The model behaves well in the description of the diaromatics content and it is within the experimental error for the triaromatics estimation. Instead, it has problems in the estimation of monoaromatic concentration. The origin of this discrepancy is due to the different competition effect of hydrogenation and hydrodesulfurization on the active sites because of the different levels of sulfur and nitrogen respect to the corresponding levels in the calibration test. Nevertheless, the nitrogen effect affects

only the monoaromatics concentration and not that of diaromatics and triaromatics because, under these operating conditions, the diaromatics and triaromatics are close to equilibrium conditions. Consequently, this allows to correctly describing their concentration even in absence of nitrogen. Unlike the reaction of monoaromatics is controlled by the direct reaction and, although the constant kinetic is the same of that calibrated with the Set#5 it is necessary to correctly describe the denominator of Langmuir-Hinshelwood kinetics considering the nitrogen compounds competition.

8.5 Hydrogenation results for a high level of temperature: catalyst 1 (cat 1)

The increase of temperature determines an increase of the kinetic constant on one side but intensifies the limitation due to the thermodynamic equilibrium on the other one. Starting from the constants estimated at 330°C, the activation energies and the heats of reactions have been calibrated.

8.5.1 Calibration test (Set #3)

For the catalyst 1, only one test is available for high values of temperature. This test belongs to the Set#3 that at 330°C has been used as a validation test.

Two runs are available at 345 and 365°C and they are used to estimate the activation energies by Arrhenius formula and the heats of reaction by Van't Hoff equation.

The feed of the test, a pure LCO, is the same reported in the Table 8.5.

The results are reported in the Fig.8.6 for temperature equal to 365°C.

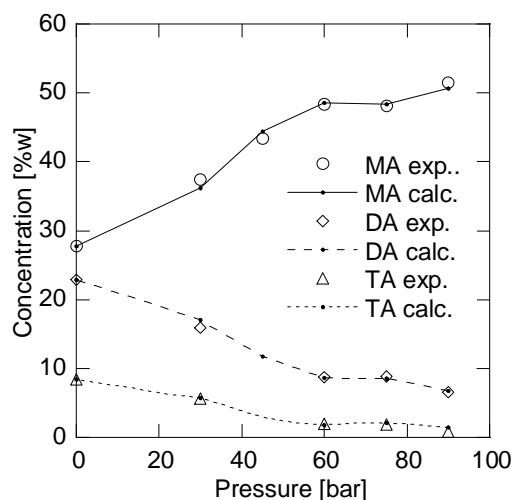


Fig.8. 6 Hydrogenation: Comparison between experimental data and model results at 365°C (Set#3)

The five runs reported in the graph differ for the pressure values that vary from 30 to 90 bar and for the LHSV, which range between 1.7 and 2.5 h⁻¹.

The results are only in terms of mono-, di-, and triaromatics but they show how the model is able to correctly represent the LHSV variations. It is very important to underline how the monoaromatic, diaromatic and triaromatic profiles are qualitatively similar to the second validation test at 330°C varying the pressure.

8.6 Hydrogenation results for a high level of temperature: catalyst 2 (cat 2)

8.6.1 Calibration and validation tests (Set #5 and Set #7)

In this case, Set#5 used as a validation test at low temperature, is used, jointly Set#7, as one of the calibration test at high levels of temperature (350 and 365°C).

The goal is estimating the activation energies typical of catalyst 2 for the several reactions of hydrogenation starting from the kinetic constants calibrated at 330°C. The equilibrium constants at the higher temperature levels are calculated applying the Van't Hoff equation considering the equilibrium constants at 330°C as temperature reference. The hydrogenation heats of reaction ΔH are taken from the literature. The feed of Set#5 has been presented in the Table 8.7 while the characteristics of feed for the Set#7, made of a mixture 70% SRGO and 30% LCO, are reported in the Table 8.11.

Proprieties	S.I. Unit	Value	Method
Density	kg/m ³	873.1	ASTM D4052-96
Sulfur	wppm	6686	ISO 14596 ASTM D5453-04
Nitrogen	wppm	180	ASTM D4629-02
Monoaromatics	%w	17.3	
Diaromatics	%w	15.2	
Triaromatics	%w	2.3	EN 12916-2000
Total Aromatics	%w	34.8	

Table 8.11 Properties of feed (SRGO) used in Set#6

Concerning the operating conditions, both tests have been carried out at two levels of temperature (350 and 365°C) and for each temperature, only one level of pressure has been chosen (75 bar for the Set#5 and 90 bar for the Set#7). Totally, four runs are available, three of which have been used in the calibration phase. They are both runs of the Set#5 and the run at 350°C of the Set#7 while the remaining run of Set#7 has been used in direct prediction.

However, the information coming from these tests is limited and they allowed estimating the activation energy of triaromatics and biphenyls but not that of naphthalenes because under these operating conditions their reaction is controlled by the equilibrium. Probably, the values of LHSV (2 for the Set#5 and 1.5 for the Set#7) are too low to avoid that the equilibrium takes place. The equilibrium control has been demonstrated observing that sensibly changing the naphthalenes kinetic constant, the concentration of this lump does not undergo significant variations.

The results are reported in two tables. The former (Table 8.12) concerning Set#5 in the calibration phase and the last one Set#7, partially in calibration and partially in prediction (Table 8.13).

		Set#5 (75 bar)			
Feed [%w]		350°C		365°C	
		Experimental Data [%w]	Model Results [%w]	Experimental Data [%w]	Model Results [%w]
MONO	16.6	21.7	22.41	18.8	17.30
DI	10.4	3.8	2.91	3.6	2.66
TRI	1.8	0.5	0.54	0.2	0.51

Table 8.12 Comparison between experimental data and model results, high temperature (Set#5)

		Set#7 (90 bar)			
Feed [%w]		350°C		365°C	
		Experimental Data [%w]	Model Results [%w]	Experimental Data [%w]	Model Results [%w]
MONO	17.3	25.1	26.39	21.9	18.85
DI	15.2	1.5	2.19	1.2	1.71
TRI	0.23	0.2	0.38	0.3	0.31

Table 8.13 Comparison between experimental data and model results, high temperature (Set#7)

Tables 8.12 and 8.13 summarize the comparison between the experimental data and model results in terms of aromatic macro-classes. A deviation from the experimental data for the diaromatic compounds could be observed. An analysis of the class behavior has been realized comparing the Table 8.12 with the Table 8.8. It shows that experimentally the diaromatic concentration in the hydrotreated product increases from 330°C to 350°C and decreases from 350°C to 365°C. On the other hands, the model describes only the decrease of such concentration increasing the temperature because of the kinetic regime detected into the model.

8.7 Hydrogenation results for different feeds: catalyst 2 (cat 2)

The feeds used along this work are gasoil, LCO, or their mixture but some experiments have been carried out using feeds with different properties. Such feed is a HVGO used to test the reliability of the model using the same parameters estimated using gasoil without any adjustment. The set of runs is called Set#8 and HVGO properties are shown in the following table

Proprieties	S.I. Unit	Value	Method
Density	kg/m ³	926	ASTM D4052-96
Sulfur	wppm	21136	ISO 14596 ASTM D5453-04
Nitrogen	wppm	1547	ASTM D4629-02
Monoaromatics	%w	18.7	
Diaromatics	%w	9.7	EN 12916-2000
Triaromatics	%w	17.1	
Total Aromatics	%w	45.5	

Table 8.14 Properties of HVGO used in Set#8

Three tests have been realized in such contest for one level of temperature and two levels of pressure. For the first pressure value only one LHSV has been chosen (1.3h^{-1}) while for the second, two (1 and 1.3h^{-1}) have been used.

Initially, these runs have been simulated using the values of ΔH from literature to calculate the equilibrium constants at different temperature levels by the Van-t Hoff equation. The results showed a good prediction of monoaromatic and diaromatic total contents but some problems in the description of the triaromatic compounds. Such discrepancy is related to the fact that the range of molecular weight in the HVGO is higher than that of gasoil. Therefore, the triaromatic class includes also structures with more than three aromatic rings that are not present in the calibration test.

Indeed, at this moment, the analytical methodology is not able to distinguish triaromatics from the other polyaromatic compounds and the model is obliged to simulate them into a single lump. This introduces an error depending on the nature of the processed feed because polyaromatic compounds are characterized by a different adsorption constant respect to the triaromatic species. Because of the impossibility to identify separately tri- and polyaromatic compounds, the kinetic constant has been properly changed by estimation of a new value for the runs with HVGO in order to account the presence of the polyaromatic compounds and correctly estimate the concentration of their lump in the hydrotreated product.

Results obtained by this approach are reported in the Table 8.15.

	Feed [%w]	<u>1st run: 75 bar and</u>		<u>2nd run: 90 bar and</u>		<u>2nd run: 90 bar and</u>	
		<u>1.3h⁻¹</u>		<u>1h⁻¹</u>		<u>1.3h⁻¹</u>	
		Exp Data [%w]	Model Results [%w]	Exp Data [%w]	Model Results [%w]	Exp Data [%w]	Model Results [%w]
MONO	18.7	28	28	30	29.75	30.5	29.24
DI	9.7	5	5.10	4.2	4.22	3.9	4.46
TRI	17.10	10.3	10.69	8.5	8.92	9	9.53

Table 8.15 Comparison between experimental data and model results, at high temperature and two different levels of pressure and LHSV (Set#8)

8.8 Hydrodesulfurization results for a low level of temperature

8.8.1 Calibration tests for both cat 1 and cat 2(Set #1 and Set #4)

As said in the previous Chapters, most of the sulfur compounds of gasoil totally react under the typical hydroprocessing operating conditions and are included in the hydrogenation scheme. Therefore, the hydrodesulfurization results concern only the refractory sulfur compounds description.

The approach is similar to the hydrogenation one. Some sets have been used to calibrate the desulfurization constants and the remaining to test the reliability of the model when it is used in the prediction phase.

Set#1 and Set#4 have been not used only as calibration tests for cat 1 and cat 2 respectively, but they have been also used to deduce the best kinetic expression able to describe the sulfur compounds conversion.

The experimental data in terms of sulfur compounds for feed and products are reported in Tables 8.16 and 8.17.

	Refractory scale	Feed conc. [wppm]	Conc. at 30 bar [wppm]	Conc. at 45 bar [wppm]	Conc. at 60 bar [wppm]	Conc. at 75 bar [wppm]	Conc. at 90 bar [wppm]
R₁	1	113.33	23.12	20.18	18.09	15.11	12.50
R₂	2	191.75	42.82	36.27	31.16	26.16	20.53
R₃	3	382.85	102.08	91.00	81.97	71.95	61.49
R₄	4	79.33	50.57	46.27	43.60	39.56	35.30

Table 8.16 Lumps repartition of the refractory sulfur compounds (Set#1)

	Refractory scale	Feed conc. [wppm]	Conc. at 30 bar [wppm]	Conc. at 45 bar [wppm]	Conc. at 60 bar [wppm]	Conc. at 75 bar [wppm]
R₁	1	303.28	129.82	109.52	95.84	85.98
R₂	2	544.40	200.13	172.44	153.07	139.53
R₃	3	1157.53	473.45	425.93	380.12	351.99
R₄	4	268.13	160.12	150.22	132.95	122.29

Table 8.17 Lumps repartition of the refractory sulfur compounds (Set#4)

In the Table 8.16 the Set#1 lumps repartition of refractory sulfur compounds is presented. As reported in the Table 8.2, the total sulfur content of the mixture

70%SRGO-30%LCO is 2325 wppm but from summing the lumps feed concentrations only 767 wppm are refractory compounds.

Similarly, in Table 8.17 the Set#4 lumps classification is reported. In this case, the feed is the same described in the Table 8.6 where only 2273 wppm of the total sulfur content (10018 wppm) belongs to the refractory species.

For both tables it is possible to observe the increasing refractoriness of the different lumps. In particular, the last two lumps, where 4mDBT and 4,6dmDBT belong, are those with the lowest reactivity.

In terms of the operating conditions used to identify the hydrodesulfurization kinetic expressions, they are the same used for the hydrogenation, $T=330^{\circ}\text{C}$, $P=30\div 90$ bar, $\text{LHSV}=1.7\text{ h}^{-1}$ for the Set#1 and $T=330^{\circ}\text{C}$, $P=30\div 90$ bar, $\text{LHSV}=1.5\div 1.8\text{ h}^{-1}$.

The results are shown in the following graphs:

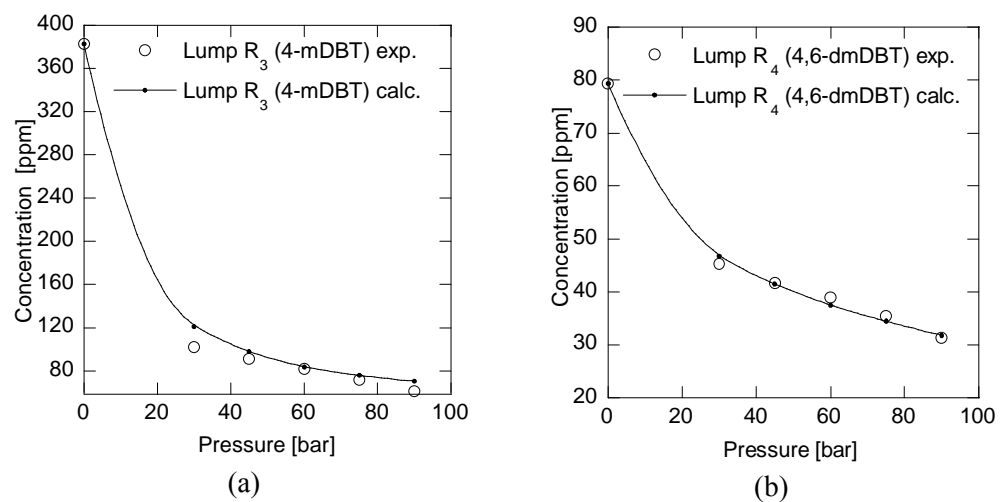


Fig.8. 7 Hydrodesulfurization: Comparison between experimental and model R₃ and R₄ concentrations, (Set#1)

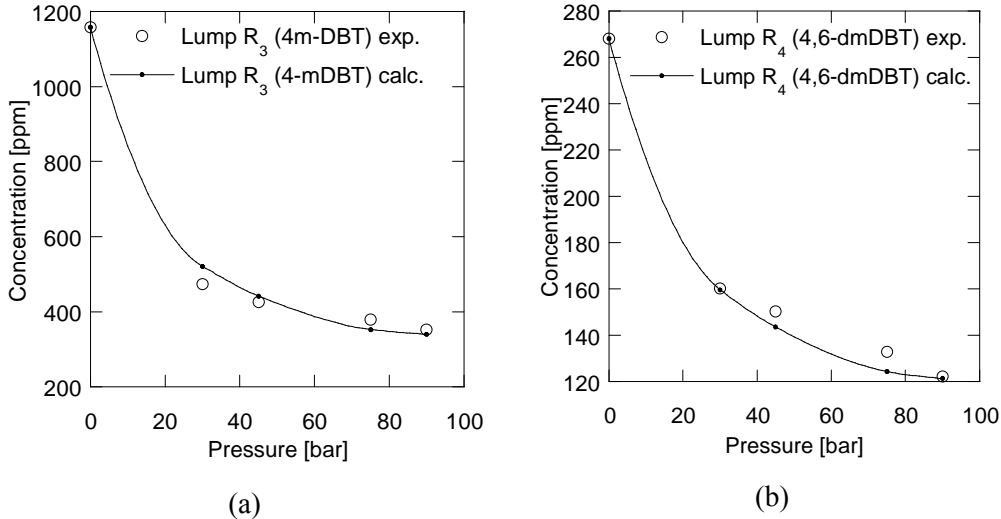


Fig. 8. 8 Hydrodesulfurization: Comparison between experimental and model R₃ and R₄ concentrations, (Set#4)

Figures 8.7a and 8.8a show the results in terms of 4-methyldibenzothiophene lump (R₃) and figures 8.7b and 8.8b those in terms of 4,6-dimethyldibenzothiophene lump (R₄). The correct description of the alkyldibenzothiophenes conversion allows obtaining a good agreement among the experimental total sulfur content (by the method EN-ISO 14596) and its value predicted by the model. A comparison between the two tests, Set#1 on the left (Fig.8.9a) and Set#4 on the right (Fig.8.9b), is following reported:

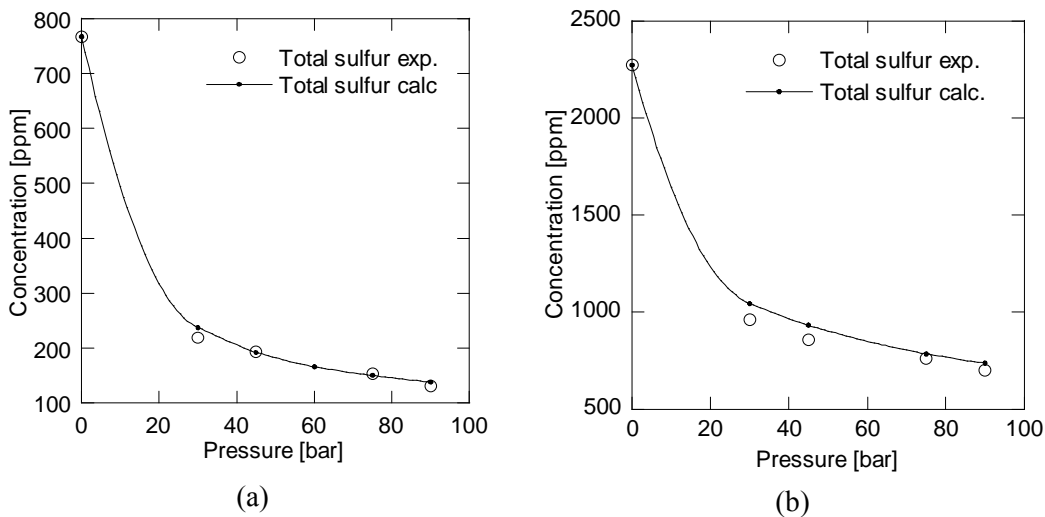


Fig.8. 9 Hydrodesulfurization: Comparison between experimental and model total sulfur content, (Set#1-Set#4)

The results allow having a confirmation of the assumptions taken concerning the speciation and classification of the refractory sulfur compounds and the hypotheses about the kinetic expression. It has been verified how removing the hydrogenation term in the hydrodesulfurization kinetics (equation 6.14), the model is not able to correctly predict the total sulfur content anymore. Especially, it has some problems to describe the runs at high level of pressure where the HYD is the favorite pathway. The compounds that mainly undergo the contribution of such term are those belonging to the lump4 of the 4,6-dimethyldibenzothiophene because they are the most refractory species and then need the hydrogenation reaction.

8.8.2 Validation test: cat 2 (Set #5 and Set#6)

No test is available for the first type of catalyst in the prediction phase. Therefore, the validation of the model has been realized only using tests carried out using the catalyst 2. One of them is the test related to the Set#5 and the other to Set#6, used also to verify the hydrogenation model. The temperature conditions are the same of the Set#4 (330°C), so the same kinetic parameters may be used to realize a direct prediction. Set#5 is characterized by a 75 bar pressure and 2h^{-1} LHSV. The experimental data and the model results are shown in the Table 8.18.

	Refractory scale	Feed Conc. [wppm]	Exp. Conc. [wppm]	Calc. Conc. [wppm]
R₁	1	304.86	124.35	122.21
R₂	2	466.47	185.75	177.90
R₃	3	1154.71	458.27	493.33
R₄	4	269.74	163.05	154.72
Total		2195.78	931.42	948.16

Table 8.18 Experimental data and model results (Set#5)

In the Set#6, two several pressure levels have been used for one level of LHSV equal to 1.5h^{-1} . The sulfur compounds repartition is presented in the Tables 8.18 and 8.19. This test is very important because the hydrotreated product has properties very close to those required from the environmental specifications, especially at 90 bar where the concentration of the total sulfur content is lesser than 50 wppm.

	Refractory scale	Feed Conc. [wppm]	Conc. at 60 bar [wppm]	Conc. at 90 bar [wppm]
R₁	1	188.98	11.53	1.81
R₂	2	363.45	23.94	4.93

R_3	3	799.54	90.65	25.12
R_4	4	190.29	47.00	13.01

Table 8.19 Lumps repartition of the refractory sulfur compounds (Set#6)

The results are reported in the Fig. 8.10 in terms of different lumps:

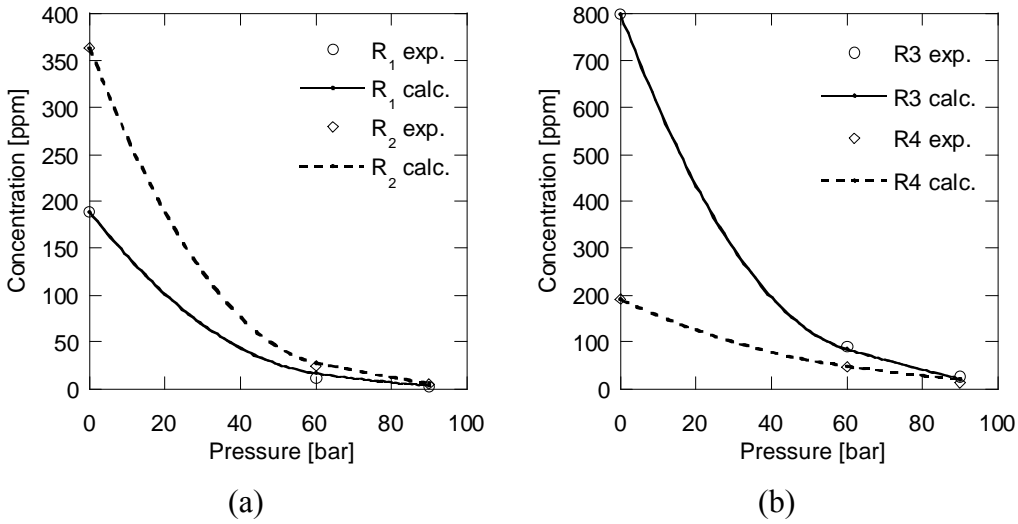


Fig.8. 10 Hydrodesulfurization: Comparison between experimental and model R_1 , R_2 , R_3 , R_4 concentrations (Set#6)

Instead, the Fig.8.11 compares the experimental and model total sulfur content:

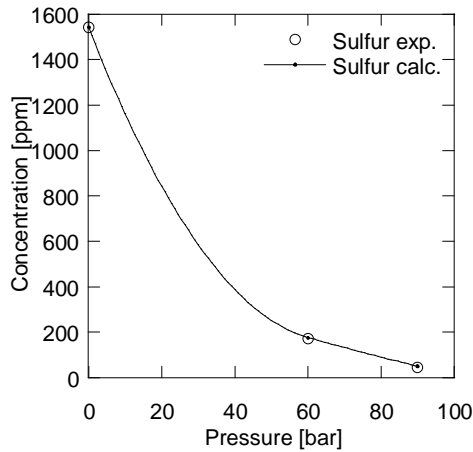


Fig.8. 11 Hydrodesulfurization: Comparison between experimental and model total sulfur concentrations (Set#6)

As said in the beginning of this Chapter, this is a test where the effect of nitrogen compounds on the hydrodesulfurization reactions is not negligible. Observing the experimental data, especially at 90 bar, a very low sulfur level is present in the hydrotreated products. That is possible because, how it will be shown in the next Paragraph, the amount of nitrogen is very close to zero in the product. The results reported above have been obtained also considering the hydrodenitrogenation reaction and a good prediction is observable both for each lump and for total sulfur content.

8.9 Hydrodesulfurization results for a high levels of temperature

8.9.1 Calibration and validation tests for cat 2

The Set#5 has been used to estimate the desulfurization kinetic constants for high temperature through the calibration of the activation energies for the DDS and HYD reactions. The feed properties are those reported in the Table 8.7 and the operating conditions used are two levels for the temperature (350 and 365°C) and one level of pressure equal to 75 bar.

As reported in the Fig.8.12, the model correctly predicts the experimental concentration of the total sulfur content for different temperature levels:

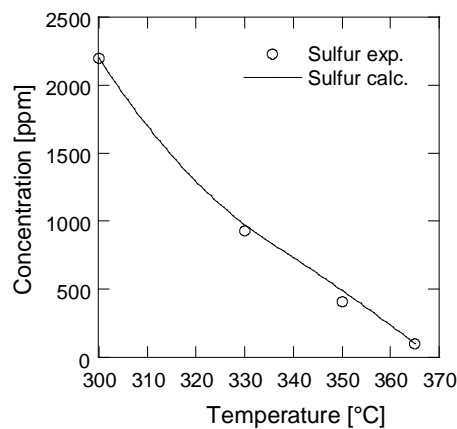


Fig.8. 12 Hydrodesulfurization: Comparison between experimental and model total sulfur concentrations (Set#5)

The activation energies estimated using Set#5 has been used to predict the total sulfur content by a simple prediction for Set#4 and Set#6, at one temperature level equal to 350°C and one pressure level: 90 and 60 bar, respectively. The results are shown in the following Table

	Sulfur exp. [ppm]	Sulfur calc. [ppm]
Set#4 (90 bar)	50	54
Set#6 (60 bar)	13	9

Table 8.20 Hydrodesulfurization at high temperature: Comparison between experimental and model total sulfur concentrations

The motivation why the experimental sulfur value at 90 bar is higher than that one at 60 bar is related to the feeds properties. The feed characteristics, reported in the Tables 8.17 and 8.19, show that the total sulfur content in Set#4 is higher than the sulfur amount in Set#6. It is worth stressing out that these results are very important because they represent the current and the future bound of sulfur compounds and the Table shown how the model is able to correctly describe both of them.

8.10 Hydrodenitrogenation results

As said in advanced, no experimental data is available for the first catalyst. Therefore, only results for the second catalyst will be presented.

8.10.1 Calibration test (Set #4)

This is the test used to calibrate the kinetic constants of basic and non-basic nitrogen compounds, according to the kinetics reported in the Chapter 7, for a temperature level equal to 330°C. The experimental data in terms of total nitrogen content for feed and products are reported in Table 8.21.

	Feed conc. [wppm]	Conc. at 30 bar [wppm]	Conc. at 45 bar [wppm]	Conc. at 75 bar [wppm]	Conc. at 90 bar [wppm]
Nitrogen	275.9	168.5	112.8	41.6	28.9

Table 8.21 Nitrogen experimental concentrations (Set#4)

As reported in the table, the concentration of nitrogen is appreciable also in the products. Therefore, that can justify why also the total sulfur content reported in the Fig.8.9b cannot reach low concentrations.

Anyway, the model ability to satisfactory describing the total nitrogen content for several levels of pressure is shown in the following figure:

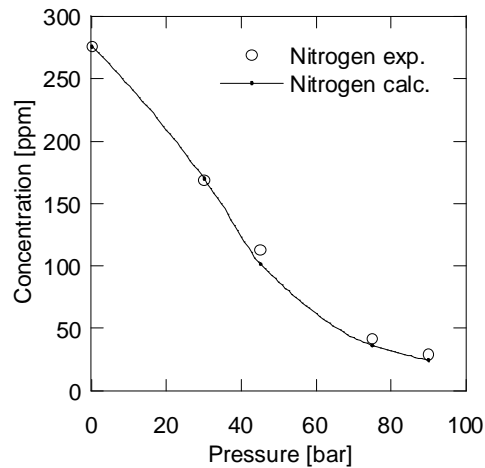


Fig. 8. 13 Hydrodenitrogenation: Comparison between experimental and model total nitrogen concentrations (Set#4)

8.10.2 Validation tests (Set #5 and Set#6)

In addition, to verify the reliability of the model for the hydrodenitrogenation Set#5 and Set#6 (used in the validation of hydrogenation and hydrodesulfurization) have been used. Even in terms of nitrogen, the former is very similar to the calibration test while the second one has lower nitrogen content and it represents the main pilot unit test where the nitrogen cross-effect has been felt very strongly.

For the Set#5 experimental data and results are following reported and a good prediction has been obtained:

	Feed conc. [wppm]	Conc. Exp. [wppm]	Conc. Calc. [wppm]
Nitrogen	232.47	53.68	51.25

Table 8.22 Nitrogen experimental concentrations (Set#5)

For Set#6, the experimental feed and product concentrations are initially shown:

	Feed conc. [wppm]	Conc. at 60 bar [wppm]	Conc. at 90 bar [wppm]
Nitrogen	176	2.287	1.143

Table 8.23 Nitrogen experimental concentrations (Set#6)

Then the prediction of the model is presented in the Fig.8.14:

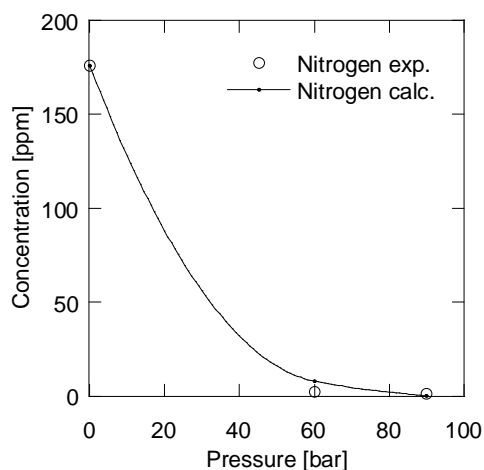


Fig.8. 14 Hydrodenitrogenation: Comparison between experimental and model total nitrogen concentrations (Set#6)

Only a small deviation exist for the model prediction at 60 bar but it is within the experimental error and however it allows to correctly predict the total sulfur content, see Fig.8.12.

Finally, the hydrodenitrogenation study has been concluded estimating the activation energy for the heterocyclic nitrogen compounds using the Set#5. The operating conditions are the same reported in the Paragraph 8.9.1, two levels for the temperature (350 and 365°C) and one level of pressure equal to 75 bar. The obtained results, reported in the following Figure, show a rather good agreement between experimental and predicted total nitrogen content.

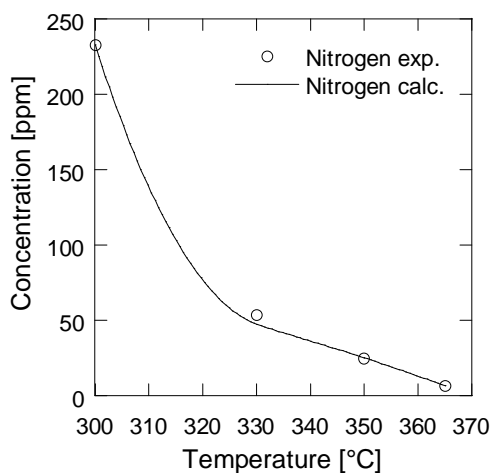


Fig.8. 15 Hydrodenitrogenation: Comparison between experimental and model total nitrogen concentrations (Set#5)

8.10 Industrial model results

The application considered that, the pilot unit the model has been developed, and the industrial plant have some important differences. Firstly, they differ for the flows direction. In fact, the industrial reactor is a trickle-bed reactor with a down-flow configuration. Then, more than one catalytic bed is present and the reactor is adiabatic. Therefore, the model is modified to describe the industrial reactor by introduction of the thermal balance. It has been written for all catalytic beds also considering the introduction of the quenches present in the industrial plant to bind the temperature increase. In particular, instance, three beds were present in the real reactor used for the simulation.

The simulation is just a direct prediction using the kinetic and equilibrium parameters estimated for the pilot unit changing as a function of the temperature following the Arrhenius and Van't Hoff equations.

Nothing can be made explicit about catalyst but the results obtained are in the following reported in terms of aromatic, sulfur and nitrogen compounds and temperature profile. Furthermore, a comparison among results without and with nitrogen cross effect has been presented to show how it is fundamental to correctly simulate the hydroprocessing plant.

Proprieties	Concentration exp. [%w]	Concentration calc. [%w.]
Monoaromatics	26	30.88
Diaromatics	2.4	2.81
Triaromatics	0.5	0.39
Sulfur	14	4.77

Table 8.24 Results without nitrogen cross effect (Industrial test)

Proprieties	Concentration exp. [%w]	Concentration calc. [%w.]
Monoaromatics	26	28.33
Diaromatics	2.4	2.74
Triaromatics	0.5	0.43
Sulfur	14	13
Nitrogen	0.5	2.7

Table 8.25 Results with nitrogen cross effect (Industrial test)

It is possible to observe that, although the concentrations of tri-, di- and monoaromatic compounds improve if the nitrogen inhibitive effect is considered, it does not strongly affect the hydrogenation reactions. On the contrary, the cross effect becomes very important versus the hydrodesulfurization reactions. In fact, in this case if it is neglected, the model underestimates the total sulfur content because none inhibitive effect controls the refractory sulfur compounds conversion. It is able to correctly predict the total sulfur content if the hydrodenitrogenation reaction is considered.

Moreover, three catalytic beds were present in such adiabatic industrial plant. The increases of the temperature into each bed are reported in the Table 8.26

	ΔT exp. [°C]	ΔT calc. [°C]
1st catalytic bed	30	29
2nd catalytic bed	9	13
3rd catalytic bed	18	19

Table 8.26 Temperature increments inside the catalytic beds (Industrial test)

Chapter 9

Cracking reactions



In this Chapter, the approach used to tackle the extremely high level of detail required for cracking reaction will be presented. Starting considering that on the hydroprocessing catalyst the only kind of cracking reaction is the dealkylation while isomerization and ring-opening are negligible, the population distribution of each molecular lump components will be derived. Finally, the cracking model and the solution method will be explained

9.1 Kinetics

In the hydroprocessing plant, the only cracking phenomena are the dealkylation reactions where the break of the side chains occurs (cf. Paragraph 4.3). On the other hand, the negligibility of the isomerization and ring-opening reactions has been observed.

As reported in the Paragraph 4.3, the lumps classification used for the hydrogenation is not detailed enough to describe the cracking reactions and the knowledge of distributions of the components characterized by side chains with different lengths is necessary. Starting from this point and assuming as hypothesis that only one chain is present or if more chains are present, a strong asymmetry exists between them. Therefore, it is assumed that only the biggest chain endures cracking.

The main problem connected to the cracking reactions is the definition of the kinetics. Only few papers are present in the literature, especially about the dealkylation over the NiMo/Al₂O₃ catalyst and in this work, a first order kinetics has been assumed. Starting from a work developed for the catalytic hydrocracking reaction on a Shell NiW/USY zeolite catalyst (Russell et al., 1994) some information are found to study the cracking kinetic constants.

Theoretically, cracking kinetics depends both on the length of the side chain and the position where the break occurs. In agreement with Russell et al. (1994), it has been assumed that cracking only depends on the distance from the aromatic rings. On the other hands, the break of chain with length equal to k in the position $i < k$ is equal to the break of the chain with length equal to m in the same position i ($i < m$). Moreover, the dealkylation near to the aromatic ring (positions α , β , γ , δ) is hampered while the kinetic constant increases proportionally to the distance from the ring up to eight atoms. After that, it becomes constant. The variation of the kinetic constant as a function of the cracking position is shown in the Fig. 9.1.

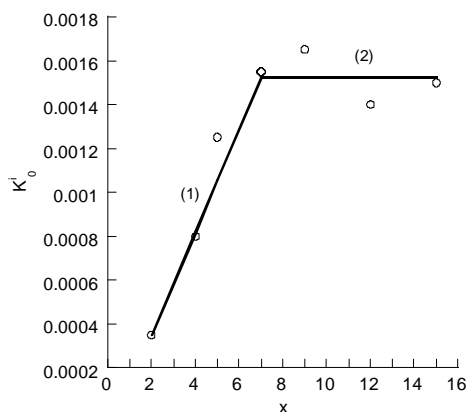


Fig.9. 1 Variation of the kinetic constant vs. cracking position (x)

The figure reports two different lines which represents two different dependences on the break position. The first is indicated with the symbol ① and the second one with the symbol ②. In this way, taken a generic lump with maximum n atoms in the side chain, the dealkylation matrix has been found (Fig.9.2):

		Break position →																
		1	2	3	4	5	6	7	8	9	10	11	n	
Chain length →	1	0	0	0	0	0	0	0	0	0	0	0	0	0	0	0	0	0
	2	0	0	0	0	0	0	0	0	0	0	0	0	0	0	0	0	0
	3	0	0	0	0	0	0	0	0	0	0	0	0	0	0	0	0	0
	4	0	0	0	0	0	0	0	0	0	0	0	0	0	0	0	0	0
	5	0	0	0	0	0	0	0	0	0	0	0	0	0	0	0	0	0
	6	0	0	0	0	①	0	0	0	0	0	0	0	0	0	0	0	0
	7	0	0	0	0	①	①	0	0	0	0	0	0	0	0	0	0	0
	8	0	0	0	0	①	①	②	0	0	0	0	0	0	0	0	0	0
	9	0	0	0	0	①	①	②	②	0	0	0	0	0	0	0	0	0
	10	0	0	0	0	①	①	②	②	②	0	0	0	0	0	0	0	0
	11	0	0	0	0	①	①	②	②	②	②	0	0	0	0	0	0	0
	...	0	0	0	0	①	①	②	②	②	②	②	0	0	0	0	0	0
	...	0	0	0	0	①	①	②	②	②	②	②	②	0	0	0	0	0
	...	0	0	0	0	①	①	②	②	②	②	②	②	②	0	0	0	0
...	0	0	0	0	①	①	②	②	②	②	②	②	②	②	0	0	0	
n	0	0	0	0	①	①	②	②	②	②	②	②	②	②	②	②	0	

Fig.9. 2 Dealkylation matrix

$$k_i^0 = 2.35 \cdot 10^{-4} i - 1.2 \cdot 10^{-4} \quad \text{at } i < 7 \quad (9.1)$$

$$k_i^0 = 1.525 \cdot 10^{-3} \quad \text{at } i \geq 7 \quad (9.2)$$

9.2 Cracking Model

After the kinetics has been found, two different approaches have been tested to solve the cracking model.

The former uses the method of moments, applied to each lump, whose elements are described by a gamma distribution (see Appendix).

$$D_{0e} \frac{\partial^2 C_i}{\partial x^2} - u_0 \frac{\partial C_i}{\partial x} - \rho_{app} r_i^{HDA} - \sum_{j=4}^{i-1} k_{i,j} \rho_{app} C_j + \sum_{j=i+1}^n k_{i,j} \rho_{app} C_j = 0 \quad (9.3)$$

The total mass balance is readily obtained by summing all the components.

$$D_{0e} \frac{\partial^2 C_{TOT}}{\partial x^2} - u_0 \frac{\partial C_{TOT}}{\partial x} - \sum_{i=1}^n \rho_{app} r_i^{HDA} - \sum_{i=1}^n \sum_{j=4}^{i-1} k_{i,j} \rho_{app} C_j + \sum_{i=1}^n \sum_{j=i+1}^n k_{i,j} \rho_{app} C_j = 0 \quad (9.4)$$

The last equation is the same one used for the hydrogenation without the cracking rate but considering that the zero, first, second and third moments are

$$M_{0i} = C_{TOTi} = \sum_{i=1}^n C_i, \quad M_{1i} = \sum_{i=1}^n i C_i, \quad M_{2i} = \sum_{i=1}^n i^2 C_i, \quad M_{3i} = f(M_{0i}, M_{1i}, M_{2i})$$

respectively. The probability gamma distribution is completely determined by a number of its moments equal to its parameters, it is possible to describe all components of each lump with only three equations in terms of moments. The resulting equations system for one lump is following reported:

$$D_{0e} \frac{\partial^2 M_{0i}}{\partial x^2} - u_0 \frac{\partial M_{0i}}{\partial x} - \sum_{i=1}^n \rho_{app} r_i^{HDA} - \sum_{i=1}^n \sum_{j=4}^{i-1} k_{i,j} \rho_{app} C_j + \sum_{i=1}^n \sum_{j=i+1}^n k_{i,j} \rho_{app} C_j = 0 \quad (9.5)$$

$$D_{0e} \frac{\partial^2 M_{1i}}{\partial x^2} - u_0 \frac{\partial M_{1i}}{\partial x} - \sum_{i=1}^n \rho_{app} r_i^{HDA} - \sum_{i=1}^n \sum_{j=4}^{i-1} k_{i,j} \rho_{app} C_j + \sum_{i=1}^n \sum_{j=i+1}^n k_{i,j} \rho_{app} C_j = 0 \quad (9.6)$$

$$D_{0e} \frac{\partial^2 M_{2i}}{\partial x^2} - u_0 \frac{\partial M_{2i}}{\partial x} - \sum_{i=1}^n \rho_{app} r_i^{HDA} - \sum_{i=1}^n \sum_{j=4}^{i-1} k_{i,j} \rho_{app} C_j + \sum_{i=1}^n \sum_{j=i+1}^n k_{i,j} \rho_{app} C_j = 0 \quad (9.7)$$

This approach is advantageous because a small system of equations is obtained but in this case, it cannot apply because of the closure problems. In fact, because of the different cracking behaviors of the several compounds inside a same distribution the

reactive term is not expressible in terms of moments. For this reason, this approach has been abandoned.

The second approach considers a balance for a population for each lump assuming that each component is formed

- Because of the hydrogenation of its corresponding reactant with the same lateral chain;
- Due to the cracking of the longer side chains of the other compounds belonging to the same distribution.

In such way a very big equations system has been obtained where the equation for each species of each lump is

$$D_{0e} \frac{\partial^2 \omega_i}{\partial x^2} - u_0 \frac{\partial \omega_i}{\partial x} - \rho_{app} r_i^{idr} - \sum_{j=4}^{i-1} k_{i,j} \rho_{app} \omega_j + \sum_{j=i+1}^n k_{i,j} \rho_{app} \omega_j = 0 \quad (9.8)$$

The number of equations in this case could be about 5-6 hundreds but in spite of its dimensions it may solved easily therefore this is the approach used to describe the cracking model.

9.3 Results

The application of the model on the Mild Hydrocracking is represented by the Set#9 reported in the Table 8.1 and the results in terms of conversion and naphtha yield:

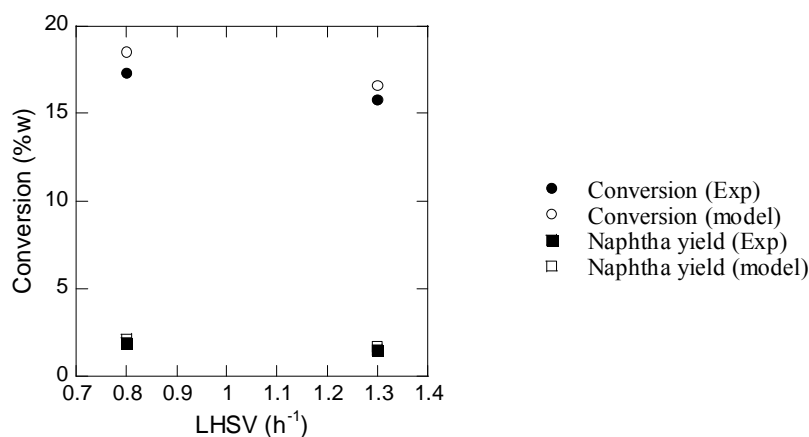


Fig.9. 3 Cracking: Comparison between experimental and model results

Conclusions

The aim of this thesis consisted of developing the most flexible phenomenological model able to describe the hydroprocessing plant both on pilot and on industrial scale. Large efforts were required due to the deep process knowledge needed. All the efforts made to study and develop completely the main hydroprocessing aspects like mass and heat balances development, kinetic expressions and experimental issues are paid back by the model ability in simulating this process under every possible situation in terms of real feeds, commercial catalysts and typical operating conditions. In fact, using this model we will be able to simulate the hydroprocessing process conditions like flow rate, temperature and pressure as a function of feed and catalyst properties.

In agreement with the approach used by Erby in her previous PhD thesis belonging to the project founded the by Ministry of University and Research too, this thesis completes the study about hydrogenation reactions. In particular, starting from the already existing feed and product characterization in terms of aromatic compounds made by HPLC analysis, the hydrogenation kinetic expressions have been modified introducing the competition effect among all the compounds present in the gasoil. Moreover, the hydrogenation approach has been extended on the new generation hydroprocessing catalysts and the conversion of monoaromatic compounds has been included.

Anyway, the major contribute given by this work concerns the hydrodesulfurization and the hydrodenitrogenation reactions study.

Ample attention has been devoted to the speciation of the refractory sulfur compounds. By the PFPD method, a deep characterization of the feed and product has been realized and the minimum number of molecular lumps sufficient to describe all refractory sulfur compounds kinetic behaviors has been found. Then the reaction mechanisms have been detailed studied allowing us to define the kinetic expressions for the sulfur compounds conversion.

The attempt to develop a flexible hydrodesulfurization model has revealed the drawback of the hydroprocessing model when the hydrodesulfurization is considered separately from the other reactions occurring in such process. In particular, the nitrogen effect importance on the hydrodesulfurization reaction has been supposed, studied and demonstrated. Therefore, hydrogenation and hydrodesulfurization kinetics have been reassessed also including the competition effect among aromatic, nitrogen and sulfur compounds. The hydrodenitrogenation kinetics expressions have

been derived although no detailed characterization of nitrogen compounds has been realized, but the simplified repartition suggested in the literature was enough.

All hydrogenation and hydrodesulfurization mechanisms have been re-examined with deeper attention on the active sites typology on the catalyst surface and different types of competitions have been described as a function of the sites where the different reactions occur. In particular, two different active sites have been proposed. On one side, the hydrogenation sites where aromatic, sulfur and nitrogen compounds compete on the other hand one the hydrogenolysis sites where only nitrogen and sulfur competition is accounted. From this point of view the new kinetics have been introduced into a global homogeneous ideal plug-flow hydroprocessing model where all reactions are simultaneously considered.

The main advantage of the model is that, although simple in comparison with the complexity of the real processes it wants to describe, it is at the same time detailed enough to achieve its goal. In particular, it is simple if compared to the complexity of the processed feedstock, but able to reach a level of gasoil characterization so deep that it has never been reached by similar works proposed up to now.

The results are obtained from *ad hoc* experiments targeted to investigate the typical ranges of pressure, temperature and LHSV using real feedstock and typical hydroprocessing catalysts. Such experiments have been chosen in order to have significant sulfur and nitrogen contents in the hydrotreated product to study the effect varying the different operating conditions even if in these cases the nitrogen cross effect was not very important. Anyway, some other tests demonstrated that the introduction of nitrogen inhibitive effect makes this model innovative respect to those already existing in the literature. In fact, when the sulfur and nitrogen contents tend to zero the nitrogen inhibition becomes appreciable and the hydroprocessing simulation cannot disregard the hydrodenitrogenation reaction.

Another important contribution introduced in the work concerns the cracking reactions. This is newness not only because usually this kind of reaction is considered negligible on the commercial hydroprocessing catalyst but also due to the used approach. In fact, even if cracking results are in the preliminary step, the combination of different experimental information allows us to answer the need of high level of detail in the feed and product characterization. This lays the foundation to extend the model also to other plants like the mild-hydrocracking plant where heavier feedstock are processed and the typical catalyst and the operating conditions determine a significant cracking of the molecules.

In conclusion, the goal proposed in the Introduction can be considered satisfactorily met because the model is able to correctly describe the hydroprocessing plant as a whole. It can consider all kinds of reactions, it can be easily adapted to different

plants and it can correctly simulate the process for all real possible combinations of feed, catalyst, temperature, pressure and LHSV.

Although not widely discussed in this thesis due to the confidential information, a further proof of the reliability of this model is the extension of it on the real plant. In fact, the real simulation demonstrates that such model can be easily adapted to find a concrete application at real level.

Appendix

Introduction

Several times, in this thesis, references to the experimental methodologies have been made. None experimental activity directly concerns the development of the model. For this reason, no dedicated Chapter has been dedicated to its description, but it is fundamental to understand some assumptions made in terms of feed and product characterization. Moreover, the presentation of the analytical techniques is important to understand their limitations respect to the deep level of detail required in this work and the approaches chosen to overcome the difficulties. In fact, as said in the Chapter 4 about the feed and product characterization, it is clear that the approach used in this work requires a level of detail that the recent analysis methods are not able to provide. In fact, they can only define the oil mixture in terms of mono, di and polyaromatics, total sulfur content and total nitrogen content.

Therefore, in the specific instance in this appendix the techniques to analyze aromatic, sulfur and nitrogen content and distribution will be presented.

Content and distribution of the aromatic compounds

The content and the distribution of the aromatic compounds are defined by a combination of an experimental activity and an analytical methodology.

The experimental activity is a method called EN 12912/2000 that allows evaluating the content of saturate, monoaromatic, diaromatic and triaromatic compounds.

The method applicability is related to the several aromatic contents. It is possible to apply the method only when the total aromatic content is included between 4 and 65%w, the monoaromatic content between 4 and 40%w, diaromatic content between 0 and 20%w and triaromatic one between 0 and 6%w.

The method employs the High Performance Liquid Chromatography (HPLC). A known mass of sample diluted with heptane is injected into the HPLC where a polar column is located. The several aromatic compounds have a different affinity to this column as a function of their different polarity. Such polarity depends on the number of aromatic rings therefore saturates, monoaromatic, diaromatic and triaromatic compounds adsorb on the polar column with a different strength. Saturates group is the first one that elute from the column due to its lowest number of aromatic rings. Then, increasing the number of the aromatic rings, the retention time increases and

monoaromatic and diaromatic elute. At a defined time, after diaromatics elute, a backflush is realized. The direction of the flow inside the column is changed in order to elute the polyaromatics all together.

The experimental section, whose scheme is shown in the Fig.A.1, is constituted by an injector, a micro-filter for the samples, a HPLC column (250 mm long, 4 mm ID), a temperature control system and backflush valve. The HPLC column is filled with very small silica particles with isopropylamine that represents the fixed phase. The sample diluted into the solvent represents the mobile phase.

The small dimension of the solid particles gives the advantage to have a high surface area. They superficially adsorb the compounds into the solvent, keeping them relatively their polarity and using the differential adsorption as separation mechanism. On the other hand the disadvantage of using small particles is the necessity to flow the mobile phase at high pressure (50÷150 bar), otherwise the elution become too slow.

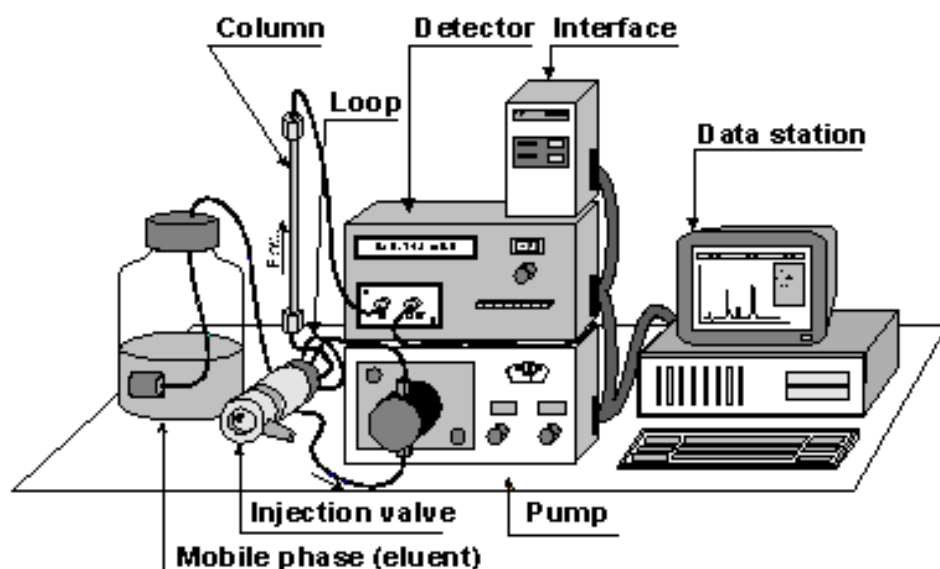


Fig.A 1 High Performance Liquid Chromatography schematization

The HPLC column is connected to an index refraction detector that registers the components gradually they elute. The electronic signal, from the detector, is continually monitored by a computer. In fact, software compares the signal width from the analyzed sample with a calibration curve obtained by previous injections of four standard solutions (A, B, C, D) reported in the Table A.1.

Calibration Standard	Ciclohexane [g/100ml of heptane]	o-xylene [g/100ml of heptane]	1 methyl naphthalene [g/100ml of heptane]	Phenanthrene [g/100ml of heptane]
A	5.0	4.0	4.0	0.4
B	2.0	1.0	1.0	0.2
C	0.5	0.25	0.25	0.05
D	0.1	0.05	0.02	0.01

Table A.1 Concentrations of the standard solutions for the calibration curve

In addition, a standard solution called System Calibration Standard, SCS, is prepared to identify the backflush point. It is made of 1g of cyclohexane, 0.5g of o-xylene, 0.05g of dibenzothiophene and 0.05g of 9-methylanthracene, diluted into heptane since to 100ml. As reported in the equation A.1, the backflush time is calculated considering the retention time of dibenzothiophene (t_{DBT}) and 9-methylanthracene (t_{9mA}) which represents the di- and triaromatic components of the SCS:

$$\text{Backflush time} = t_{DBT} + 0.4 (t_{9mA} - t_{DBT}) \quad (\text{A.1})$$

The standard solutions give information to find a relationship between the area of the peak and the concentration of the solution. In this way a concentration curve vs. peak area is obtain for each aromatic compound. A linear curve, with a correlation factor greater than 0.999 and an intercept included between $\pm 0.01\text{g}/100\text{ml}$ is required.

After that, the samples are injected, previously filtered if they contain insoluble material and analyzed. At this point the weight percentage of mono-, di- and polyaromatic compounds are estimated. The sum of such percentages represents the total aromatic content in the analyzed sample.

As said in the previous Chapters, the model development requires a deeper level of detail. For this reason, the experimental method is supported by a numerical methodology able to draw the identification and the concentrations of the subclasses of tri-, di-, monoaromatic and saturated compounds (Sassu et al., 2003). This is made through the application of the deconvolution algorithm to identify the peaks hidden in the HPLC-RI profiles (Fig.A.2a-A.2b).

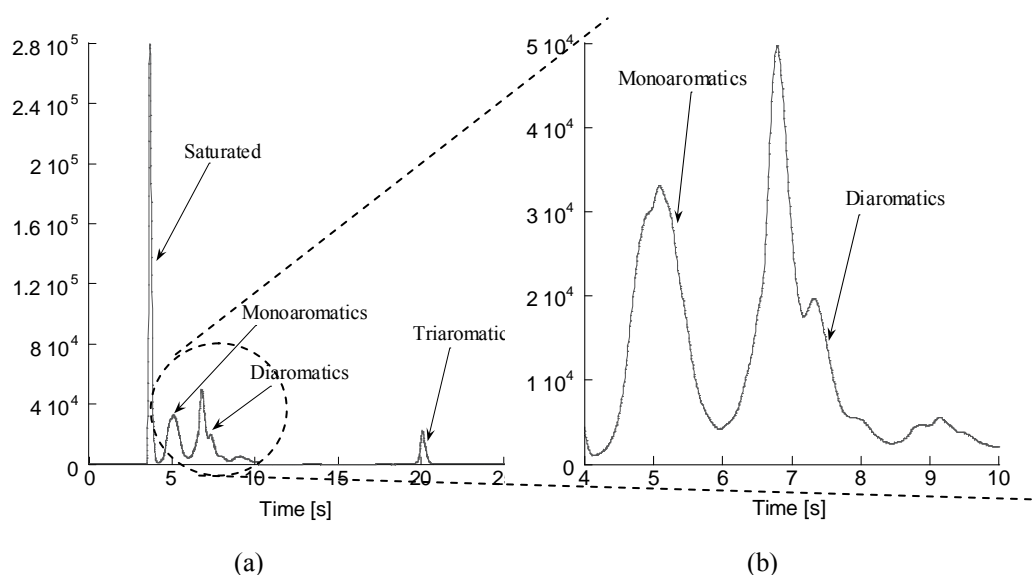


Fig.A 2 Typical chromatogram from HPLC

The chromatogram comes from the different retention times that triaromatic diaromatic, monoaromatic, and saturate compounds have in the HPLC column. Observing their peaks (Fig.A.2a), it is possible to notice that they are the result of the combination of different peaks of other compounds that belong to the several macro-classes.

Only one subclass is considered to describe the saturate and the triaromatic class, therefore as shown in Fig.A.2b the deconvolution will be realized only for the monoaromatic and diaromatic peaks.

In order to account for the diversity in structure and reactivity of aromatic compounds four sub classes are identified for the mono-aromatics (i.e. alkylbenzenes, tetralins, cyclohexylbenzenes and octahydrophenanthrenes) and six sub classes were identified for the di-aromatics (i.e. indenenes, naphthalenes, biphenyls, phenyltetralines, tetrahydrophenanthrenes,, phenylnaphthalenes, benzothiophene and dibenzothiophene). Interpretation of the chromatograms reported in the Fig.A.2b is accomplished through a Levenberg-Marquardt non-linear minimization algorithm for peak fitting finds hidden peaks through minimization of the residuals between total area and the area of the resolved peaks. The integration of the peaks is made drawing a baseline from the beginning of the monoaromatics peak to a point immediately the back-flush point. Saturates and triaromatic peaks are integrated by others two independent baselines. A relationship between peaks area and compounds concentration is expressed by the following formula:

$$\omega_j = \frac{A_j S_j + I_j}{M} V \quad (\text{A.2})$$

where j is the generic j -th component and peak, A_j is its area, S_j and I_j the slope and intercept of the calibration referred to the corresponding macro-class, M is the sample mass and V the solution volume.

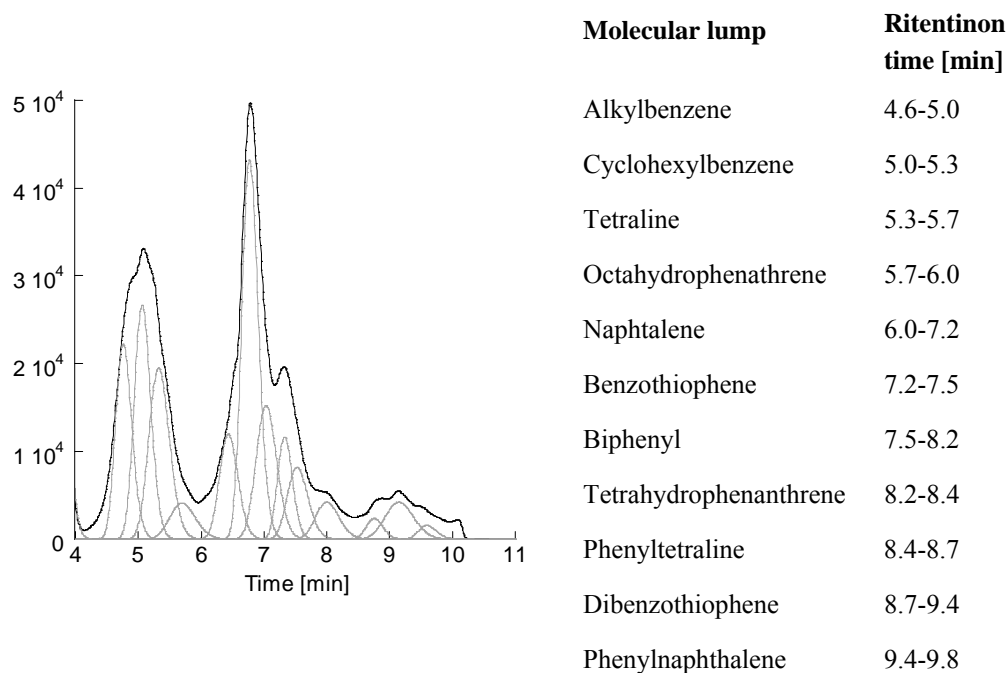


Fig.A 3 Typical gasoil deconvolution by Peakfit algorithm

The table reported into the Fig. A.3 shows the typical range of retention time for each molecular lump. The reason is that the molecular lump reported in this figure is only the key component used to represent a wider class of species that includes all the compounds that have the same aromatic structure but different lateral alkyl chains (cf. Paragraph 4.2.1). These compounds behave in the same way respect to the hydrogenation reactions but they have a different affinity to the adsorption column inside the HPLC and elute with a different retention time. Consequently, each molecular lump is represented by a peak that has an average retention time of all compounds belonging to that class. The identification of this peak is rather complicated due to its position, or the value of the average retention time, which depends also on the concentration of the class and the distribution of the several components inside it. Moreover, it depends also on the interaction with the different molecular classes and no software is able to objectively consider such effects and

identify the several peaks. The identification of the peaks is also complicated from the overlapping peaks of compounds belonging to the same lump. These are the problems related to this methodology that, although gives very good results (Sassu et al., 2003), has the disadvantage to require the ability of an operator for the chromatogram deconvolution. A solution of this problem is presented by Foddi et al. (2007) who proposed a model of chromatographic system in order to support the feed and product characterization reconstructing the elution profile of multicomponent mixture from HPLC. They concentrated the attention on the alkylbenzenes compounds but it is supposed to extend the same approach also to the other aromatic compounds.

Content and distribution of the sulfur compounds

Total sulfur content and distribution of sulfur compounds are estimated by two different experimental activities. Sulfur content could be evaluated using two different methodologies: the first one (ASTM D5453) is based on UV sulfur oxide analysis while the second one (EN ISO 14596) is an X-ray photometry of the sample. Based on ASTM D5453 method, the sample is inserted inside a high temperature tube (1075÷1100 °C) where sulfur is oxidized to SO₂ and submitted to UV ray exposure reaching an excited state SO₂. The fluorescence released by sulfur oxide once stable again gives a measure of the total sulfur content in the sample.

With the XRF analysis method (EN ISO 14596), the sample is mixed together with a zirconium solution with a given mass ratio. The homogenized mixture is exposed to the primary radiation inside an X-ray tube. By this way, it is possible to get a line spectrum of components inside the sample. Using the calibration curve based on well defined standards, the total sulfur content is obtained.

In terms of sulfur species distribution, the sample is analyzed using an own-developed analytical method running on a Gas Chromatograph equipped with a PTV injector and a Pulsed Flame Photometric Detector (PFPD). The developed method allows the improvement of the resolution between the different sulfur compounds as well as the determination of trace species (detectability 0.2 wppm) without the need for individual calibrations. The attention will be focused on the second experimental activity in order to understand how the 55 different refractory sulfur compounds have been identified. In the specific instance, in this contest, is not really important understanding how the SARTEC internal method works but how the several peaks have been recognized and how their reactivity has been studied. For this reason, the two following chromatograms will be considered:

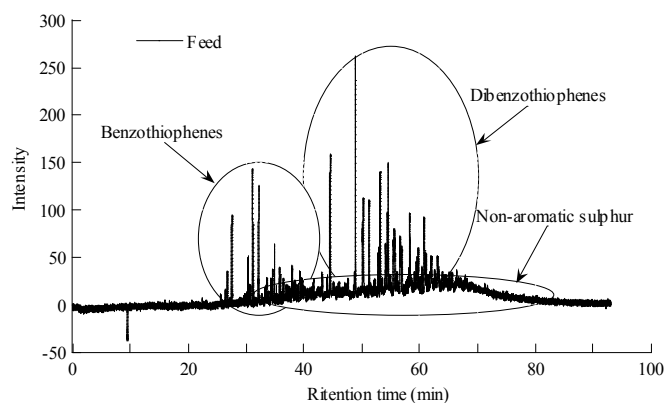


Fig.A 4 Chromatogram of feedstock obtained from the analytical method PFPD

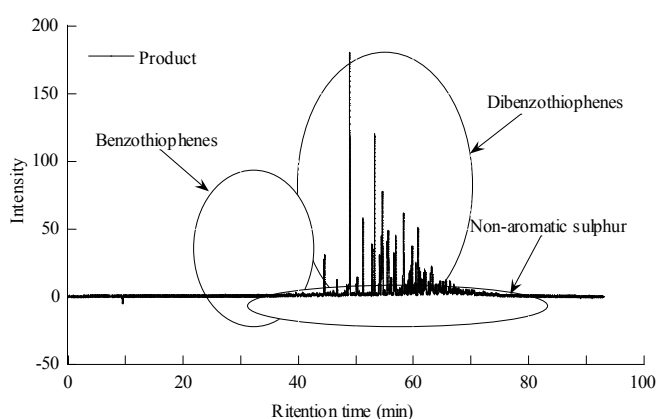


Fig.A 5 Chromatogram of product obtained from the analytical method PFPD

As said along the thesis, sulfur present in gasoil can be divided into non-aromatic and aromatic sulfur. The first group includes sulphides and mercaptans and in the analytic condition, it is eluted as a hump extending almost along the entire Gas Chromatograph (GC) profile. Aromatic sulfur includes thiophenes, eluting at approximately 10 minutes (but not seen in Figures A.4 and A.5), benzothiophenes and dibenzothiophenes. Already from a comparison between Figures A.4 and A.5, representing the GC profile for the sulfur species of feed and a mild hydrotreated product, it is seen that both non-aromatic sulfur and benzothiophenes are completely absent from the product. This makes the product chromatogram much simpler to integrate than the feed chromatogram. In fact, due to the presence of the hump, although most of the peaks are not overlapped, their integration strongly depends on the ability and objectivity of the operator. In fact, taking choice where draw the baseline of the peaks, which separates aromatic sulfur (sum of the peaks) and non-

aromatic sulfur (hump) is very difficult because each peak is partially overlapped with the hump.

Initially, two baselines have been considered as shown in the Fig. A.6. In this way some of peaks result overestimated because they also include part of the hump some others underestimated because are cut by the baseline.

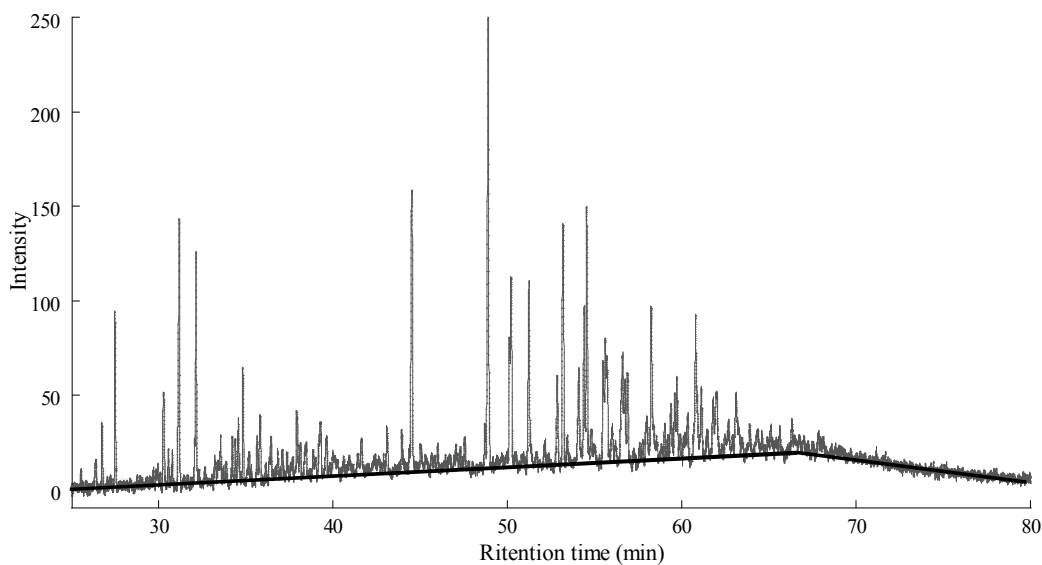


Fig.A 6 Baseline position, 1st approach

Therefore, the choice to consider one baseline for each peak has been taken. It has been drawn considering the minimum points at the beginning and at the end of the peak. In the Fig.A.7, the zoom of the small part of the chromatogram shown in the Fig.A.6 has been presented. Some peaks have been integrated showing which procedure has been chosen to do that trying to integrate peaks as objective as possible without any influence from the operator ability and trying to create a repeatable methodology.

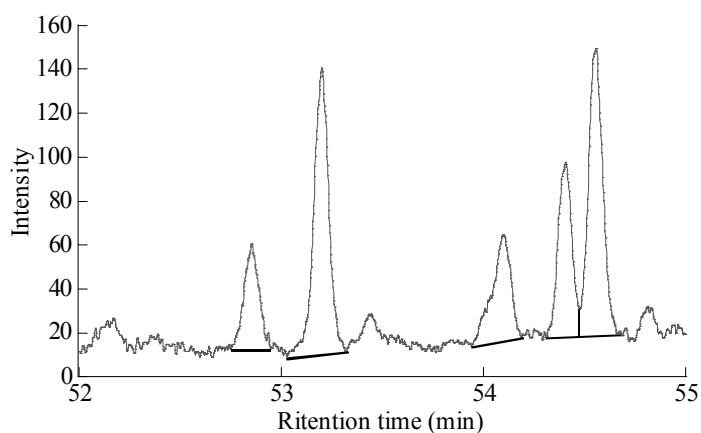


Fig.A 7 Baseline position, 2nd approach

Observing that, unless the area, the shape of each particular peak is the same changing feed and product, the uniformed procedure has been defined, in order to integrate in the same manner every chromatograms introducing the same error for each test.

Once all peaks have been integrated, the area information has been converted into concentration information, assuming that the ratio between the area of each peak and the total area below the chromatogram is equal to the ratio between the concentration of the same peak and the total sulfur content. The total sulfur content is known, the total and peaks area have been calculated, and therefore the peaks concentrations could be estimated. A key component for each refractoriness class has been identified. All other components have been allocated into these four lumps when the constancy of the ratios between each component and the four key components for different levels of pressure has been observed.

Acronyms

13C NMR	Carbon Nuclear Magnetic Resonance
AGO	Atmospheric gasoil
ASTM	American Society for Testing and Materials
CARB	California Air Resources Board
CNG	Compressed Natural Gas
DDS	Direct Desulfurization pathway
DME	Dimethyl Ether
EMA	Engine Manufacturers Association
EOR	End of Run
EPA	Environmental Protection Agency
EXAFS	Extended X-ray Absorption Fine Structure
FBR	Flooded Bed Reactor
FCC	Fluid Catalytic Cracking
GC	Gas Chromatograph
HCGO	Heavy Coker Gasoil
HDA	Hydrogenation
HDM	Hydrodemetallization
HDN	Hydrodenitrogenation
HDO	Hydrodeoxygenation
HDS	Hydrodesulfurization
HYD	Hydrogenolysis + Hydrogenation pathway
HPLC	High Performance Liquid Chromatography
HPS	High Pressure Separator
HVGO	Heavy Vacuum Gasoil
IPMT	Intra Particle Mass Transfer
LCGO	Light Coker Gasoil
LCO	Light Cycle Oil
LHHW	Langmuir-Hinshelwood- Hougen- Watson kinetics
LHSV	Liquid Hourly Space Velocity
LNG	Liquefied Natural Gas
LPG	Liquefied Petroleum Gas
MES	Mössbauer Emission Spectroscopy
MHC	Mild Hydrocracking
PAH	Polyaromatic Hydrocarbons
PFPD	Pulsed Flame Photometric Detector

PID	Proportional Integral Derivative controller
PFR	Plug Flow Reactor
POM	Polycyclic Organic Matter
SCS	System Calibration Standard
SOL	Structure-Oriented Lumping
SOR	Start of Run
SRGO	Straight Run Gasoil
STM	Scanning Tunneling Microscope
TBR	Trickle Bed Reactor
THDBT	Tetrahydrodibenzothiophene
ULSD	Ultra Low Sulfur Diesel
VOC	Volatile Organic Compound
VGO	Vacuum Gasoil
VSBGO	Visbreaking Gasoil
WABT	Weighted Average Bed Temperature
XRF	X-Ray Fluorescence

Bibliography

1. Al-Dahhan, M. H., Larachi, F., Dudukovic, M. P., Laurent, A., (1997). "High-pressure trickle-bed reactors: a review", *Ind. Eng. Chem. Res.*, 36, 3292-3314.
2. Ancheyta, J., Rana, M.S., and Furimsky, E., (2005). "Hydroprocessing of heavy petroleum feeds: Tutorial", *Catalysis Today*, 109, 3-15.
3. Angelici, R.J., (1997). "An overview of modeling studies in HDS, HDN and HDO catalysis", *Polyhedron*, Vol. 16, No. 18, pp. 3073-3088.
4. Aubert, C., Durand, R., Geneste, P., and Moreau C., (1988). "Factors affecting the Hydrogenation of Substituted Benzenes and Phenols over a Sulfided NiO-MoO₃/γ-Al₂O₃ Catalyst", *J. Catal.*, 112, 12-20.
5. Bataille, F., Lemberton, J.-L., Michaud, P., Perot, G., Vrinat, M., Lemaire, M., Schulz, E., Breysse, M., Kasztelan, S., (2000). "Alkyldibenzothiophenes hydrodesulfurization-promoter effect, reactivity, and reaction mechanism", *Journal of Catalysis*, 191, 409-422.
6. Bettati, A., Zeuthen, P., Hidalgo-Vivas, A., (2005). "Nitrogen tolerance og hydrocracking catalysts", in Topsøe A.S. Hydrocracking Catalyst and Technology Seminar, Copenhagen (Dk).
7. Biardi, G., and Baldi, G., (1999), "Three-phase catalytic reactors", *Catalysis Today*, 52, 223-234.
8. Bunch, A., Zhang, L., Karakas, G., Ozkan, U. S., (2000). "Reaction network of indole hydrodenitrogenation over NiMoS/γ-Al₂O₃ catalysts", *Applied Catalysis A: General*, 190, 51-60.
9. Chowdhury, R., Pedernera, E., and Reimert, R., (2002). "Trickle-bed Reactor Model for Desulfurization and Dearomatization of Diesel", *AIChE Journal*, 48, No. 1, 126-135.
10. Chu, C-I., and Wang, I. (1982). "Kinetic Study of Hydrotreating", *Ind. Eng. Chem. Process Des. Dev.*, 21, 338-344.
11. Cooper, B.H., and Donnis, B.B.L., (1996). "Aromatic Saturation of Distillates: an Overview", *Applied Catalysis A: General*, 137, 203-223.

12. De Wind, M., Plantenga, F. L., Heinerman, J. J. L., and Homan Free, H. W. (1988). "Upflow versus downflow testing of hydrotreating catalyst", *Applied Catalysis*, 43, 29-42
13. Edvinsson, R., Irandoust, S., (1993). "Hydrodesulfurization of dibenzothiophene in a monolithic catalyst reactor", *Ind. Eng. Chem. Res.*, 32, 391-395.
14. Erby, L., Diana, M. L., Medde, M., Baratti, R., Melis, S., (2005). "A lumped model for the hydrodesulfurization of the refractive compounds during gasoil hydroprocessing", *Chemical Engineering Transactions*, 7th Italian Conference on Chemical and Process Engineering (IcheaP-7), Giardini di Naxos (Italy), Vol.6, 269-274.
15. Evans, G. C., and Gerald, C. F., (1953). "Mass transfer from benzoic acid granules to water in fixed and fluidized beds at low Reynolds numbers", *Chem. Eng. Progr.*, 49 (3), 135
16. Foddi, O., Leoni L., Melis, S., Tronci, S., (2007). "Simulation of chromatographic for multicomponent mixtures of aromatic compounds", 8th International IFAC Symposium on Dynamics and Control of Process System, Vol.2, June 6-8, Cancun, Mexico, 309-314
17. Froment, G. F., Depauw, G. A., Vanrysselberghe, V., (1994). "Kinetic Modeling and Reactor Simulation in Hydrodesulfurization of Oil Fractions", *Ind. Eng. Chem. Res.*, 33, 2975-2988.
18. Furimsky, E., and Massoth, F.E., (1999). "Deactivation of hydroprocessing catalysts", *Catalysis Today*, 52, 381-495.
19. Gates, B.C. and Topsøe, H., (1997). "Reactivities in deep catalytic hydrodesulfurization: challenges, opportunities, and the importance of 4-methyldibenzothiophene and 4,6-dimethyldibenzothiophene", *Polyhedron*, Vol. 16, No. 18, 3213-3217.
20. Gianetto, M.J., and Specchia, V., (1992). "Trickle bed reactors: state of art and perspectives", *Chemical Engineering Science*, 47, (13/14), 3197-3213.
21. Gierman, H., (1988). "Design of laboratories hydrotreating reactors scaling down of trickle-flow reactor.", *Applied Catalysis*, 43, 277-286

22. Gioia, F., and Lee, V., (1986). "Effect of hydrogen pressure on catalytic hydrodenitrogenation of quinoline", *Ind. Eng. Chem. Proc. Des. Dev.*, 25, 918-925.
23. Girgis, A., and Gates, B.C., (1991). "Reactivities, Reaction Networks, and Kinetics in High-Pressure Catalytic Hydroprocessing", *Ind. Eng. Chem. Res.*, 30, 2021-2058.
24. Goto, S. and Smith, J.M., (1975). "Trickle-Bed Reactor Performance. Part I. Holdup and Mass Transfer Effects", *AIChE Journal.*, 21, 706-713.
25. Gultekin, S., Khaleeq, M., Al-Saleh, M. A., (1989). "Combined effect of hydrogen sulfide, water, and ammonia on liquid-phase hydrodenitrogenation of quinoline", *Ind. Eng. Chem. Res.*, 28, 729-738.
26. Helveg, S., Lauritsen, J.V., Lægsgaard, E., Stensgaard, I., Nørskov, J.K., Clausen, B.S., Topsøe, H., and Besenbacher, F., (2000). "Atomic-Scale Structure of Single-Layer MoS₂ Nanoclusters", *Physical Review Letters*, 84, 951-954.
27. Ho, T. C., and Sobel, J. E., (1991). "Kinetics of dibenzothiophene hydrodesulfurization", *Journal of Catalysis*, 128, Issue 2, 581-584.
28. Houalla, M., Broderick, D.H., Sapre, A.V., Nag, N.K., De Beer, V.H.J., Gates, B.C., and Kwart, H., (1980). "Hydrodesulfurization of Methyl-Substituted Dibenzothiophenes Catalyzed by Sulfided Co-Mo/ γ -Al₂O₃", *Journal of Catalysis*, 61, 523-527.
29. Jian, M., and Prins, R., (1998a). "Determination of the nature of distinct catalytic sites in hydrodenitrogenation by competitive adsorption", *Catalysis Letters*, 50, 9-13.
30. Jian, M., and Prins, R., (1998b). "Mechanism of the hydrodenitrogenation of Quinoline over NiMo(P)/Al₂O₃ Catalysts", *Journal of Catalysis*, 179, 18-27.
31. Kabe, T., Ishihara, A., Zhang, Q., (1993). "Deep desulfurization of light oil. Part 2: hydrodesulfurization of dibenzothiophene, 4-methyldibenzothiophene and 4,6-dimethyldibenzothiophene", *Applied Catalysis A: General* 97, L1-L9.
32. Kim, S. C., and Massoth, F. E., (2000). "Hydrodenitrogenation activities of methyl-substituted indoles", *Journal of Catalysis*, 189, 70-78.

33. Koltai, T., Macaud, M., Guevara, A., Schulz, E., Lemaire, M., Bacaud, R., Vrinat, M., (2002). "Comparative inhibiting effect of polycondensed aromatics and nitrogen compounds on the hydrodesulfurization of alkyldibenzothiophenes", *Applied Catalysis A: General* 231, 253-261.
34. Korre, S.C., Klein, M.T, and Quann, R.J.,(1995). "Polynuclear Aromatic Hydrocarbons Hydrogenation. 1.Experimental Reaction Pathways and Kinetics", *Ind. Eng. Chem. Res.*, 34, 101-117.
35. Korre, S.C., Neurock, M., Klein, M.T., and Quann, R.J., (1994). "Hydrogenation of Polynuclear Aromatic Hydrocarbons. 2. Quantitative Structure/Reactivity Correlations", *Chemical Engineering Science*, 49, 24A, 4191-4210.
36. Korre, S.C., and Klein, M.T.,(1996). "Development of temperature-independent quantitative structure/reactivity relationships for metal- and acid-catalyzed reactions", *Catalysis Today*, 31, 79-91.
37. Kwak, C., Lee, J.J., Bae, J. S., Moon, S. H., (2001). "Poisoning effect of nitrogen compounds on the performance of CoMoS/Al₂O₃ catalyst in the hydrodesulfurization of dibenzothiophene, 4-methyldibenzothiophene, and 4,6-dimethyldibenzothiophene", *Applied Catalysis B: Environmental* 35, 59-68..
38. Laredo, G. C., De Los Reyes, J. A., Cano, J.L., and Castillo, J. J., (2001). "Inhibition effects of nitrogen compounds on the hydrodesulfurization of dibenzothiophene", *Applied Catalysis A: General*, 207, 103-112.
39. Laredo, G. C., Leyva, S., Alvarez, R., Mares, M. T., Castillo, J. J., Cano, J.L., (2002). "Nitrogen compounds characterization in atmospheric gasoil and light cycle oil from a blend of Mexican crudes", *Fuel*, 81, 1341-1350.
40. Laredo, G. C., Altamirano, E., and De Los Reyes, J. A., (2003). "Inhibition effects of nitrogen compounds on the hydrodesulfurization of dibenzothiophene", *Applied Catalysis A: General* 243, 207-214.
41. Laredo, G. C., Montesinos, A., and De Los Reyes, J. A., (2004). "Inhibition effects observed between dibenzothiophene and carbazole during the hydrotreating process", *Applied Catalysis A: General* 265, 171-183.
42. Lauritsen, J.V., Helveg, S., Lægsgaard, E., Stensgaard, I., Clausen, B.S., Topsøe, H., and Besenbacher, F., (2001). "Atomic-Scale Structure of Co-

- Mo-S Nanoclusters in Hydrotreating Catalysts-Priority communication”, *Journal of Catalysis*, 197, 1-5.
43. Lauritsen, J.V., Bollinger, M.V., Lægsgaard, E., Jacobsen, K.W., Nørskov, J.K., Clausen, B.S., Topsøe, H., and Besenbacher, F., (2004). “Atomic-scale insight into structure and morphology changes of MoS₂ nanoclusters in hydrotreating catalysts”, *Journal of Catalysis*, 221, 510-522.
44. La Vopa, V., and Satterfield, C. N., (1988). “Poising of thiophene hydrodesulfurization by Nitrogen Compounds”, *Journal of catalysis*, 110, 375-387.
45. Lindfors, L. P.; Salmi, T., 1993. “Kinetics of Toluene Hydrogenation on a Ni/Al₂O₃ Catalyst”, *Ind. Eng. Chem. Res.*, 32, 34.
46. Lylykangas, M. S., Rautanen, P. A., and Krause, A. O. I., (2002). “Liquid-Phase Hydrogenation Kinetics of Multicomponent Aromatic Mixtures on Ni/Al₂O₃.”
47. Ma, X., Sakanishi, K., and Mochida, I., (1994). “Hydrodesulfurization Reactivities of Various Sulfur Compounds in Diesel Fuel”, *Ind. Eng. Chem. Res.*, 33, 218-222.
48. Machida, M., Sakao, Y., Ono, S., (1999). “Influence of hydrogen partial pressure on hydrodenitrogenation of pyridine, aniline and quinoline”, *Applied Catalysis A: General*, 187, L73-L78.
49. Macías, M.J., and Ancheyta, J., (2004). “Simulation of an isothermal hydrodesulfurization small reactor with different catalyst particle shapes”, *Catalysis Today*, 98, 243–252.
50. Mears, D. E., (1971). “The role of axial dispersion in trickle-flow laboratory reactors”, *Chem. Eng. Sci.*, 26, 1361-1366.
51. Meille, V., Schulz, E., Lemaire, M., and Vrinat, M., (1997). “Hydrodesulfurization of alkyl-dibenzothiophenes over a NiMo/Al₂O₃ catalyst: kinetics and mechanism”, *Journal of Catalysis*, 170, 29–36.
52. Meille, V., Schulz, E., Lemaire, M., and Vrinat, M., (1999). “Hydrodesulfurization of 4-methyl-dibenzothiophene: a detailed mechanism study”, *Applied Catalysis A: General* 187, 179-186.

53. Mijoin, J., Pérot, G., Bataille, F., Lemberon, J.L., Breysse, M., Kasztelan, S., (2001). "Mechanistic considerations on the involvement of dihydrointermediates in the hydrodesulfurization of dibenzothiophene-type compounds over molybdenum sulfide catalysts", *Catalysis Letters*, 71, No.3-4, 139-145.
54. Nagai, M., Goto, Y., Irisawa, A., and Omi, S., (2000). "Catalytic activity and surface properties of nitrided molybdena-alumina for carbazole hydrodenitrogenation", *Journal of Catalysis*, 191, 128-137.
55. Ng, K.M. and C.F. Chu, 1987. "Trickle-Bed Reactors", *Chemical Engineering Process*.
56. Piché, S., Larachi, F., Iliuta, I., and Grangjean, B., (2002). "Improving the prediction of liquid back-mixing in trickle-bed reactors using a neural network approach", *Journal of Chemical Technology & Biotechnology*, 77(9); 989-998.
57. Prins, R., Jian, M., and Flechsenhar, M., (1997). "Mechanism and kinetics of hydrodenitrogenation", *Polyhedron*, Vol.16, No.18, 3235-3246.
58. Quann, R.J., and Jaffe, S.B., (1992). "Structure-Oriented Lumping: Describing the Chemistry of Complex Hydrocarbon Mixtures", *Ind. Eng. Chem. Res.*, 31, 2483-2497.
59. Rabarihoela-Rakotovo, V., Brunet, S., Berhault, G., Perot, G., and Diehl, F., (2004). "Effect of acridine and octahydroacridine on the HDS of 4,6-dimetyldibenzothiophene catalyzed by sulfided NiMoP/Al₂O₃", *Applied Catalysis A: General* 267, 17-25.
60. Rautanen, P., (2002). "Liquid phase hydrogenation of aromatic compounds on nickel catalyst", *Industrial Chemistry Publication Series*, No. 14, Espoo 2002.
61. Rautanen, P.A., Aittamaa, J.R., and Krause, A. Outi I., (2000). "Solvent Effect in Liquid-Phase Hydrogenation of Toluene", *Ind. Eng. Chem. Res.*, 39, 4032-4039.
62. Rautanen, P.A., Aittamaa, J.R., and Krause, A. Outi I., (2001). "Liquid phase hydrogenation of Tetralin of Ni/Al₂O₃", *Chemical Engineering Science*, 56, 1247-1254.

63. Rautanen, P.A., Lylykangas, M. S., Aittamaa, J.R., and Krause, A. Outi I., (2002). "Liquid phase hydrogenation of Naphthalene and Tetralin of Ni/Al₂O₃: Kinetic Modeling", *Ind. Eng. Chem. Res.*, 41, 5966-5975.
64. Russell, C. L., Klein, M. T., Quann R. J., Trewella, J., (1994). "Catalytic hydrocracking reaction pathways, kinetics, and mechanisms of n-alkylbenzenes", *Energy & Fuels*, 8, 1394-1400.
65. Sapre, A.V. and Gates, B.C., (1981). "Hydrogenation of Aromatic Hydrocarbons Catalyzed by Sulfided CoO-MoO₃/γ-Al₂O₃. Reactivities and Reaction Networks", *Ind. Eng. Chem. Proc. Des. Dev.*, 20, 68-73.
66. Sapre, A.V. and Gates, B.C., (1982). "Hydrogenation of Biphenyl Catalyzed by Sulfided CoO-MoO₃/γ-Al₂O₃. The Reaction Kinetics", *Ind. Eng. Chem. Proc. Des. Dev.*, 21, 86-94.
67. Sassu, L., Delitala, C., Leoni, L., Baratti, R., Melis, S., (2003). "Class separation of aromatic compounds in diesel fuels", *Chem. Eng. Trans.*, 3, 491-496.
68. Satterfield, C. N., and Smith, C. M., (1986). "Effect of water on the catalytic reaction network of quinoline hydrodenitrogenation", *Ind. Eng. Chem. Process., Des. Dev.*, 25, 942-949.
69. Schuit, G.C.A., and Gates, B.C., (1973). "Chemistry and Engineering of Catalytic Hydrodesulfurization", *AIChE Journal, Journal review*, Vol. 19, No. 3, 417-438.
70. Sie, S. T., (1991). "Scale effects in laboratory and pilot-plant reactors for trickle-flow processes", *Revue de l'Institut français du petrol*, 46, No 4, 501-515.
71. Specchia, V., Baldi, G., Gianetto, A., (1978). "Solid liquid mass transfer in co-current two-phase flow through pace beds", *Ind. & Eng. Chem. Proc., Des. Dev.*, 17, 362.
72. Spry, J. and Sawyer W., (1975). Paper presented at 68th Annual AIChE Meeting, Los Angeles, November 1975.
73. Stanislaus, A., and Cooper, B.H., (1994). "Aromatic Hydrogenation Catalysis: A Review", *Catal. Rev. – Sci. and Eng.*, 36 (1), 75-123.

74. Stefanidis, G.D., Bellos, G.D., Papayannakos, N.G., (2005). "An improved weighted average reactor temperature estimation for simulation of adiabatic industrial hydrotreaters", *Fuel Processing Technology*, 86, 1761-1775.
75. Sun, M., Nelson, A., E., Adjaye, J., (2005). "First principles study of heavy oil organonitrogen adsorption on NiMoS hydrotreating catalysts", *Catalysis Today*, 109, 49-53.
76. Topsøe, H., and Clausen, B.S., (1984). "Importance of Co-Mo-S Type Structures in Hydrodesulfurization", *Catal. Rev. – Sci. and Eng.*, 26, (3 & 4), 395-420.
77. Toppinen, S., Rantakyla, T.-K., Salmi, T., and Aittamaa, J., (1996a). "Kinetics of the liquid phase hydrogenation of benzene and some monosubstitute Alkylbenzenes over a Nickel Catalyst", *Ind. Eng. Chem. Res.*, 35, 1824-1833.
78. Toppinen, S., Rantakyla, T.-K., Salmi, T., and Aittamaa, J., (1996b). "Kinetics of the Liquid Phase Hydrogenation of Di- and Trisubstituted Alkylbenzenes over a Nickel Catalyst", *Ind. Eng. Chem. Res.*, 35, 4424-4433.
79. Toppinen, S., Salmi, T., Rantakyla, and T.-K., Aittamaa, J., (1997). "Liquid-Phase Hydrogenation Kinetics of Hydrocarbons Mixtures", *Ind. Eng. Chem. Res.*, 36, 2101-2109.
80. Trambouze, P., (1993). "Engineering of hydrotreating processes", *Chemical Reactor Technology for Environmentally Safe Reactors and Products*, 425-442.
81. Van Krevelen, D., and Krekels, J. T. C., (1948). "Rate of dissolution of solid substances", *Rec. Trav. Chim.*, **67**, 512.
82. Van Parijs, I.A. and Froment, G.F. (1986a). "Kinetics of Hydrodesulfurization on CoMo/ γ -Al₂O₃ Catalyst. 1. Kinetics of the Hydrogenolysis of Thiophene", *Ind. Eng. Chem. Prod. Res. Dev.*, 25, 431-436.
83. Van Parijs, I.A., Hosten, L.H., and Froment, G.F., (1986b). "Kinetics of Hydrodesulfurization on CoMo/ γ -Al₂O₃ Catalyst. 2. Kinetics of the Hydrogenolysis of Benzothiophene", *Ind. Eng. Chem. Prod. Res. Dev.*, 25, 437-443.

84. Wiwel, P., Knudsen, K., Zeuthen, P., and Whitehurst, D., (2000). "Assessing compositional changes of nitrogen compounds during hydrotreating of typical diesel range gas oils using a novel preconcentration technique coupled with gas chromatography and atomic emission detection", *Ind. Eng. Chem. Res.*, 39, 533-540.
85. Zeuthen, P., Knudsen, K. G., and Whitehurst, D. D., (2001). "Organic nitrogen compounds in gas oil blends, their hydrotreated products and the importance to hydrotreatment", *Catalysis Today*, 65, 307-314.